Ion channel mediated mechanotransduction in chondrocytes

Inaugural-Dissertation
to obtain the academic degree
Doctor rerum naturalium (Dr. rer. nat.)
submitted to the Department of Biology, Chemistry and Pharmacy
of Freie Universität Berlin

by
Martha Rocío Servín Vences
from Mexico City, Mexico

2017

The present work was carried out under the supervision of Prof. Dr. Gary R. Lewin from September 2012 to October 2017 at the Max Delbrück Center for Molecular Medicine in the Helmholtz Association.

1st reviewer: Prof. Dr. Ursula Koch

2nd reviewer: Prof. Dr. Gary R. Lewin

Date of the defense: 12 January 2018

1 Table of contents

2 Abstract

Articular cartilage is a protective tissue that covers joints with large degree of movement such as knees and elbows. Its main function is to support and distribute forces generated during body locomotion. Cartilage is comprised of individual chondrocytes that are embedded in a specialized matrix formed by collagens, proteoglycans, other non-collagenous proteins and water. Chondrocytes experience a complex mechanical environment and are able to respond to changes in mechanical loads in order to maintain cartilage homeostasis by inducing synthesis or degradation of matrix proteins. It has been proposed that mechanically-gated ion channels are of functional importance in chondrocyte mechanotransduction. Application of mechanical load in chondrocytes induce protein synthesis that is inhibited in the presence of gadolinium, a non-specific inhibitor of mechanically-gated ion channels. However, there was no direct evidence of mechanically-gated currents in these cells. Channel-mediated mechanotransduction is known as mechanoelectrical transduction, and the molecular players mediating this process remained elusive in chondrocyte biology. The aim of this thesis was to identify and characterize the mechanosensitive ion channels that are important for chondrocyte mechanoelectrical transduction. To study this, we used elastomeric pillar arrays to apply mechanical stimuli at the cell-substrate interface while clamping the membrane potential of murine chondrocytes in whole-cell configuration. We found that TRPV4 and Piezo1 channels contribute to currents produced by stimuli applied at the cell-substrate interface. In addition, only Piezo1 contributes to the stretch-activated current in chondrocytes. This is the first direct demonstration of mechanically-gated ion channel activity in primary murine chondrocytes. To study the activation mechanism of Piezo1 and TRPV4, the channels were overexpressed in HEK-293 cells. As observed before, Piezo1 is activated by membrane stretch, cellular indentation and substrate deflection. In contrast, TRPV4 was only slightly activated by membrane stretch, was not activated by cellular indentation, but was efficiently activated by substrate deflections. These results suggest that TRPV4 requires cellular components to efficiently transfer the force to gate the channel. Additionally, the data demonstrate that mechanical stimuli applied to distinct membrane compartments are transduced by separate, but overlapping transduction pathways.

Zusammenfassung

Gelenkknorpel ist ein Schutzgewebe, das Gelenke mit großer Beweglichkeit bedeckt, wie z.B. Knie und Ellenbogen. Seine Hauptverteilung ist die Dämpfung und Verteilung von Kräften während der Bewegung des Körpers. Knorpel besteht aus individuellen Chondrozyten, die in eine spezielle Matrix aus Kollagenen, Proteoglykanen, anderen nicht-kollagenen Proteinen und Wasser eingebettet sind. Chondrozyten befinden sich in einer komplexen mechanischen Umgebung und können auf unterschiedliche mechanische Belastung reagieren, um ein Gleichgewicht innerhalb des Knorpels zu erhalten, indem sie die Synthese oder den Abbau von Matrixproteinen anregen. Es wird vermutet, dass mechanisch gesteuerte Ionenkanäle eine wichtige Funktion bei der Mechanotransduktion der Chondrozyten spielen. Durch mechanischen Druck auf Chondrozyten wird Proteinsynthese induziert, die durch Gadolinium, einen unspezifischen Inhibitor mechanisch gesteuerter Ionenkanäle, inhibiert wird. Allerdings gab es bisher keinen Nachweis von mechanisch gesteuerten Strömen in diesen Zellen. Durch Kanäle gesteuerte Mechanotransduktion ist als mechanoelektrische Transduktion bekannt, und bisher sind die an diesem Prozess beteiligten Moleküle in der Biologie der Chondrozyten noch unbekannt. Ziel dieser Arbeit ist es, die mechanosensitiven Ionenkanäle zu identifizieren und zu charakterisieren, die eine wichtige Rolle bei der mechanoelektrischen Transduktion der Chondrozyten spielen. Um dies zu untersuchen, haben wir elastomere Pillar Arrays verwendet, um mechanische Reize an der Zell-Substrat-Grenze auszuüben, und dabei Gesamtzell-Ableitungen an den murinen Chondrozyten vorgenommen. Dabei haben wir herausgefunden, dass TRPV4- und Piezo1- Kanäle zu Strömen beitragen, die durch Reize an der Zell-Substrat-Grenze ausgelöst wurden. Darüber hinaus ist nur Piezo1 an dehnungsaktivierten Strömen in Chondrozyten beteiligt. Damit wurde erstmals mechanisch gesteuerte Ionenkanalaktivität in primären murinen Chondrozyten gezeigt. Um den Aktivierungsmechanismus von Piezo1 und TRPV4 zu untersuchen, wurden die Kanäle in HEK-293 Zellen überexprimiert. Wie vorher beobachtet, wird Piezo1 durch Dehnung der Membran, Eindellung der Zelle und Substratablenkung aktiviert. Im Gegensatz dazu wird TRPV4 nur leicht durch Dehnung der Membran, nicht durch Eindellung der Zelle und sehr gut durch Substratablenkung aktiviert. Diese Ergebnisse lassen vermuten, dass TRPV4 zelluläre Komponenten benötigt, um das Signal der Krafteinwirkung zur Öffnung des Kanals weiterzugeben. Diese Daten zeigen, dass mechanische Reize, die auf bestimmte Membranabschnitte einwirken, durch unterschiedliche, sich überschneidende Transduktionswege weitergeleitet werden.

3 Abbreviations

$[Ca^{2+}]_I$	intracellular calcium concentration
2D	two-dimensional
3D	three-dimensional
AA	arachidonic acid
ATP	adenosine triphosphate
cDNA	complementary DNA
DAG	diacylglycerol
DNA	deoxyribonucleic acid
DRG	dorsal root ganglion
ECM	extracelular matrix
FCS	fetal calf serum
GAG	glycosaminoglycans
GFP	green fluorescent protein
HEK-293	human embryonic kidney cells 293
HSPC	high-speed pressure clamp
Hz	Hertz
IL4	interleukine 4
IP3	inositol triphosphate
KD	knockdown
MEC-10	mechanosensory abnormality protein 10 (from *C. elegans*)
MEC-4	mechanosensory abnormality protein 4 (from *C. elegans*)
min	minutes
mmHg	millimeter of mercury
MPa	megapascal
mRNA	messenger RNA
ms	millisecond
MscS	small conductance mechanosensitive channel
MscL	large conductance mechanosensitive channel
mV	millivolts
N2a	neuro 2a cells
NK1	neurokinin 1

nm	nanometers
NOMPC	no mechanoreceptor potential C (from *Drosophila*)
P2	purinergic receptor type 2
P2Y2	purinergic receptor type Y2
P_{50}	half-activation pressure
pA	picoampere
PDMS	polydimethylsiloxane
PKC	protein kinase C
PLA2	phospholipase A2
PLC	phospholipase C
PLL	poly-L-lysine
PPADS	pyridoxal-phosphate-6-azophenyl-2´,4´-disulphonic acid
RNA	ribonucleic acid
RT-qPCR	real time qPCR
s.d.	standard deviation
s.e.m.	standard error of the mean
SHG	second harmonic generation
siRNA	small interfering RNA
SK	small conductance Ca^{2+} dependent K^+ channel
SOX9	SRY-box 9
SP	substance P
TRP	transient receptor potential
TRPC6	transient receptor potential cation channel subfamily C member 6
TRPM7	transient receptor potential cation channel subfamily M member 7
TRPV4	transient receptor potential cation channel subfamily 4anilloid 4
WT	wild type
τ_1	activation time constant
τ_2	inactivation time constant

4 List of figures

5 Introduction

Articular cartilage is a highly specialized connective tissue whose primary function is to provide a low-friction environment between opposing bones, and to support and distribute the forces generated during body motion (Buckwalter et al. 2005). It does so by responding to physical and biological cues, such as changes in mechanical load and secretion of inflammatory molecules. This ability is mediated by specialized cells called chondrocytes, which produce the cartilage (Grodzinsky et al. 2000). These cells regulate the synthesis and degradation of extracellular matrix (ECM) proteins. Maintaining balance between these two processes is extremely important for homeostasis of the tissue. A disturbance of the equilibrium leads to diseases of the joints such as osteoarthritis or rheumatoid arthritis that together with ageing reduce the regenerative properties of the cartilage (Buckwalter et al. 2005). Therefore, it is important to study the mechanisms that allow chondrocytes to respond to changes in mechanical load to maintain homeostatic balance of the tissue.

Articular cartilage covers the surface of bones within joints that facilitate body locomotion and provide a large degree of movement, for instance knees, shoulders, wrists, elbows and hips (Figure 1 A-B) (Mansour 2009). The body also has other types of cartilage, classified according to their functions. Elastic cartilage that maintains the shape of the ear and trachea, and fibrocartilage covers joints whose movement is restricted, such as the annulus fibrosus of the internal disc. From here on, I will focus only on the articular cartilage.

In the following introductory section, I will highlight the importance of cartilage composition and the different types of forces detected by the cartilage. Next, I will review what is known about the signaling pathways in chondrocytes that are activated by mechanical load, emphasizing the techniques that have been used to perform mechanical stimulation. This is followed by the aim, objectives, scope, hypothesis (Section 7) and methods used in this thesis (Section 8).

In Section 9, I present the results obtained in this thesis, starting with the establishment and characterization of the cellular model –primary murine chondrocytes. Section 9.2 contains a description of the mechanosensitive currents found in chondrocytes using different methods to stimulate the cells, followed by the identification of the ion channels mediating these currents (Section 9.3). Next, the results from the expression of the candidate channels in a heterologous system are explained (Section 9.4). The last section

of the results is dedicated to the question of whether the presence of Transient Receptor Potential Vanilloid 4 (TRPV4) ion channel could affect the ECM structure of the cartilage. To this aim, entire femoral heads were imaged using a label-free technique, namely Second Harmonic Generation microscopy (Section 9.5).

Section 10.1 contains a short discussion about the importance of using differentiated chondrocytes to draw physiologically relevant conclusions. Section 10.2 elaborates into the relevance of the different techniques to understand the activation modalities of mechanical activated ion channels. Section 10.3 and 10.4 discuss the parallel mechanoelectrical transduction pathways that can be activated in chondrocytes. Section 10.5 provides an insight into the mechanical activation mode of TRPV4. The last section of the discussion expands on the activation modes of TRPV4 and Piezo1 by mechanical stimulation. Section 11 contains the conclusions of the current study.

5.1 Articular cartilage organization

Articular cartilage consists of a dense ECM and sparsely dispersed chondrocytes (Figure 1C). The thickness of this cartilage varies depending on the joint and within the joint, which in humans ranges from 1 to 5 mm (Fox et al 2009). Articular cartilage lacks blood vessels, lymphatic vessels and nerves. Chondrocytes occupy only 2 to 5% of the cartilage volume, the rest consists of water, ions and a complex meshwork structure composed of ECM proteins (Figure 1E) (Kuettner 1992). The ECM is formed by collagens, proteoglycans and glycosaminoglycans (GAG). The proper proportions of these components as well as their interactions are essential for the adequate mechanical properties of the healthy cartilage (Buckwalter et al. 2005; Goldring & Marcu 2009).

Distinct layers of cartilage can be determined based on the size, shape and orientation of chondrocytes relative to the bone (Figure 1C). These layers are known as the superficial zone, transitional zone, deep zone and calcified zone. Each region has different proportion of ECM components, different orientation of collagen fibers and different density and arrangement of chondrocytes. This heterogeneity makes it difficult to define a sharp morphological distinction between zones. Moreover, the protein and collagen composition of the ECM changes in relation to its proximity to chondrocytes, leading to a further classification into pericellular matrix, territorial matrix and interterritorial matrix (Figure 1D). This structural complexity provides cartilage with the mechanical properties to protect the joints.

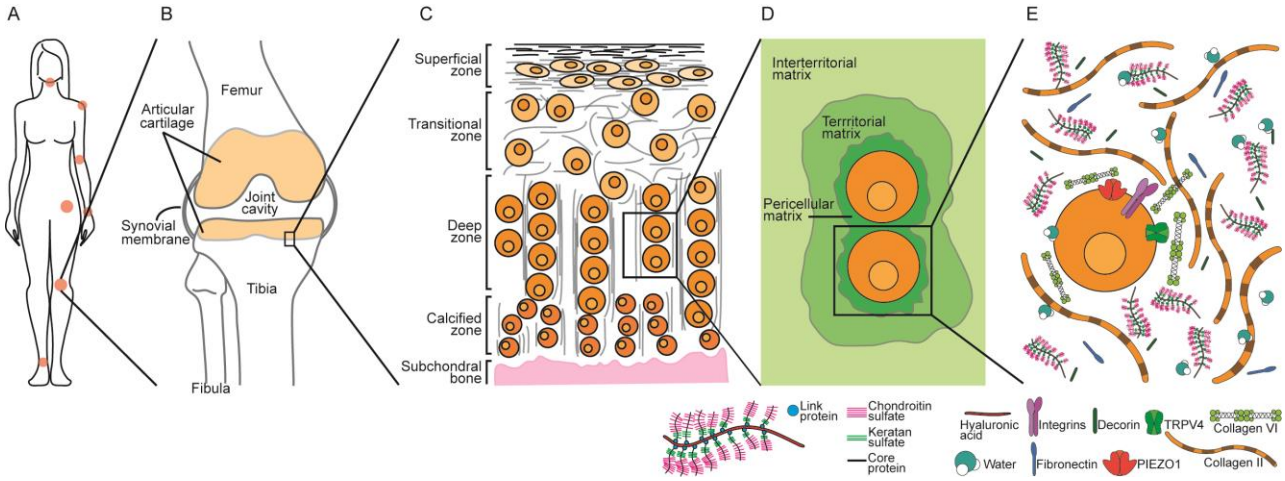

Figure 1: Scheme of structure and composition of articular cartilage.
A) Examples of some diarthrodial joints in the body, from top to bottom: neck, shoulder, elbow, hip, wrist, knee, and ankle. The orange dots represent the location of diarthrodial joints. B) Articular cartilage in the knee. The cartilage covers the femur and tibia. In between the joints there is a cavity containing synovial fluid. C) Articular cartilage zones. Chondrocytes present different shapes and orientation of collagen fibers (gray lines) depending on zonal localization. These zones are the superficial, transitional, deep and calcified zones. D) Position of the cartilage matrices relative to chondrocyte proximity. The pericelullar matrix immediately surrounds chondrocytes, followed by the territorial matrix with the interterritorial matrix comprising the rest of the cartilage. E) Molecular composition of the cartilage. The cartilage contains chondrocytes and a network of ECM proteins such as collagens, proteoglycans, and non-collagenous proteins; the water that comprises the majority of the cartilage content is also shown.

5.2 Structure of articular cartilage

5.2.1 Zonal organization of the articular cartilage

The **superficial zone** is the first layer of cartilage that starts from the articular surface, from the distal part of the bone (Figure 1C). This thin layer is very important for the articular cartilage protection since it is the first shield against mechanical loads. It consists of a thin sheet of fine collagen fibrils, followed by ellipsoid-shaped chondrocytes arranged with their major axis parallel to the articular surface. Collagen II and collagen IX are the most abundant collagen isoforms in the superficial layer (Buckwalter et al. 2005). The fibrillar structure and parallel alignment of these collagens provide higher stiffness and tensile strength in comparison with deeper zones. Additionally, the dense matrix of collagen fibrils affects the permeability of the articular cartilage and the transport of molecules through the cartilage. In the superficial zone, the proportion of collagens is higher in comparison with proteoglycans and relative to other cartilage layers. The superficial zone makes up 10% to 20% of the articular cartilage thickness (Buckwalter et al. 2005; Fox et al. 2009).

The **transitional zone** follows the superficial zone proximally to the bone; this layer forms a transition between the superficial and the deep zone of the cartilage (Figure 1C). It is composed of spherical and sparse chondrocytes that synthesize proteoglycans and collagens (Fox et al. 2009). The concentration of proteoglycans is higher than in the superficial zone. Collagen fibers consist mainly of Collagen II, and their arrangement is more heterogeneous, creating an elastic network that provides resistance against compression and shear stress. The water concentration is lower in comparison to the superficial zone. This zone covers approximately 40% to 50% of the cartilage thickness (Cohen et al. 1998).

The **deep zone** provides a great resistance against compressive forces that impact the cartilage because it contains the highest proteoglycan concentration, with perpendicularly aligned collagen fibers and low water content (Figure 1C) (Cohen et al. 1998). This layer comprises around 30% of the cartilage; the chondrocytes have a spherical shape and are aligned in columns perpendicular to the superficial zone (Buckwalter et al. 2005; Fox et al. 2009). Collagen fibrils are aligned in parallel to these columns.

The **calcified zone** is the functional layer in which the turnover from cartilage to bone takes place (Figure 1C). In this layer the chondrocytes are smaller than in the other zones and they undergo terminal differentiation to form bone. These chondrocytes are considered hypertrophic because they leave the cell cycle, stop proliferating and are gradually replaced by bone (Aigner et al. 2007; Leung et al. 2011; Araldi & Schipani 2010). This thin layer consists of approximately 10% of the tissue and is the boundary between cartilage and the subchondral bone (Cohen et al. 1998; Buckwalter et al. 2005).

5.2.2 Matrix organization of the articular cartilage

Within the cartilage, the ECM also shows variations in terms of composition and fiber orientation depending on the proximity to the chondrocytes. Therefore, the matrix has been further categorized as: pericellular matrix, territorial matrix and interterritorial matrix (Figure 1D).

The **pericellular matrix** immediately surrounds the chondrocytes (Figure 1D) and has been proposed to be important for the initiation of signals between ECM and chondrocytes (Zhang 2014). This thin layer is mainly composed of collagen VI, a non-fibrillar collagen. The pericellular matrix can surround a single chondrocyte or a small group of them in a complex known as the “chondron” (Zhang 2014; Poole et al. 1992). The **territorial matrix** is a thick ECM that surrounds the pericellular matrix (Figure 1D). In this area, the collagen fibers tend to arrange parallel to the articular surface (Buckwalter et al. 2005). The

interterritorial matrix forms the bulk of the cartilage, it is the largest of the ECM divisions and is not in direct contact with chondrocytes (Figure 1D). Proteoglycans are abundant in this space, and the orientation of the collagen fibrils varies depending on the zone (Cohen et al. 1998; Buckwalter et al. 2005). In the superficial zone the collagens lie parallel to the bone surface and each other. Collagens in the transitional zone have various orientations. In the deep zone, they are aligned in parallel columns that stand perpendicular to the bone surface. In the calcified zone the collagen fibers follow the same arrangement as in the deep zone.

In summary, Chondrocytes are the unique cell type of the cartilage. They occupy 2 to 5% of the total cartilage volume (Kuettner 1992), and produce and maintain the ECM (Grodzinsky et al. 2000). This complex ECM is composed of collagens, proteoglycans, GAG, non-collagenous proteins and water (Figure 1E). ECM proteins have to be expressed and deposited in precise amounts to achieve particular proportions on each cartilage zone. Therefore, the proper amount of components and their interactions are essential for the mechanical properties of a healthy cartilage. For instance, the tensile strength is provided by the aligned collagen fibers from the superficial zone, and resistance to compression is provided by the high amount of proteoglycans interacting with the collagen fibers in the deep zone.

5.2.3 Structure, composition and behavior of articular cartilage

Chondrocytes are specialized cells that produce, maintain and repair the **extracellular matrix** (ECM) of the articular cartilage (Figure 1E) (Grodzinsky et al. 2000). They detect extrinsic factors such as mechanical forces and biological stimuli including cytokines, growth factors and differentiation factors (Grodzinsky et al. 2000; Mobasheri et al. 2002). They respond by modulating gene expression to regulate the synthesis and degradation of ECM proteins. This permits the articular cartilage maintain tissue homeostasis when coping with the external stimuli (Buckwalter et al. 2005; Cohen et al. 1998; Mansour 2009; Fox et al. 2009). Chondrocytes additionally, synthesize diverse types of collagens, proteoglycans and other non-collagenous proteins (Dreier 2010; Buckwalter et al. 2005; Fox et al. 2009), and express different types of receptors that mediate interactions between cells and ECM, including integrins, CD44, P2 receptors and ion channels.

5.2.3.1 Biphasic components of the cartilage matrix

The cartilage **extracellular matrix** is a porous, permeable and highly organized structure. To better understand the function of cartilage, it is often considered as a biphasic material that is composed of a structural and a fluid component (Cohen et al. 1998; Lu & Mow 2008). The structural phase comprises all

the macromolecules that form the protein meshwork. The fluid phase consists of water, ions and metabolites. Interactions between the proteins and the fluid phase give the cartilage its particular stiffness and resilience to mechanical loads. These features allows the tissue to withstand the mechanical stress placed on joints with body motion (Lu & Mow 2008).

The **fluid component** contains gases, small proteins, metabolites and cations that counterbalance the negative charges of the proteoglycans. An essential role is to transport nutrients, growth factors and cytokines to the tissue. 80% of the wet weight of the cartilage is water (Cohen et al. 1998; Lu & Mow 2008). The **structural component** of the ECM is composed of proteins such as: collagens, proteoglycans, glycoproteins and non-collagenous proteins. This protein network traps the water inside, 20-40% of the wet weight of the cartilage is composed of proteins (Fox et al. 2009; Cohen et al. 1998; Lu & Mow 2008).

5.2.3.2 Protein composition of the cartilage matrix

Collagens are the most abundant proteins in mammals; they are deposited in the ECM where they form supramolecular assemblies (Heino 2007; van der Rest & Garrone 1991; Ricard-Blum 2011). These proteins have a structural function and contribute to the mechanical properties and shape of tissues. Collagens include in their structure one or more triple-helical domains and 28 members of the family have been described (van der Rest & Garrone 1991; Ricard-Blum 2011). These proteins can be arranged in diverse supramolecular structures, for example collagen I and II form fibrillar filaments, while collagen VI forms beaded microfilaments (Figure 1E) (Cescon et al. 2015). Additionally, collagens are able to interact with cells via different receptor families and some collagens have a restricted tissue distribution (Heino 2007; van der Rest & Garrone 1991; Ricard-Blum 2011).

The different types of collagens contribute approximately 60% to the cartilage by dry weight. They provide the tensile strength to the cartilage, and cohesiveness by trapping large proteoglycans (Cohen et al. 1998).

The bulk material of cartilage is mainly composed of collagens, such as collagen II, VI, IX, X and XI. The collagen II network is the most abundant and it is stabilized by collagen IX and XI, in particular, collagen IX stabilizes the interaction of collagen II network with proteoglycans. In addition, collagen type II is the most abundant protein in the cartilage contributing 90-95% of the collagen in this tissue, and it is also used as a cartilage marker (Lovell-Badge et al. 1987). On the other hand, collagen VI surrounds the chondrocytes and forms part of the pericellular matrix, to which the chondrocytes bind (Zhang 2014; Poole 1997; Wilusz et al. 2014). Moreover, in the calcified zone, there is a turnover of ECM components and the most abundant

collagen is type X, which is additionally considered as a marker for hypertrophic chondrocytes (Leung et al. 2011; Araldi & Schipani 2010).

Proteoglycans consist of a protein core and glycosaminoglycan (GAG) chains (Figure 1E). The proteoglycan aggregates coupled with GAG chains determine the stiffness of the cartilage (Buckwalter et al. 2005) by binding to the collagen meshwork or staying trapped inside the network.

There are two types of protein cores in the proteoglycans: large aggrecans and small proteoglycans. The most abundant large proteoglycan is aggrecan, which comprises about 90% of the proteoglycan mass in the cartilage. The aggrecan is commonly found in a complex with large numbers of chondroitin sulfate and keratin sulfate chains (Figure 1E). On the other hand, examples of small proteoglycans are decorin, biglycan and fibromodulin, which together constitute 10% of the cartilage proteoglycans (Cohen et al. 1998).

The **glycosaminoglycans** (GAG) are long, unbranched and highly polar polysaccharides. They bind to the proteoglycan core (Figure 1E) and confer its negative charge which is important to provide the compressive resistance of the cartilage. The ECM contains different types of GAGs such as hyaluronic acid, chondroitin sulfate, keratin sulfate and dermatan sulfate (Cohen et al. 1998; Fox et al. 2009).

Non-collagenous proteins and **glycoproteins** are involved in stabilizing the matrix by mediating the binding between chondrocytes and the ECM in the cartilage. These proteins make up 15%-20% of the dry weight of the cartilage and include proteins such as anchorin CII, fibronectin and tenascin.

In summary, the structure and organization of the articular cartilage is necessary to confer adequate mechanical properties that allow cartilage to respond to exogenous and endogenous cues. This is achieved by the interaction between chondrocytes and the ECM. However, an imbalance in the function of this tissue produces joint diseases such as osteoarthritis and rheumatoid arthritis, the incidence and prevalence of which increase with age (Litwic et al. 2013). Therefore, more work is needed to understand the molecules involved in the function of articular cartilage, which can advance our understanding of these diseases.

5.3 Mechanical environment of the articular cartilage

Articular cartilage receives a combination of mechanical stimuli, including compressive forces, tensile forces and shear forces (Figure 2) in a wide range of static and dynamic modes. The biomechanical behavior of the cartilage can be better understood when viewed as a biphasic material with a solid and fluid phase.

For instance, when contact forces are initiated in joints, for example when running, there is an immediate increase in the fluid pressure due to compression which causes the fluid to flow out of the ECM, thereby generating shear stress and frictional drag on the matrix (Mansour 2009; Lu & Mow 2008; Mow et al. 1984; Cohen et al. 1998).

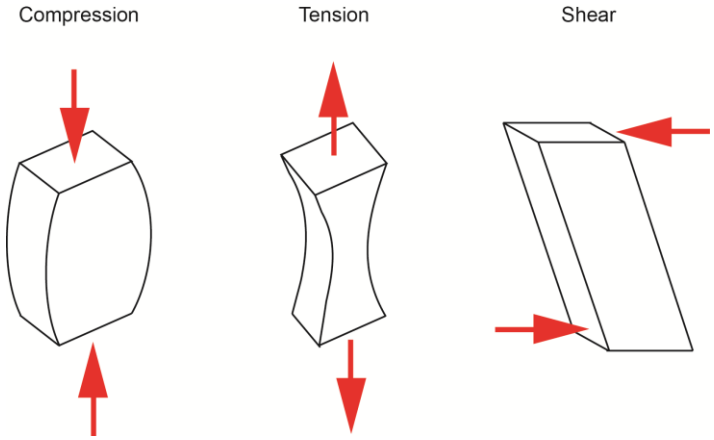

Figure 2. Schematic of forces detected by cartilage.
Compression, tension and shear stress are exemplified in the figure, the red arrow represent the direction in which the force is applied.

To understand the role of the different types of forces encountered by the cartilage, studies using different macroscopic loading configurations have been performed. Including confined stimulation of cartilage explants, unconfined, static and dynamic compression, shear stress, osmotic swelling, and tissue indentation (Han et al. 2011).

The following section contains a summary of the mechanical forces that affect the cartilage, as well as the role that each ECM component plays to withstand them.

5.3.1 Compressive forces

Compressive forces are exerted when pressure is applied over a body that causes it to become compacted (Figure 2, left). Compression of the cartilage induces fluid flow through the solid matrix. This is the primary factor responsible for the viscoelastic behavior observed in articular cartilage. A viscoelastic material is characterized by a time-dependent response to a constant load or deformation; these responses are known as creep and stress-relaxation (Mansour 2009; Lu & Mow 2008; Cohen et al. 1998). The creep response occurs when the cartilage is subjected to a constant load and the tissue responds with a fast deformation,

followed by a slower deformation until it reaches its equilibrium, at this point the load is balanced and deformation stops. The stress-relaxation behavior takes place when the cartilage is constantly deformed. The stress will rapidly increase, reach a peak and progressively decrease over time until equilibrium is achieved, at this point the stress is zero (Mansour 2009; Lu & Mow 2008; Cohen et al. 1998).

Additionally, the negative charges from the proteoglycans help to resist compression. For instance, the cartilage matrix is compacted after compression; therefore, the negative charges of the proteoglycans come closer which increase the repulsion forces. In turn, the aggrecan molecules spread and occupy a larger volume inside the collagen network which results in compressive stiffness of the cartilage. Damage to the collagen framework also reduces the compressive stiffness of the tissue, since the aggregated proteoglycans are contained less efficiently (Buckwalter et al. 2005).

5.3.2 Tensile forces

Tensile stress is the strain applied on a material to stretch it (Figure 2). Tensile strength is the resistance of a material to break under this type of force. The cartilage tensile resistance is provided by the collagen meshwork, which is mainly composed of collagen II. The orientation of the collagen fibers strongly influences the tensile strength (Cohen et al. 1998).

In particular, the superficial zone plays an important role in the tensile force protection of the cartilage; as it is the first layer facing the articular surface it withstands the load and protects the deeper levels. The dense and parallel-aligned collagen meshwork in the superficial zone provides the highest tensile strength of all the cartilage layers. Therefore, the ECM protects the chondrocytes from the high loads coming from daily activities through a combination of mechanical forces, such as: light jogging 7.7 megapascales (MPa), standing up 9.2 MPa, and stair climbing 10 MPa (Adams 2006).

5.3.3 Shear forces

Shear stress occurs when forces are applied in a perpendicular direction relative to the surface of a material as exemplified in Figure 2. Although the predominant load in cartilage is compressive, important shear stresses take place within the tissue, particularly in the deep zone. These stresses can have clinical relevance when degeneration of the basal layer of the cartilage takes place. Normally shear stress is produced as a consequence of the compressive load; the shear stress develops at the interface between the soft thin layer

of cartilage and the much stiffer subchondral bone to which it is attached. Additionally, the randomly distributed fibers from the transitional zone of the cartilage are important to resist the stretching caused by the shear stress (Fox et al 2009).

In summary, the articular cartilage constantly experiences a combination of compressive, tensile and shear forces, and the particular structure and composition of the ECM is essential to withstand them and to provide resilience to the cartilage.

5.4 Mechanisms of chondrocyte mechanotransduction

Mechanotransduction is important in chondrocytes and is vital for their role in cartilage function and maintenance. Different types of protocols have been implemented to study the mechanical response of chondrocytes (isolated or within cartilage). These studies showed that chondrocytes are able to respond and modify their gene expression to make adaptive changes to their environment that include modifying the ECM composition (Conor et al. 2014; Kaupp et al. 2012; Buschmann et al. 1995; Mouw et al. 2007; D. A. Lee et al. 2000).

However, what remains unknown is the precise sequence of events activated by mechanical load that modulates chondrocyte mechanotransduction. In fact, the response of chondrocytes to mechanical load can be assigned to different temporal scales, ranging from seconds and minutes to hours and days. The first responses are due to the activation of a variety of intracellular signaling pathways that include activation of ion channels, integrins, changes in Ca^{2+} concentration, activation of Phospholipase C (PLC), Protein kinase C (PKC), protein phosphorylation, secretion of ATP, substance P (SP) and Interleukin 4 (IL4) and hyperpolarization of the plasma membrane. In contrast, the long-term effects (hours to days) include changes in synthesis and degradation of aggrecan, collagen type II, proteoglycans and proteases, resulting in a different ECM composition through remodeling (Mobasheri et al. 2002; Millward-sadler et al. 2004).

5.4.1 Summary of events during chondrocyte mechanotransduction

The response of chondrocytes to mechanical stimulation is transduced through the ECM, in particular the pericellular matrix which physically interacts with receptors in the plasma membrane. These receptors include integrins, CD44, anexins and other related proteins that bind to collagens, fibronectin, laminin, vitronectin and hyaluron (Mobasheri et al. 2002).

It has been proposed that collagens, fibronectin, laminin, and vitronectin interact with integrins, which subsequently activate several cytoskeletal-associated proteins such as paxilin, tensin and focal adhesion kinase (Millward-Sadler & Salter 2004). In the focal adhesions more proteins are recruited including the actin cytoskeleton, which activate specific kinases to induce the release of SP. The Neurokinin 1 (NK1) receptor is activated by SP to induce IL4 secretion (Millward-Sadler & Salter 2004). Subsequently, IL4 interacts with its receptor, causing PKC and PLC to activate a K^+ channel, most likely the small conductance Ca^{2+} dependent K^+ channel (SK) (Millward-Sadler et al. 1999). SK channel activation leads to a K^+ efflux that induces membrane hyperpolarization Figure 3. This response is seen approximately 20 min after application of mechanical stimuli. The hyperpolarization is very important for the adequate response to mechanical stimuli because chondrocytes derived from osteoarthritic cartilage show a depolarization instead (Millward-Sadler & Salter 2004). This imbalance therefore has been suggested to be an important characteristic for the progression of osteoarthritis (Millward-sadler et al. 2004; Millward-Sadler & Salter 2004; Mobasheri et al. 2002).

In short, different signaling pathways activated by mechanical load have been identified and characterized in chondrocytes. The following section contains a summary of these routes focusing on the ion channels that have been related to these processes.

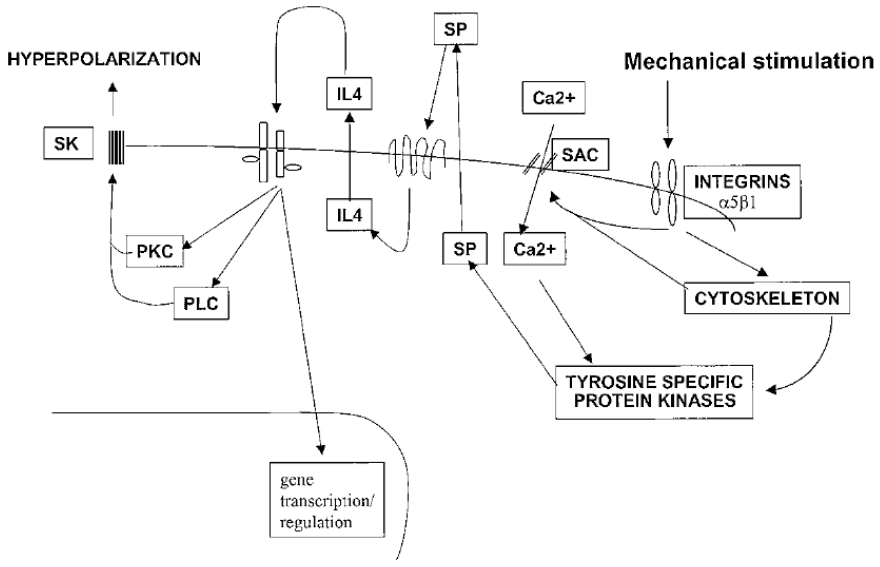

Figure 3. Mechanotransduction pathways activated in human articular cartilage by 0.33 Hz stimulation.
After mechanical cyclical stimulation, α5β1 integrin is activated which results in signaling pathways that leads to SP and IL4 secretion and modulation of gene transcription. Taken from Millward-Sadler & Salter 2004.

5.4.2 Intracellular Calcium fluxes induced by mechanical stimulation in chondrocytes

Calcium ions are an important second messenger with crucial roles in several cellular processes and multiple cell types, and chondrocytes are no exception. Experiments performed on chondrocytes using fluorescent Ca^{2+} indicators showed that a transient Ca^{2+} increase is one of the earliest events in the cascade activated by mechanical load. For example, experiments performed with *in situ* chondrocytes describe a rise in the intracellular Ca^{2+} concentration ($[Ca^{2+}]_i$) induced by cyclical compression of the cartilage explant. The first $[Ca^{2+}]_i$ increase starts 5.9 (± 4.4) sec after the first stimulation and the second after 12.3 (± 3.8) sec (3 and 2 MPa loading conditions respectively) (Han et al. 2012).

Using primary chondrocytes grown in monolayer and indented with a glass micropipette, a Ca^{2+} rise was observed 2 s after the stimulation (Kono et al. 2006). In addition, experiments using chondrocytes seeded in a 3D agarose culture, the $[Ca^{2+}]_i$ increase in response to a single static strain was observed with a delay of 225 s (± 95) (Roberts et al. 2001).

The variations observed in latency of response could arise from a number of differences in the experimental methodology. For example, whether the experiments were performed in static or cyclical conditions, the magnitude of the applied force, as well as the frequency of the stimulation. Furthermore, the differences in culture conditions are very important for the chondrocyte response, this issue is addressed later in the introduction. One important factor is that chondrocytes grown on monolayer produce less ECM than chondrocytes grown in 3D culture (Caron et al. 2012). This is relevant because ECM proteins are crucial for transduction of the mechanical stimuli by chondrocytes.

5.4.3 Molecules involved in chondrocyte mechanotransduction

Chondrocytes are capable of detecting mechanical signals that are continuously impacting their environment. To detect and transduce these inputs, chondrocytes need cell membrane mechanoreceptors. Potential candidates for this role include mechanosensitive ion channels and integrin receptors (Lee et al. 2000). The following section summarizes pathways activated by such cell membrane receptors.

5.4.3.1 Integrins

Integrins are a family of heterodimeric integral membrane glycoproteins that connect the extracellular environment with the intracellular space. They have a large extracellular domain, which works as a receptor for different ECM proteins such as laminins, collagen, fibronectin, and vitronectin among others (Millward-Sadler et al. 1999; Barczyk & Carracedo 2010). Integrins also have an intracellular domain that anchors them to the cytoskeleton and allows them to interact with other intracellular proteins. Integrins are therefore a bridge that connect and communicate between the extracellular environment and the interior of the cell. Thus, mediating bidirectional interactions between cells and ECM proteins.

Integrins are constituted by an alpha (α) and a beta (β) subunit to form a functional heterodimer. Previous work performed in chondrocytes demonstrated using antibodies against α5 and β1 integrins that integrin blockade inhibits the hyperpolarization induced by mechanical stimuli in these cells. These data suggest that integrin activation is connected to the hyperpolarization that is observed 20 min after mechanical stimulation (Wright et al. 1997).

5.4.3.2 Ion channels

5.4.3.2.1 Purinergic ion channels, signaling events leading to intercellular communication

An important cellular messenger that is released by chondrocytes after mechanical stimulation is ATP (identified in experiments performed using cyclic compression). To address the role of ATP, Ca^{2+}signaling studies have been performed in chondrocytes cultures in monolayer and 3D matrices (Andrea 1996; Roberts et al. 2001; Pingguan-Murphy et al. 2006; Kono et al. 2006). These studies revealed a Ca^{2+} rise mediated by influx of extracellular Ca^{2+} and Ca^{2+} release from stores (Andrea 1996; Roberts et al. 2001; Pingguan-Murphy et al. 2006; Kono et al. 2006). Purinergic receptor (P2) blockers like suramin and basilien blue, reduced the Ca^{2+} rise induced by ATP. An additional piece of evidence that supports the role of P2 receptors in chondrocyte mechanotransduction comes from the detection of mRNA for P2Y2 channels by RT-qPCR (Millward-sadler et al. 2004). Together this evidence strongly suggests that P2Y2 channels mediate Ca^{2+} influx in response to ATP released after mechanical stimulation.

Interestingly, it has been shown that P2Y2 receptors are able to interact with the αV β3/5 integrin; therefore, they might be acting together to transduce mechanical signals in the cell (reviewed in Peterson et al., 2010). Moreover, chondrocytes release other molecules in addition to ATP, such as SP and IL4 which might be acting as mediators of intercellular communication within the cartilage.

5.4.3.2.2 SK channels and the hyperpolarization response

Mechanical stimulation in chondrocytes activates a series of signaling pathways that induce membrane hyperpolarization. This response has been observed approximately 20 min after stimulus onset (cyclical mechanical stimulation at 0.33 Hz) (Wright et al. 1997; Millward-Sadler et al. 2000; Millward-Sadler & Salter 2004). To investigate the nature of this response different blockers were used including P2 receptor antagonists (suramin and PPADS pyridoxal-phosphate-6-azophenyl-2´,4´-disulphonic acid), a SK selective blocker (apamin), and a Ca^{2+} dependent K^+ channel blocker (quinide), all of which decreased the membrane hyperpolarization in chondrocytes. Suggesting that P2 receptors, SK channels and Ca^{2+} dependent K^+ channel participate in the signaling pathway leading to hyperpolarization (Millward-Sadler et al. 1999; Millward-Sadler et al. 2000; Millward-sadler et al. 2004). So far, pharmacological data mainly implicates the P2Y2 receptor in Ca^{2+} influx, and SK channels in K^+ efflux. However, other channels cannot be excluded.

SK channels are characterized by low single-channel conductance (10-20 pS), voltage independence and activation by submicromolar concentration of intracellular Ca^{2+} (Adelman et al. 2012). Thus, these channels can be activated via Ca^{2+} influx and Ca^{2+} release from intracellular stores, or by a combination of both pathways. This suggests that the SK channels should have fine spatiotemporal regulation that allows the channels to be activated 20 min after the mechanical stimulation and not just after the initial $[Ca^{2+}]_i$ increase, just seconds after the stimuli.

In summary, chondrocytes display an intracellular Ca^{2+} increase seconds to minutes after the onset of stimulation with P2Y2 receptors or other Ca^{2+} permeable channels mediating this event. Following the initial increase, Ca^{2+} oscillations can be observed due to Ca^{2+} mobilization from internal stores that are activated by IP3 receptors or Ryanodine receptors. This Ca^{2+} signaling is necessary to activate SK channels and produce the hyperpolarization response observed 20 min after the stimulus onset. A parallel signaling pathway involves ATP release by hemi-channels, anion channel or via exocytosis, 5 to 15 min after the mechanical stimulation. ATP is recognized by the P2Y2 receptor allowing Ca^{2+} and Na^+ influx to depolarize the plasma membrane and open Voltage Operated Calcium Channels, to induce a massive Ca^{2+} influx. Furthermore, the P2Y2 receptor is activated via G_q protein, which activates the PLC pathway leading to the production of inositol triphosphate (IP3) and diacylglycerol (DAG). In turn, Ca^{2+} is released from intracellular stores and subsequently PKC is activated (Graff et al. 2000; Millward-sadler et al. 2004; Pingguan-Murphy et al. 2006). According to this proposed mechanism (Figure 4), the Ca^{2+} increase mediated by the P2Y2 receptor should be downstream of the Ca^{2+} influx mediated by mechanically activated

ion channels. However, the order of the events following mechanical stimulation of chondrocytes is unknown.

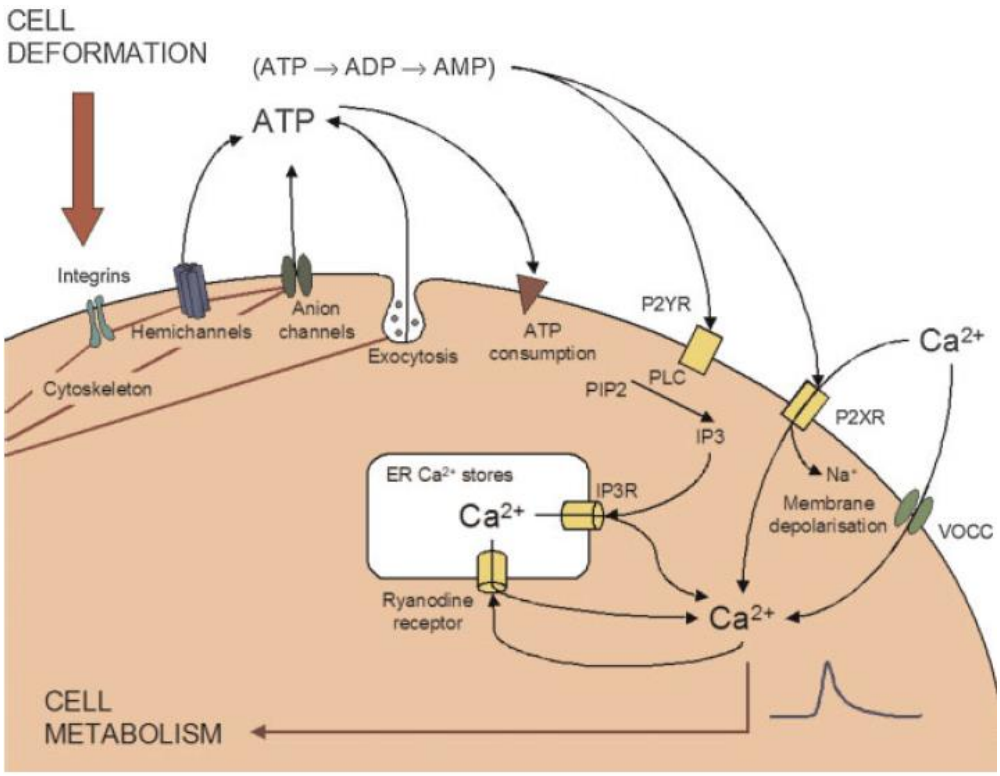

Figure 4. Mechanotransduction pathways activated in chondrocytes after mechanical stimulation.
Activation of mecanosensitive transduction pathways that lead to ATP release to active P2 receptors. Image taken from Pingguan-Murphy et al. 2006.

5.4.3.2.3 Mechanically activated ion channels and the calcium response

Mechanically activated ion channels are transmembrane proteins capable of opening in response to a mechanical stimulus. Thus, the open probability of the ion channel increases with mechanical stress to allow ion flux across the membrane. It is important to mention that a mechanosensitive ion channel is a term used to categorize ion channels that are directly or indirectly activated by mechanical stimuli but involved in a mechanosensitive pathway. Examples of ion channels that are directly activated by changes in the lipid bilayer tension (Figure 5A) are bacterial ion channels such as the small conductance mechanosensitive channel (MscS) and the large conductance mechanosensitive channel (MscL) (Sukharev et al. 1994; Martinac 2001; Levina et al. 1999), and the eukaryotic ion channels: Piezo1, TRAAK and TREK1 (Coste et al. 2012; Syeda et al. 2016; Charles D Cox et al. 2016; Brohawn et al. 2014); these channels are also known as stretch-activated ion channels (Figure 5A). In contrast the term mechanosensitive ion channels may also refer to channels with diverse types of activation such as: 1) ion channels activated by mechanical

stimuli with help of a tether protein (Figure 5B-C). 2) Channels coupled to a mechanosensitive pathway, without the ion channel being the mechanosensor (Figure 5D). 3) Stretch-activated ion channels (Figure 5A). From here on, I will refer to stretch-activated ion channels when the stretch mechanism has been proven and mechanically-activated ion channels when the channel opening mechanism has not yet been fully elucidated.

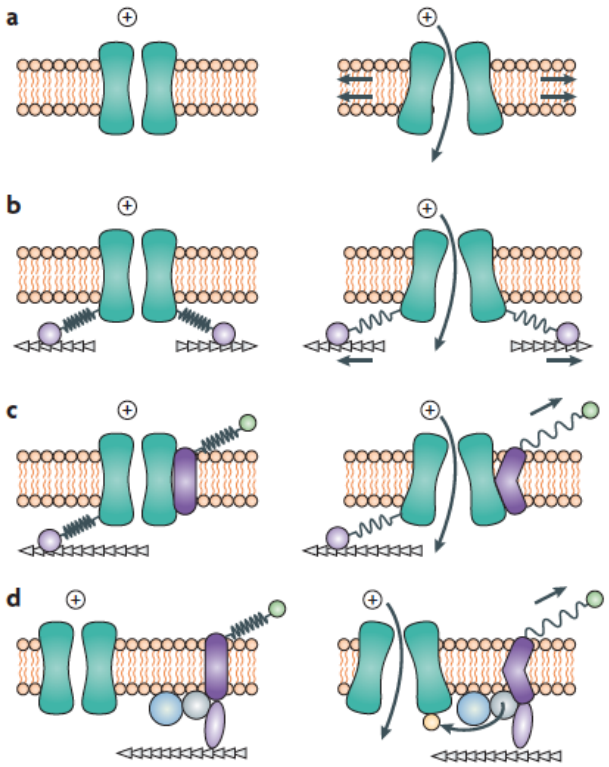

Figure 5. Schematic of activation modes for channels gated by mechanical stimuli.
Activation mode for stretch-sensitive ion channels. In this model, the force is delivered to the channels by changes in lipid bilayer tension, which favors the channel opening. B and C) In the tether model, accessory proteins such as ECM or cytoskeletal proteins are bound to the channel to transfer the mechanical force to gate the channels. D) Activation mode in which the channel is considered mechanically sensitive because the channel is activated through a signaling pathways but not directly gated through mechanical stimuli. Image taken from Christensen & Corey 2007.

Mechanically-activated ion channels have been implicated in chondrocyte mechanotransduction by the use of gadolinium, a broad blocker of mechanosensitive ion channels. Chondrocytes loaded with Ca^{2+} fluorescent probes and stimulated with cyclic compression display a Ca^{2+} influx that is sensitive to gadolinium block (Roberts et al. 2001; Pingguan-Murphy et al. 2006). Additionally, gadolinium also prevents the hyperpolarization and tyrosine phosphorylation induced by mechanical load (Lee et al. 2000; Millward-Sadler et al. 2000). This strongly suggests the involvement of a mechanosensitive ion channel however, the molecular identity of these channels in chondrocyte mechanotransduction is unknown.

In summary, Ca^{2+} regulation is very important for chondrocyte physiology, the fine spatiotemporal regulation of Ca^{2+} mobilization is crucial for chondrocytes to display an adequate response to mechanical stimulation. Although some candidates have been proposed such as Piezo channels, which are *bona fide* mechanically activated ion channels, and TRPV4, which has been linked to mechanotransduction processes in different cell types as well as chondrocytes. In support of this hypothesis, it has been shown that the mRNA of Piezo channels and TRPV4 is present in porcine chondrocytes (Lee, et al. 2014). This evidence suggested a role for these proteins in chondrocyte mechanotransduction. However, there is no electrophysiological evidence supporting an essential function for these channels in chondrocyte mechanotransduction.

5.4.3.2.3.1 TRPV4 channel

The Transient Receptor Potential cation channel subfamily V member 4 (TRPV4) belongs to the TRPV subgroup of the TRP family. It was cloned for the first time in 2000 (Strotmann et al. 2000; Wissenbach et al. 2000; Liedtke et al. 2000). TRPV4 is a highly cation permeable channel that poorly discriminates between monovalent cations (K^+>Cs^+>Rb^+>Na^+>Li^+; and permeability values relative to Na^+ are 6-10 for Ca^{2+} and 2-3 for Mg^+) (Liedtke et al. 2000; Strotmann et al. 2000; Voets et al. 2002). It was first described as an osmosensitive channel but can also be gated by heat and chemical agonists such as phorbol ester compounds, arachidonic acid and endocanabinoids (Vriens et al. 2004; Nilius et al. 2004). Therefore, TRPV4 is a polymodal ion channel, a property shared by many members of the TRP family.

It has been shown that TRPV4 mRNA is widely expressed and has been detected in heart, endothelium, brain, liver, placenta, lung, trachea and salivary glands (Plant & Strotmann 2007). Additionally, TRPV4 has been detected in dorsal root ganglion (DRG) neurons (Cao et al. 2009; Lechner et al. 2011). In bladder urothelium, kidney epithelium and vascular epithelium where TRPV4 has a role in volume regulation and osmosensing (Gevaert et al. 2007; Janssen et al. 2016; Tian et al. 2004; Filosa et al. 2013). In the inner ear, pulmonary aortic smooth muscle, cardiac fibroblasts, myocytes and skeletal muscle fibers TRPV4 has a mechanosensing role (Nilius & Voets 2013; Shen et al. 2006; Adapala et al. 2013; Ho et al. 2012). TRPV4 together with the transcription factor SRY-box 9 (SOX9) has an important role in chondrocyte differentiation (Muramatsu et al. 2007).

Mouse models with a targeted deletion of *Trpv4* gene are viable and fertile, however they were reported to have impaired pressure and osmotic sensation (Liedtke & Friedman 2003; Suzuki, Mizuno, et al. 2003; Mizuno et al. 2003; Lechner et al. 2011) as well as impaired stretch sensitivity in the bladder wall (Gevaert

et al. 2007; Mochizuki et al. 2009). TRPV4 mutant mice have been reported to display a normal thermal response *in vivo* (Lee et al. 2005), and normal response to thermal and mechanical hyperalgesia (Alessandri-Haber et al. 2008). TRPV4 is additionally involved in endothelial mechanotransduction and arterial vasodilatation (Hartmannsgruber et al. 2007; Earley et al. 2009; Mendoza et al. 2010). Moreover, mice lacking TRPV4 have defects in the formation of the intercellular junction barrier in the skin (Sokabe et al. 2010) and impaired osteoclast differentiation, hearing alteration and compromised pain sensing (Tabuchi et al. 2005; Everaerts et al. 2010). TRPV4 is necessary to increase lung permeability after induced acute lung injuries (Yin et al. 2008; Jian et al. 2008; Alvarez et al. 2006; Hamanaka et al. 2007).

Osmotic imbalance detection has also been related to mechanosensation because osmotic changes cause swelling or shrinking of the cells, which affects the plasma membrane. TRPV4 functions as an osmosensor allowing Ca^{2+} influx in chondrocytes in hypotonic conditions (Phan et al. 2009). Therefore, TRPV4 is an important protein for chondrocyte physiology that has been linked to mechanotransduction, however there is controversy regarding the activation mechanism in this process.

To further support the role of TRPV4 in chondrocyte physiology, several mutations that cause human arthropathies and skeletal dysplasias were mapped to the *Trpv4* channel gene. Interestingly, there is a cluster of mutations affecting only the skeletal system in the ankyrin repeat domain of TRPV4 (Nilius & Voets 2013; Lamandé et al. 2011b). Additionally, mice lacking TRPV4 are more likely to develop osteoarthritis and this risk increases with age and high body weight (Andrea L. et al. 2010; O'Conor et al. 2013; O'Conor et al. 2016).

It has been shown that chondrocytes embedded in agarose constructs (i.e. 3D culture) secrete more ECM proteins after mechanical load is applied (O'Conor et al. 2014). ECM synthesis was inhibited by a TRPV4 antagonist (GSK205) and protein synthesis can be induced using a TRPV4 agonist (GSK1016790A) without mechanical stimulation (O'Conor et al. 2014). This evidence strongly suggests an involvement of TRPV4 in chondrocyte mechanotransduction, however it is not known whether TRPV4 is the mechanosensor, being directly activated by changes in the mechanical load.

5.4.3.2.3.2 Piezo channels

The Piezo channels are genuine mechanically-activated ion channels. They are pore-forming subunits that open in response to mechanical stimuli and are non-selective cation permeable channels (Coste et al. 2012). They were first cloned and described in 2010 (Coste et al. 2010). The Piezo channels have orthologs in

plants, insects, and fish throughout the mammalian kingdom (Coste et al. 2010; Coste et al. 2012; Prole & Taylor 2013).

Piezo2 is mainly expressed in the nervous system; particularly in dorsal root ganglia neurons, Merkel cells and auditory hair cells (Coste et al. 2010; Wu et al. 2016). Piezo2 has been implicated in proprioception (Ranade et al. 2014; Chesler et al. 2016) and touch transduction (Woo et al. 2014; Ikeda et al. 2014; Maksimovic et al. 2014). In addition, in patch-clamp experiments it has been observed that Piezo2 mediates mechanically activated currents when the channel is overexpressed and the cells are indented with a polished glass probe applied to the apical surface, (Coste et al. 2010). Mutations in Piezo2 are associated with a family of diseases that cause congenital joint contractures, distal arthrogryposis, Gordon syndrome and Marden-Walker syndrome (Coste, et al. 2013). These three diseases are characterized by multiple contractures of joints, which points to the relevance of Piezo2 in the musculoskeletal system.

On the other hand, Piezo1 has a broader expression outside the nervous system. In mouse, it has been found in erythrocytes, epithelial cells, endothelial cells, urothelial cells, and renal tubular epithelial cells (Andolfo et al. 2013; Zarychanski et al. 2012; Gudipaty et al. 2017; Peyronnet et al. 2013). It is involved in red blood cell volume regulation, cell division and cell extrusion of epithelial cells, vasculature development, pressure regulation in urothelium, regulation of mouse circadian rhythm, and axonal growth in *Xenopus* retinal ganglion neurons (Gudipaty et al. 2017; Cahalan et al. 2015; Ranade et al. 2014; Miyamoto et al. 2014; Ihara et al. 2017; Koser et al. 2016). Piezo1 mediates mechanically-activated currents in the neuroblastoma Neuro 2a cell line (N2a), where it was first described (Coste et al. 2010; Poole et al. 2014; Lewis & Grandl 2015; Syeda et al. 2016; Cox et al. 2016). So far, the first evidence of mechanically-gated currents in primary cells comes from renal tubal epithelial cells, where the channel was knocked down and the mechanically gated currents were absent (Peyronnet et al. 2013).

Additionally, it has been proven that the Piezo1 gating is promoted by differential tension in the lipid bilayer (Coste et al. 2010; Syeda et al. 2016; Cox et al. 2016; Lewis & Grandl 2015); therefore it is a stretch activated ion channel. In contrast, there is no evidence of membrane stretch gating for Piezo2 so far.

A recent report showed the mRNA expression of Piezo1 and Piezo2 in porcine, murine and human chondrocytes. Compression of pig chondrocytes with an atomic force microscopy (AFM) cantilever induces Ca^{2+} increase in porcine chondrocytes. The Ca^{2+} transient was diminished when the expression of Piezo1 and Piezo2 was reduced using a siRNA to knockdown the channels (Lee, et al. 2014). All the evidence

suggests a role of these ion channels as putative mechanosensors in chondrocytes, however no electrophysiological evidence has been presented.

5.5 Current status of the study of chondrocyte mechanotransdution

Several approaches have been used to study the mechanosensitive properties in chondrocytes focusing on population or single cell studies. The population studies are generally done conducted on cartilage explants or isolated chondrocytes embedded in 3D matrices such as agarose or alginate. Single cell studies have been generally performed in chondrocytes that were cultured in monolayers. Experimental design is important because chondrocytes are very sensitive to their mechanical environment. In fact, when primary chondrocytes are cultured in monolayer, the cells tend to dedifferentiate showing a fibroblast-like morphology (Minegishi et al. 2013; Caron et al. 2012). Additionally, there is a decrease in the expression of the transcription factor SOX9, collagen II and proteoglycans with high molecular weight that maintain the differentiated state of chondrocytes (Minegishi et al. 2013; Caron et al. 2012; Ma et al. 2013; Benya & Shaffer 1982). Moreover, there is an increase in expression of collagen type X and type I, and proteoglycans with low molecular weight. However, the dedifferentiated chondrocytes can be redifferentiated back into chondrocytes by culturing the cells in 3D matrices. Chondrocytes cultured in a 3D environment continue producing collagen II and SOX9, together with other chondrocyte markers (Caron et al. 2012; Brand et al. 2012). 3D cultures are also used to maintain isolated chondrocytes in their proper differentiation state.

5.5.1 Single cell stimulation with glass pipette indentation

This section will review studies focused on the initial part of chondrocyte mechanotransduction, emphasizing the type of mechanical stimulation that was used and the readout of the study. For organizational purposes I will make subsections referring to the different experimental configurations used to perform the mechanical stimulation: local (glass pipette indentation) and global (compression, fluid flow, ultrasonic stimulation).

Experiments performed using primary chondrocytes grown in a monolayer and indented with a glass micropipette, showed a Ca^{2+} rise seconds after the stimulation onset (Table 1). This was followed by a Ca^{2+} rise in the adjacent cells to the stimulated cell (Andrea 1996; Guilak et al. 1999; D'Andrea et al. 2000; Kono et al. 2006). Amiloride decreased the percentage of cells responding without affecting the amplitude of the Ca^{2+} increase of the responding cells (Guilak et al. 1999) Additionally, gadolinium reduced the amplitude of the Ca^{2+} peak from the stimulated cells (Guilak et al. 1999)indicating that mechanically gated ion

channels are involved in this response. The Ca^{2+} rise from adjacent cells has been attributed to the activation of purinergic receptors activated by ATP secreted by mechanically-stimulated chondrocytes (Kono et al. 2006).

Importantly, all the previous studies performed using single chondrocytes have used fluorometric Ca^{2+} imaging as a readout because of technical difficulties coming from coupling patch clamp recording in primary differentiated cells (which are 10 μm in diameter) together with a successful implementation of mechanical stimulation. In fact, a study in 2014 reported that indentation using a glass micropipette in patch clamp recordings, and pipette suction in cell-attached configuration was not successful to induce mechanically activated currents in primary porcine chondrocytes. One reason likely is the cellular destruction occurred before a signal could be measured (Lee, et al. 2014).

5.5.2 Population stimulation with cyclic and static compression

To study the chondrocyte response to compressive forces, embedded chondrocytes in 3D matrices such as agarose or cartilage explants in compression chambers have been widely used (Table 1). Different loading protocols and readouts have been measured in these types of studies. Mechanical stimulation was performed with static compression using only one long stimulus or with dynamic compression where several cycles of compression are performed, and different frequency and amplitudes tested. As a readout for these experiments, Ca^{2+} dynamics, ATP release and protein content can be measured. For instance, in an experimental setup using rabbit cartilage explants loaded with two fluorescent probes to perform ratiometric measurements, Ca^{2+} rises were observed after each compression cycle (Han 2011). Unfortunately, 3D studies are not suitable for electrophysiology as the compression chamber and the patch clamp setups are not compatible.

Studies using agarose constructs detected a Ca^{2+} rise using 1 or 100 cycles of cyclic compression, indicating an increase in Ca^{2+} signaling independent of the number of cycles (Pingguan-Murphy et al. 2005). However varying the frequency and strain rate differentially modulated the number of responding cells and the rise and decay of the Ca^{2+} transient (Pingguan-Murphy et al. 2006). Additionally, Ca^{2+} transients were decreased using the nonspecific inhibitor of mechanosensitive ion channels gadolinium, apyrase (an enzyme that hydrolyzes ATP) and P2 receptor inhibitors. Thus similar to pipette indentation, cyclic compression activates mechanically activated ion channels which in turn induce ATP release (Garcia 2009) and activates

P2 receptors, causing a combination of extracellular Ca^{2+} influx and Ca^{2+} release from internal stores (Pingguan-Murphy et al. 2006).

Table 1. Summary of methods used to mechanically stimulate chondrocytes and the downstream effect measured as response.

Mechanical stimulation	Application	Organism	2D/3D culture	Readout	Reference
Cyclic compression	Global	Rabbit, bovine, human	3D cartilage explant, 3D agarose construct, 2D monolayer	Calcium, ATP release, protein phosphorylation	Lee et al. 2000; Pingguan-Murphy et al. 2006; Mouw et al. 2007; Garcia & Knight 2010; Han et al. 2012; O'Conor et al. 2014
Static compression	Global	Dog, bovine, human	3D cartilage explant, agarose construct	Protein content	Burton-wurster et al. 1993; Mouw et al. 2007
Fluid flow (static and pulsatile)	Global	Bovine	2D monolayer, 3D alginate constructs	Calcium	Yellowley et al. 1997; Yellowley et al. 1999; Degala et al. 2011
Ultrasonic stimulation	Global	Rabbit	2D monolayer culture	Calcium, ATP release,	Kono et al. 2006
Pipette indentation	Single cell	Pig, bovine, rabbit	2D monolayer	Calcium	Andrea 1996; Guilak et al. 1999; D'Andrea et al. 2000; Kono et al. 2006

To study the relation between mechanical stimulation and protein synthesis, chondrocytes embedded in agarose constructs were stimulated with cyclic compression, resulting in protein synthesis activation measured by total GAG and collagen content (O'Conor et al. 2014). On the other hand, in conditions where cartilage explants or agarose constructs were exposed to static compression, the synthesis of GAGs, proteoglycans, fibronectin, aggrecan, collagen II and general protein synthesis was inhibited (Burton-Wurster et al. 1993; Mouw et al. 2007).

In addition, to study the role of TRPV4 in protein synthesis induced by mechanical stimulation in chondrocytes, a TRPV4 antagonist (GSK205) was used during cyclic compression. This resulted in a diminished protein synthesis that could be rescued in the presence of a TRPV4 agonist (GSK1016790A) in absence of cyclic compression (O'Conor et al. 2014). This evidence strongly suggests a role for TRPV4 in chondrocyte mechanotransduction pathways.

5.5.3 Population stimulation with fluid flow

As mentioned before, chondrocytes are subjected to fluid flow in the cartilage. To study this type of stress, bovine chondrocytes in 2D and 3D cultures were subjected to fluid flow where they showed an increase in $[Ca^{2+}]_i$. This response is inhibited by removing the extracellular Ca^{2+} and by the presence of gadolinium (Table 1) (Yellowley et al. 1997; Yellowley et al. 1999; Degala et al. 2011). Interestingly, ATP does not seem to be involved in the fluid-flow response because the presence of suramin (a broad inhibitor of P2 receptors) had no effect on the Ca^{2+} signaling (Yellowley et al. 1999). Therefore, mechanically gated ion channels seem to be involved in the initial response to fluid flow, but ATP does not mediate the continuation of the Ca^{2+} signal as it was observed for cyclical compression. This suggests that parallel mechanotransduction pathways are triggered by different mechanical stresses.

6 Statement of the problem

In summary, most of the current studies in chondrocyte mechanotransduction have focused on the outcomes of mechanotransduction signaling pathways, such as protein synthesis modulation. Therefore, more information is needed about the initial activation of pathways, mainly about the mechanoreceptors. In addition, there is indirect evidence suggesting early activation of mechanosensitive ion channels. In these studies researchers observed an inhibition of protein synthesis induced by cyclical mechanical stimulation when gadolinium was used (Roberts et al. 2001; Pingguan-Murphy et al. 2006). This evidence together with data reporting expression of different ion channels in chondrocytes suggests that these proteins are strong candidates for mediating force transduction in chondrocytes. However, until now due to technical limitations, there has been a lack of electrophysiological evidence supporting this hypothesis. Hence, is important to determine whether 1) mechanical stimulation of chondrocytes is followed by an inflow of current. 2) The identity of the molecular players generating this current. 3) The biophysical properties and the requirement for the generation of such currents.

7 Aim, scope and hypothesis of the study

As previously mentioned, there is a gap in the knowledge regarding the identity of the early mediators of force transduction in chondrocytes. Experimental evidence strongly suggests that mechanosensitive ion channels may play a pivotal role in mediating fast mechanotransduction processes. Therefore, the aim of this study is: *the identification of mechanosensitive ion channels participating in chondrocyte mechanotransduction*.

The hypothesis is: *chondrocytes respond to mechanical stimulation by mechanosensitive ion channel activation*.

This study focuses on the identification and characterization of mechanosensitive ion channels expressed in differentiated murine chondrocytes, the identification of molecules responsible for the mechanically gated currents and the characterization of the identified ion channels in heterologous expression system using different techniques to convey the mechanical stimulation.

7.1 Significance of the study

By understanding how mechanical forces activate mechanosensitive ion channels, we can achieve a broader knowledge of how these types of proteins work at the molecular level. These results can also be helpful to understand the role of these proteins in other cell types. Additionally, this study can lead to an advancement of our knowledge that can further develop new therapies to treat osteoarthritis or to increase cartilage production to treat joint injuries and diseases.

Moreover, this study will broaden our understanding of ion channels, in particular mechanosensitive ion channels and channels from the TRP family. The findings of this research may be extended to other tissues where Piezo1 and TRPV4 are expressed.

8 Materials and methods

8.1 Materials

8.1.1 Chemicals

Name	Supplier	Catalog number
ACA	Calbiochem, EMD Millipore	104550
Alginate (alginic acid sodium salt from Brown algae)	Sigma	71238
$CaCl_2$	Sigma	C4901
Cal-520	AAT-Bioquest	21091
Chloroform	Sigma	67-66-3
Cytochalasin D	Santa Cruz Biotechnology	SC-201442
dNTPs	Invitrogen	P/N55082-85
EGTA	Sigma	E4378
Ethanol	Roth	K928.4
FuGene	Promega	E231A
Glucose	Sigma	G8270
GSK1016790A	Sigma Aldrich	G0798
GSK205	Calbiochem	616522
HEPES	Roth	9105.4
Isopropanol	Sigma	67-63-0
KCl	Roth	6781.3
Lipofectamine LTX and Plus reagent	Invitrogen	15338-100
$MgCl_2$	Merk	1.05833
Na Citrate	Sigma	S-4641
NaCl	Roth	3957.3
Oligo(dT) Primer	Invitrogen	18418020
PDMS (syligard 184 silicone elastomer kit)	Dow Corning Corporation	(240)4019862

PFA	Merk	1.04005
PLL (P-L-lysine hydrobromide)	Sigma	P1524
ProLong Gold antifade reagent	ThermoFisher Scientific	P36934
Random hexamers	Invitrogen	N8080127
RNase-Exitus Plus (spray)	AppliChem	A7153
Triton X-100	Sigma	X-100
Trizol	Ambion	10296028
Universal Probe Library Set, mouse	Roche	04913949001
Water RNAse and DNAse free	Sigma	W3513

8.1.2 Reagents for cell culture

Name	**Supplier**	**Catalog number**
Amphotericin B solution	Sigma	A2942
Penicillin-Streptomycin (PIS)	Gibco	15140122
Primocin	InvivoGen	Ant-pm-2
Fetal calf serum (FCS)	PAN biotech, Germany	P40-37500

8.1.3 Commercial kits

Name	**Supplier**	**Catalog number**
TaqMan Universal PCR Master Mix	Roche	4304437
RNAeasy microkit	Qiagen	74004
TURBO DNA-free kit	Ambion	Ant-pm-2

8.1.4 Plasmids

Name	**Fluorescent marker**	
mouseTrpv4	None	Dr. Veit Flockerzi
mousePiezo1	GFP	Dr. Mirko Moroni

miRNA targeting mousePiezo1	GFP	Previously cloned using Block-iT Poll II miR RNAi by Regina Herget
miRNA scrambled	GFP	Previously cloned using Block-iT Poll II miR RNAi by Regina Herget
LifeAct	GFP	Dr. Liudmila Lapatsina

8.1.5 Enzymes for molecular biology

Name	**Supplier**	**Catalog number**
SuperScript III	Invitrogen	18080-044
TURBO-DNA free kit	Ambion	AM1907

8.1.6 Enzymes for dissociation

Name	**Supplier**	**Catalog number**
Collagenase D	Roche	1108888 2001
Trypsin-EDTA (0.05% Trypsin, 0.02% EDTA in PBS without Ca^{2+}, Mg^{2+}.)	PAN-Biotech	P10-023100

8.1.7 RT-qPCR Primers

Name	**Sequence**	**Probe number**
β-actin	AAGGCCAACCGTGAAAAGAT GTGGTACGACCAGAGGCATAC	56
Hprt1	TCCTCCTCAGACCGCTTTT CCTGGTTCATCATCGCTAATC	95
Piezo1	GACGCCTCACGAGGAAAG GTCGTCATCATCGTCATCGT	17
Piezo2	ACGGTCCAGCTTCTCTTCAA CTACTGTTCCGGGTGCTTG	34
Sox9	TATCTTCAAGGCGCTGCAA TCGGTTTTGGGAGTGGTG	101
Collagen II	CGGTCCTACGGTGTCAGG TCTTTATACCTCTGCCCATTCTG	79
Aggrecan	CCAGCCTACACCCCAGTG GAGGGTGGGAAGCCATGT	76

The qPCR primers were synthesized and purified with HPLC by TIB Biolmol GmbH, Germany. RT-qPCR machine (Abi7000 Sequence Detection System, Applied Biosystems) was used with TaqMan probes (from the Universal Probe Library, Roche) to perform the gene expression essays.

8.1.8 Buffers and solutions

Name	Composition
PBS (from Gibco)	14190-094
PFA 4%	PFA 4%, 1 M PBS
Alginate solution	Alginate 1.2% w/v, 25mM HEPES, 118mM NaCl, 5.6 mM KCl, 2.5 mM $MgCl_2$, pH 7.4
Gelation solution (used to make alginate beads)	22mM $CaCl_2$, 10mM HEPES, pH 7.4
Washing alginate bead solution	150 mM NaCl
Extracellular solution for whole-cell patch clamp	140mM NaCl, 4mM KCl, 2mM $CaCl_2$, 1 mM $MgCl_2$, 4mM glucose, 10mM HEPES. pH adjusted with NaOH to 7.4
Intracellular solution for whole-cell patch clamp	110mM KCl, 10mM NaCl, 1mM $MgCl_2$, 1mM EGTA, 10mM HEPES. pH adjusted with KOH to 7.3
Extracellular solution for HSPC	150mM NaCl, 5mM KCl, 2mM $CaCl_2$, 1mM $MgCl_2$, 10mM glucose, 10mM HEPES. pH adjusted with KOH to 7.4
Intracellular solution for HSPC	140mM KCl, 1mM $MgCl_2$, 1mM EGTA, 10mM HEPES. pH adjusted with KOH to 7.3

8.1.9 Antibodies

Primary antibodies

Name	Organism	Dilution	Application	Supplier	Catalog number
Anti-aggrecan	Mouse monoclonal	1:100	Immunofluorescence	Abcam	Ab3778
Anti-collagen II	Rabbit polyclonal	1:200	Immunofluorescence	Abcam	Ab300
Anti-collagen X	Mouse monoclonal	1:2000	Immunofluorescence	Abcam	Ab49945

Anti-SOX9	Rabbit polyclonal	1:500	Immunofluorescence	Abcam	Ab59265

Secondary antibodies

Name	**Organism**	**Dilution**	**Application**	**Supplier**	**Catalog number**
Alexa-fluor 488	Goat anti-rabbit	1:2000	Immunofluorescence	Life Technologies	A-11034
Alexa-fluor 555	Goat anti-rabbit	1:2000	Immunofluorescence	Life Technologies	A-31630
Alexa-fluor 633	Goat anti-mouse	1:2000	Immunofluorescence	Life Technologies	A-21050

8.1.10 Cell culture

Cell lines

Name
Human embryonic kidney cells 293 (HEK-293)
Neuro 2a cells (N2a) from mouse

Primary cells

Name	**Composition**
Articular chondrocytes	Isolated from knees and femoral heads from 4-5 days old pups (C5Bl/l and *Trpv4*$^{-/-}$)

Cell culture media and dissociation buffers

Name	**Composition/supplier**
Chondrocyte Basal Medium	Lonza, USA (CC-3226)
Chondrocyte Differentiation Medium	Lonza, USA (CC-3225)
DMEM/F12 (1:1) 1x	Gibco (21331)
OptiMem	Gibco (11058)
Collagenase D (3 mg/ml)	Collagenase D 3 mg/ml in Chondrocyte Basal Medium, Lonza, USA with 10% FCS

Collagenase D (0.5 mg/ml)	Collagenase D 0.5 mg/ml in Chondrocyte Basal Medium. Lonza, USA with serum
Trypsin-EDTA solution	Trypsin 0.25w/v EDTA 0.02%

8.1.11 Electrophysiology equipment

Name	Company
Plasma cleaner	Diener electronic
MM3A micromanipulator	Kleindiek nanotechnik
Zeiss 200 inverted microscope	Zeiss
40 X objective, LD Achroplan. 40x/0.60 Korr Ph2 ∞/0-2	Zeiss
CoolSnapEZ camera	Visitron Systems GmbH, Germany
EPC-10 amplifier	HEKA, Elektronik GmbH, Germany
High Speed Pressure Clamp	ALA Scientific
DMZ puller	Zeitz Instruments
Thick walled electrodes (1.17 mm x 0.87 mm)	Harvard Apparatus
Micro Forge (MF-830)	Narishige, Japan

8.1.12 Software

Name	Company
VisiView	Visitron Systems GmbH, Germany
ImageJ	National Institute of Health, USA
Igor Pro	WaveMetrics, Inc., USA
Patchmaster	HEKA, Elektronik GmbH, Germany
Fitmaster	HEKA, Elektronik GmbH, Germany
Metafluor	Molecular Devices, USA
Prism5	GraphPad, USA

8.2 Mouse lines

Trpv4$^{-/-}$ mice were generated by introduction of a neomycin cassette in exon 4 of the *Trpv4* gene (Mizuno et al. 2003) and acquired from the Jackson Laboratory. The line was maintained in a C57Bl/6 background and used for isolation of primary chondrocytes from knees and femoral heads.

All experiments involving mice were carried out in accordance with protocols approved by the German Federal authorities (State of Berlin).

Name	**Provider**	**Genotyping**
WT C57Bl/6	Charles River	
Trpv4$^{-/-}$ MGI ID: 2667379 on C57Bl/6 background	Jackson laboratory	Primers targeting neo cassette: F: GCTGCATACGCTTGATCCGGCTAC R: TAAAGCACGAGGAAGCGGTCAGCC Primers targeting Trpv4 exon 4 cassette: F: TGTTCGGGGTGGTTTGGCCAGGATAT R: GGTGAACCAAAGGACACTTGCATAG

8.3 Methods

8.3.1 Molecular biology

Preparation of plasmid DNA

DNA plasmids that contain mouseTrpv4, mousePiezo1 and miRNAs were obtained using large-scale bacterial culture (200 ml maxiprep). Single colonies from transformed bacteria or from glycerol stocks were picked into LB medium containing (ampicillin or kanamycin), grown overnight at 37 °C with shaking. The maxi-preps were carried out according to the manufacture´s protocol. Plasmid DNA was diluted in water and the DNA concentration was measured using the NanoDrop2000 spectrophotometer (Thermo Fisher Scientific, USA).

Genotyping

To confirm the interruption of *Trpv4*, the parents of mouse litters were genotyped using primers targeting exon 4 of the *Trpv4* gene to identify the wild types, or with primers directed against the neomycin cassette for mutant identification.

To further confirm the lack of functional TRPV4 in the *Trpv4*$^{-/-}$ mice, the harvested chondrocytes were loaded with a Ca^{2+} dye to observe their response to the TRPV4 agonist: GSK1016790A and monitored using Ca^{2+} imaging.

RNA extraction and cDNA preparation

RNA extraction from cultured cells

Confluent cells were washed with PBS and 1 ml of Trizol Reagent was added to the 25 cm^2 flask. A cell scraper was used to lyse and homogenize the sample. The mixture was incubated for 5 min and 0.2 ml of chloroform was added; the samples were mixed for 15 sec and incubated for 2-3 min at room temperature. Then, the samples were centrifuged at 12,000 g for 15 min at 4 °C; the resulting colorless upper aqueous solution was transferred to a fresh tube. To precipitate the RNA, 0.5 ml of 100% isopropanol was added to the aqueous solution, mixed and incubated at room temperature for 10 min. The mixture was centrifuged at 12,000 g for 10 min, the resulting pellet was washed with 75% ethanol, air dried and dissolved in 30 µl of RNAse-free water. To eliminate genomic DNA contamination, the samples were washed with the TURBO DNA free kit according to manufacturer's instructions. The RNA concentration was measured with a NanoDrop2000 and RNA saved at -80 °C or used immediately for cDNA preparation.

In order to maintain the same quantities of cDNA across different assays only 2 µg of total RNA were taken. cDNA synthesis was performed using SuperScriptTM III Reverse Transcriptase according to manufacturer's instructions together with random primers and Oligo(dT).

RNA extraction from encapsulated chondrocytes

To prepare RNA, chondrocytes had to be recovered from alginate. Shortly, chondrocyte beads were washed with 150 mM NaCl, transferred to a 1.5 ml Eppendorf tube and bathed with 1.5 ml of Na Citrate solution (55 mM). The mixture was shaken until the alginate beads were dissolved and the chondrocytes were centrifuged (400 g, 10 min). The supernatant was removed and cell lysis buffer from the RNAeasy microkit, (Qiagen, Germany) was added. The RNA extraction was performed following manufacturer's instructions

using the RNAeasy microkit, (Qiagen, Germany). RNA was resuspended in water and RNA concentration measured using a NanoDrop2000. The cDNA was prepared as previously described.

Real Time qPCR

In order to detect relative expression of candidate genes, RNA was reverse transcribed to obtain cDNA and perform real time qPCR (RT-qPCR). The RT-qPCR reactions were performed using probes from the Universal ProbeLibrary Set, (Roche, Germany).

The primers that were designed using the Universal Probe Library on-line tool from Roche were BLASTed to avoid off-target detection and designed to span exon-exon junctions. The primers were purchased from TIB molbiol GmbH (Germany) and HPLC purified.

To prepare the RT-qPCR reactions, cDNA obtained from the retrotranscription was diluted 1:5 in RNAse free-water. A 10 µl reaction was used per pair of primers, the mix contained 5 µl of 2X Universal PCR Master Mix from Roche, 0.1 µl of Probe from mouse Universal ProbeLibrary Roche, 0.4 µl of primers (0.2 µM final) and 1 µl of cDNA or water to achieve 10 µl of final volume.

Samples were loaded into 384 well plates and run on an ABI 7900 Sequence Detection System using a two-step protocol with a denaturation step at 95 °C for 10 min, followed by 40 cycles of 95 °C for 10 sec, 60 °C for 60 sec. Three technical replicates and negative controls without cDNA were performed in every round with at least 3 biological replicates. The relative expression levels were calculated using the 2-ΔCt method with *β-actin* and *Hprt1* as housekeeping genes (Schmittgen & Livak 2008).

8.3.2 Cell biology

Primary mouse chondrocyte culture

In order to prepare primary chondrocytes for cell culture, WT C57Bl/6 from Charles Rivers or *Trpv4*$^{-/-}$ (Jackson Laboratory, MGI ID: 2667379) mice were used. A litter of pups 4-5 days old were sacrificed by decapitation. The knees and femoral heads were extracted and cut into small pieces. The cut tissue was placed in a strainer (100 µm) and rinsed 3 times with sterile PBS in a sterile flow hood. The clean tissue was transferred to a 100 mm dish with 10 ml of collagenase D (3 mg/ml) in Chondrocyte Basal Medium (10% fetal bovine serum (FBS)), incubated for 45 min at 37 °C, 5% CO_2. After the incubation the tissue

was washed with PBS and the enzymatic digestion step was repeated. The partially digested tissue was rinsed with PBS and incubated overnight with collagenase D (0.5 mg/ml with PIS 1%, amphotericin B 0.5 mg/ml and primocin 0.1mg/ml) dissolved in Chondrocyte Basal Medium with 10% serum. The following day, the digested tissue was vigorously agitated and centrifuged at 400 g for 10 min. The tissue was treated with 0.05% trypsin-EDTA at 37 °C, 5% CO2 for 10 min, the reaction stopped with Chondrocyte Basal Medium with FBS and centrifuged again. The recovered chondrocytes were plated at 8 x 10^3 cells/cm^2 or encapsulated in alginate to maintain their differentiated state. Chondrocytes cultured in flask were used only until passage 3 to perform the redifferentiation protocol and kept with Chondrocyte Differentiation Medium, Lonza.

Freezing and thawing primary murine chondrocytes

The freshly harvested chondrocytes were seeded on 25 cm^2 flasks and cultivated until 90% confluence. P1 chondrocytes were washed and incubated with PBS (without divalent cations) for 5 min. Then, 1 ml of 0.05% Trypsin-EDTA was added and cells incubated for 5 min at 37 °C, 5% CO2. Chondrocyte Basal Medium with 10% FBS was added to stop the trypsin enzymatic activity; the cells were centrifuged at 400 g for 10 min. The pellet was resuspended in 500 µl of Chondrocyte Differentiation Medium, 400 µl of FBS and 100 µl of DMSO. The solution was gently pipetted and transferred to a cryovial, which was located in a freezing container (Mr. FrostyTM) and kept at -80 °C.

To thaw the chondrocytes, the cryovial was warmed in a 37 °C bath for one minute and immediately transferred to a tube with 9 ml of pre-warmed Chondrocyte Growth Medium. The solution was centrifuged at 400 g for 10 min and the supernatant was removed. The chondrocytes were resuspended in 5 ml of Chondrocyte Growth Medium and seeded in a 25 cm^2 flask.

Chondrocyte redifferentiation by encapsulation

Chondrocytes are very sensitive to their mechanical environment and tend to dedifferentiate when cultured in monolayer turning into fibroblast-like cells and changing their protein expression. In order to redifferentiate the dedifferentiated cells into chondrocytes, an encapsulation protocol was used. Cells were encapsulated after harvesting chondrocytes from cartilage or after cell expansion.

Confluent chondrocytes grown in monolayer for no longer than 3 passages were used for the encapsulation protocol. The chondrocytes were washed and incubated for 5 min in sterile PBS without divalent cations. Then, 1 ml of trypsin was added to the 25 cm^2 flask and incubated for 5 min at 37 °C, 5% CO_2. The

enzymatic reaction was stopped by adding chondrocyte medium with serum and centrifuged at 400 g for 10 min. The cells were counted and centrifuged again. The supernatant was removed, and alginate (1.2 %) was added to reach a cell density of 8 x 10^5 cell/ml. The solution with chondrocytes was transferred into a syringe with a 22-gauge needle. The syringe needle was held near a beaker with a constant mixing gelation solution. The alginate mix was added to the gelation solution drop wise. The high salt concentration in the gelation solution facilitates crosslinking of the alginate to promote gelation which occurs as soon as the alginate comes in contact with the solution. The alginate beads were agitated in the gelation solution for 15 min, washed with a NaCl solution (150 mM) and transferred to 12 well plates containing Chondrocyte Basal Medium, (Lonza, USA). The chondrocytes were kept for at least 4 days in alginate with Chondrocyte Differentiation Medium, (Lonza, USA) (which contains FBS and R3-IGF-1, insulin, TGFβ-1, transferrin, gentamicin and amphotericin B) before they were used for experiments.

Recovery of chondrocytes from alginate beads

To recover chondrocytes from the alginate beads, the beads were washed with 150 mM NaCl solution. Then, 5-10 beads were transferred to a 1.5 ml Eppendorf tube and bathed with 1.5 ml of Na citrate solution (55 mM). The mixture was shaken in a Thermomixer compact (Eppendorf) at 800 rpm, at 37 °C for 30 min. Chondrocytes were then centrifuged at 400 g for 10 min at 4 °C and the supernatant removed. Recovered chondrocytes were used for RNA extraction, for immunostainings or for patch-clamp recordings. For RNA extraction, the cell pellet was resuspended in cell lysis buffer from the RNAeasy microkit (Qiagen, Germany) and extraction continued according to the manufacturer´s instructions. For immunostainings, chondrocytes were resuspended in Chondrocyte Basal Medium and seeded onto Poly-Lysine (PLL) glass coverslips. Due to the low number of recovered chondrocytes for patch-clamp recordings, we used cloning cylinders on top of the pillar arrays to restrict the seeding surface for the cells.

Transfection of primary chondrocytes

Fresh or thawed chondrocytes not older than passage 2 were used for transfection. The dedifferentiated cells had higher transfection efficiency, therefore all the transfections were performed on the fibroblast-like cells. 24 hours after the transfection, the dedifferentiated cells were encapsulated to redifferentiate them into chondrocytes and later seeded onto pillar arrays to assess their mechanosensitivity.

To transfect plasmid DNA, dedifferentiated chondrocytes not older than passage 2 were plated in 12 well dishes and allowed to attach for at least 6 hr. Chondrocytes were washed with PBS and medium changed to Chondrocyte Basal Medium (without serum and growth factors). In a 1.5 ml Eppendorf tube, 2.5 µg of

plasmid DNA was mixed with 150 µl of OptiMem and 2.5 µl of PlusReagent. In a different tube, 150 µl of OptiMem was mixed with 7.5 µl of LTX Lipofectamine. The contents of the 2 tubes were mixed, incubated for 5 min at room temperature and added to wells for transfection.

Twenty-four hours after transfection, cells were encapsulated to redifferentiate them into chondrocytes. Cells were kept in alginate for a minimum period of 4 days for redifferentiation into chondrocytes.

The miRNA sequence targeting *Piezo1* was previously cloned using the Block-iT Poll II miR RNAi system (Invitrogen) and validated with a control scrambled miRNA that does not target any known vertebrate gene (Poole et al. 2014).

Target	Top strand	Bottom strand
Piezo1	5´- TGCTGTAAAGATGTCCTTCAGGTCCAGTTTTGG CCACTGACTGACTGGACCTGGGACATCTTTA-3'	5'- CCTGTAAAGATGTCCCAGGTCCAGTCAGTCAGT GGCCAAAACTGGACCTGAAGGACATCTTTAC-3'

Cell line culture

HEK-293 cells were used as a heterologous system to overexpress mechanosensitive ion channels. HEK-293 cells were grown and maintained at 37 °C in a humidified incubator supplied with 5% CO_2 on 25 cm^2 dishes. HEK-293 cells were cultured in DMEM medium containing 10% FBS and 1% penicillin, streptomycin. The growth medium was removed from 80% confluent flasks, and cultures washed and incubated for 5 min with PBS at room temperature. The PBS was removed, and the cells were incubated with 1 ml Trypsin-EDTA for 3 min. Growth medium containing 10% serum was added to stop trypsin enzymatic activity. The cells were spun down at 1,500 rpm. Cells were usually seeded in a 1 to 5 dilution to maintain cultures.

HEK-293 cells were tested regularly to confirm the absence of mycoplasma, using a luminescence kit from Epo GmbH (Germany), as per manufacturer's instructions. The identity of the cultured cells was authenticated by Eurofins Medigenomix Forensik, GmbH (Germany), with PCR-single-locus-technology using 21 independent PCR reactions.

Transfection of HEK-293 cells

Cells were plated onto PLL glass coverslips or PLL covered pillar arrays in medium without serum and let them attach for at least 4 hours. For the transfection, 1 µg of DNA was mixed with 3 µl of FuGeneHD and 300 µl of OptiMem. After 15 min of incubation at room temperature, the mixture was added to each well. Cells were incubated at 37 °C in 5% CO_2 overnight. Efficiently transfected cells could be detected by a fluorescent marker signal at least 24 hr after transfection.

8.3.3 Poly-L-Lysine coating

Poly-L Lysine (PLL) coverslips and PLL pillar arrays were used to seed primary chondrocytes and HEK-293 cells. Round coverslips (15 mm diameter) and pillar arrays were coated with PLL. Clean coverslips and plasma-cleaned pillar arrays were bathed with (10 µg/ml) PLL for one hour inside a laminar flow hood, rinsed with sterile water, and the coverslips allowed to air-dry. After drying, the PLL- coverslips were UV illuminated overnight.

8.3.4 Immunostaining of cultured cells

Freshly isolated chondrocytes were plated onto PLL glass coverslips, allowed to settle and attach for at least 1 hour. The cells were washed with PBS and fixed with 4% PFA for 15 min at room temperature. Subsequently, cells were washed 3 times with PBS and when stained for intracellular components, permeabilized with 0.25% Triton-X 100 for 10 min. Chondrocytes were washed 3 times with PBS and blocked with a solution composed of PBS and 3% serum for 1 hr at room temperature. A solution of PBS-3% serum with the appropriate concentration of primary antibody was added to the cells and incubated for 1 hr at room temperature. Coverslips were washed 3 times for 10 min with a solution of PBS and 3% serum. Secondary antibody solution (1:2000) was added to the cells and incubated for 1 hr at room temperature. Coverslips were rinsed 3 times with PBS and mounted onto slides using ProLong Gold glue. After drying, the cells were visualized with a Zeiss microscope (Axio Observer z.1).

The same protocol was used for freshly isolated chondrocytes, chondrocytes recovered from alginate and for dedifferentiated cells at different time points after seeding.

8.3.5 Morphological analysis of chondrocytes and dedifferentiated cells

Chondrocytes are round cells in contrast to dedifferentiated cells that display a fibroblast-like morphology. Therefore, a morphologic analysis was performed on chondrocytes and dedifferentiated cells that were stained with SOX9. After cells were redifferentiated in alginate, chondrocytes were recovered, seeded on glass coverslips, fixed and stained with anti-SOX9 antibody. Samples were imaged using epifluorescent and bright-field imaging. The morphology of the cells was analyzed using ImageJ software to calculate the degree of circularity from bright-field images, where 1 defines a perfect circle. The degree of circularity was plotted against the normalized SOX9 signal, which was derived from epifluorescent imaging. SOX9 intensity was normalized to the highest value measured on each sample

8.3.6 Electrophysiology

Patch clamp

Whole-cell patch clamp recordings were made at room temperature, HEK-293 cells and chondrocytes were prepared as described above. Patch pipettes were pulled from thick walled electrodes (Harvard apparatus 1.17 mm x 0.87 mm, external and internal diameter respectively) using a DMZ puller (Germany) and polished to a final resistance of 3 to 5 MΩ with a microforge (MF-830, Narishige, Japan). Currents were acquired at 10 kHz and filtered at 3 kHz using an EPC-10 amplifier with Patchmaster software (HEKA, Elektronik GmbH, Germany) in combination with a Zeiss 200 inverted microscope and were analyzed using FitMaster software (HEKA, Elektronik GmbH). The bath solution contained (in mM) 140 NaCl, 4 KCl, 2 $CaCl_2$, 1 $MgCl_2$, 4 glucose and 10 HEPES, adjusted to pH 7.4 with NaOH. The internal solution contained (in mM) 110 KCl, 10 NaCl, 1 $MgCl_2$, 1 EGTA and 10 HEPES, adjusted to pH 7.3 with KOH. The membrane potential was held at −40 mV in chondrocyte measurements (Sánchez and Wilkins, 2003; Sánchez et al., 2006) and at −60 mV for HEK-293 cell measurements.

GSK205 (Calbiochem, Billerica, MA, 616522) was used at a concentration of 10 µM and cells were treated for 3 min. ACA (Calbiochem, 104550) was used at a concentration of 20 µM and applied directly via the patch pipette. We allowed solution exchange for at least 3 min before collecting data.

Pillar arrays

Preparation of pillar arrays

Pillar arrays were prepared as described previously (Poole et al. 2014). Shortly, a silanized negative master was coated with degassed PDMS mixed at 10:1 ratio (silicone elastomeric base, curing agent). After 30 min,

the PDMS was covered with a glass coverslip (thickness 2) and placed at 110 °C for 1 hr. After curing, the pillar array was gently peeled from the negative master. Before use, the pillar arrays were activated by plasma cleaning (Deiner Electronic GmbH, Germany) and coated with PLL.

The arrays were cast under curing conditions that result in an elasticity of the PDMS equal to 2.1 MPa and the dimensions of the elements within the array were: radius = 1.79 µm; length = 5.87 µm (Poole et al., 2014). The spring constant of each individual pilus was therefore 251 pN/nm.

Assessing mechanoelectrical transduction with pillar arrays

The pillar arrays were used to study the mechanoelectrical transduction events that are sensitive to substrate deflections. Therefore, chondrocytes were recovered from alginate before the experiment took place and seeded onto pillar arrays. The cells were allowed to attach attached for a minimum of 1 hr before pillar array experiments. This time frame was chosen because the chondrocytes easily dedifferentiate into fibroblast-like cells. HEK-293 cells were seeded onto pillar arrays one day before experiments.

To generate quantitative data on mechanoelectrical transduction an individual pilus underlying a cell was deflected using a polished glass probe (approx. 2 µm in diameter) driven by a MM3A micromanipulator (Kleindiek Nanotechnik, Germany). The electrical response of the cells was monitored using whole-cell patch-clamp recording.

To quantify the magnitude of the stimulus, a bright-field image was taken before pillar deflection, during the applied stimulus and after the release of the stimulus. Bright-field images were taken using a 40x objective and a CoolSnapEZ camera (Photometrics, Tucson, AZ). To calculate the pillar deflection, bright-field images were used to determine the center point of the relevant pilus using a 2D Gaussian fit of the intensity values in the images (Igor, Wavemetrics, TIgard, OR); the resulting distance calculated from consecutive images represents the stimulus magnitude. The estimated error of the calculated stimulus size was 7 nm, as previously described (Poole et al., 2014).

Assessing mechanoelectrical transduction with High Speed Pressure Clamp

To study ion channels sensitive to membrane stretch, High-Speed Pressure Clamp (HSPC) was used to stimulate membrane patches, by pulling outside-out patches from chondrocytes and HEK-293 cells. Currents were elicited by applying protocols of positive pressure to the membrane patch via the patch pipette using a HSPC (ALA Scientific, Farmingdale, NY). Within 30 s of pulling the patch, a protocol of pressure

steps was applied (duration 600 ms, application 0.1 Hz). The pressure protocol ranging from 10 mmHg to 150 mmHg, in 20 mmHg steps was applied to cells while holding the patch at −60 mV. The sensitivity of stretch-activated channels for each patch was estimated by fitting individual pressure response curves to the Boltzmann equation. Extracellular solution had the following composition (in mM): 150 NaCl, 5 KCl, 10 HEPES, 10 glucose, 1 $MgCl_2$, 2 $CaCl_2$. The intracellular solution contained (in mM): 140 KCl, 10 HEPES, 1 EGTA, 1 $MgCl_2$. Thick walled electrodes were pulled with a DMZ puller and polished to a final resistance of 6 to 8 MΩ. The sensitivity of stretch-activated channels for each patch was estimated by fitting individual pressure response curves to the Boltzmann equation.

Cell-attached recordings were performed using extracellular solution in the pipette and at a holding voltage of −60 mV. Negative pressure steps were applied with the same frequency amplitude as described for outside-out patches.

Assessing mechanoelectrical transduction with cellular indentation

Cellular indentation studies were performed as described previously (Hu and Lewin, 2006). Briefly, cells were indented using a fire-polished glass probe, with a diameter of approximately 2 µm. The probe was moved toward the cell until a small compression of the surface was observed. Indentation stimuli (between 0.5–11 µm) were then applied by driving the glass probe into the cell using the MM3A micromanipulator. Cellular responses were simultaneously monitored using whole-cell patch-clamp.

8.3.7 Calcium imaging

Chondrocytes were plated on PLL-coated glass coverslips and loaded with Cal-520 (5 µM) for 1 hr (AAT-Bioquest, Sunnyvale, CA). Cells were placed in 200 µl of solution in a chamber that allows laminar flow and a fast solution exchange. Calcium images were acquired and analyzed using Metafluor (Molecular Devices, Sunnyvale, CA). A DG4 (Sutter Instruments, Novato, CA) was used as a light source and fluorescent images were acquired every 5 sec. The basal fluorescence was acquired for 10 cycles and used to normalize the fluorescence of the whole experiment. Fluorescence values were calculated and plotted according to the formula $\Delta F/F = (F-F_0)/(F_0)$ where F_0 is baseline fluorescence for Cal-520 and F is the fluorescence intensity at a determined time point. Yoda1 (10 µM) (Syeda et al. 2015)was applied for 90 sec, followed by a washout period of 5 min, whereas GSK1016790A (50 nM) was applied for 15 sec.

8.3.8 Second Harmonic Generation imaging of murine cartilage

Second Harmonic Generation (SHG) is a second order coherent process in which two lower energy photons are converted to twice the incidence frequency (half the wavelength) of an excitation laser (Campagnola 2011)

In order to compare ECM structure, femoral heads from 4-5 days old pups were taken. This age was chosen because at this point of development the skeleton is not yet calcified, instead it consists of cartilage. Therefore, the cartilage volume is much larger compared to an adult, in which the cartilage would be a very thin layer covering the femur. In addition, the femoral heads have a homogeneous morphology that ease the handling and preparation of the samples.

The femoral heads were taken from WT and *Trpv4*$^{-/-}$ pups (Figure 6), washed with PBS, immediately immersed in glycerol (80%) and frozen. The samples were used within two weeks from the extraction. On the day of the experiment, the samples were thawed on iced and washed with PBS to remove the excess of glyceraldehyde. The samples were mounted using low-melting-point agarose (LMP agarose). The femoral heads were located with the ligament facing upwards as shown in Figure 6, trying to reproduce the same orientation on every sample.

The tiles were stitched with the plugin "Grid/Collection stitching" from ImageJ/Fiji (Preibisch et al. 2009). The stitched images were background corrected using the option in ImageJ/Fiji (Figure 6). A "radial profile" from ImageJ/Fiji was used to analyze transversal images from the femoral heads.

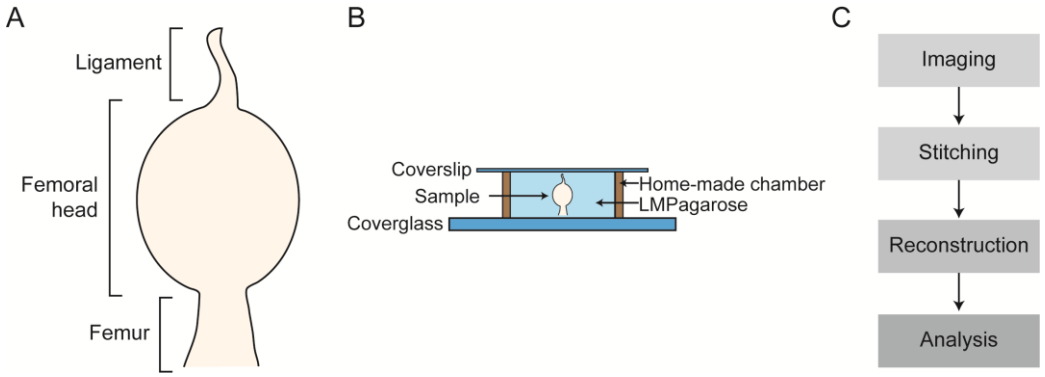

Figure 6. Scheme of sample preparation and workflow for imaging analysis.
A) Scheme of the femoral head morphology after extraction from 4-5 days old pups. **B**) Scheme of sample preparation. The femoral head was thawed, washed and embedded in a home-made chamber with low-melting-point agarose (LMP agarose); a coverslip was added on the top to avoid sample drying. After mounting, the femoral heads were immediately imaged. **C**) Analysis workflow. After acquiring images, the pictures were stitched, reconstructed and analyzed.

The femoral heads were imaged from the ligament to the base of the tissue using a multiphoton microscope (Trimscope, LaVision Biotech, GmbH). A diagram of the setup is shown in the Figure 7. The 860 nm output of a Ti:Sapphire laser (Chamaleon Ultra II, Coherent) was used to pump an optical parameter oscillator (OPO) and to obtain the excitation wavelength at 1100 nm. The SHG signal was detected in a backward configuration using a band pass filter 560/40 nm. Images were acquired using a water immersion objective lens (Olympus 20x). The field of view was set at 400 □m x 400 □m. z-stacks were acquired every 2 □m for a depth of 500 □m. A total of 3 x 3 fields (tiles) were collected to cover the whole surface of the femoral head.

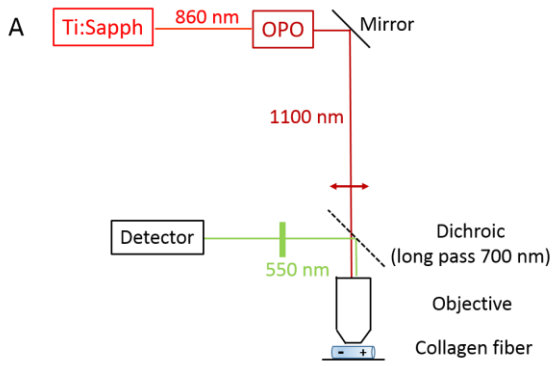

Figure 7. SHG system to image cartilage.
A) Schematic of the multiphoton microscope used to aquire the SHG images of the femoral heads (4-5 days old pups).

8.3.9 Statistical analysis

All data sets were tested for normality: parametric data sets were compared using a two-tailed, Student's t-test, paired or unpaired depending on the experimental setup, nonparametric data sets were compared using a Mann-Whitney test. In order to compare the overall response of samples to deflection stimuli, we conducted two-way ANOVA. Data are displayed as mean ± s.e.m. unless otherwise stated.

The stimulus-response data collected from experiments performed in the pillar arrays have variation in x (deflection) and y (current amplitude). Therefore, the responses were grouped in bins of different sizes for comparisons. The size of the bins is as follows: 0–10, 10–50, 100–250, 250–500 and 500–1000 nm. For each cell, the current amplitudes within the bins were averaged, and these data averaged across cells.

Categorical data were compared using Fisher's exact test. One-way ANOVA and Tukey post-hoc tests were used to compare RT-qPCR data sets.

9 Results

9.1 Establishment of a cellular model to study mechanoelectrical transduction in chondrocytes

Articular chondrocytes have been studied in 2D and 3D cultures. Chondrocytes dedifferentiate to fibroblast-like cells when cultured as a monolayer; however, 3D cultures promote redifferentiation of dedifferentiated cells into chondrocytes, and when differentiated chondrocytes are cultured in 3D matrices cells do not dedifferentiate. The dedifferentiation process includes changes in morphology, gene expression and protein synthesis (Stokes et al. 2001; Thirion & Berenbaum n.d.; Gosset et al. 2008). In particular, chondrocyte morphology changes from a round to an elongated and spread-out cell shape, similar to fibroblasts. In addition, changes in gene expression result in an alteration of the typical chondrocyte protein expression (Layman et al. 1972; Caron et al. 2012; Minegishi et al. 2013; Ma et al. 2013; Lefebvre et al. 2001). These three aspects were analyzed to characterize chondrocytes and dedifferentiated cells in primary cultures. Subsequently, a redifferentiation protocol (Brand et al. 2012) was tested to transform dedifferentiated cells back into chondrocytes, and the same molecular and cellular characterizations were performed to determine the functionality of the protocol.

9.1.1 Morphological characterization of chondrocytes and dedifferentiated cells

In order to discriminate between chondrocytes and dedifferentiated cells in monolayer cultures, a correlation between the cellular morphology and the transcription factor SRY-box 9 (SOX9) signal was investigated. SOX9 is a very important transcription factor which is highly expressed during chondrogenesis, and its expression decreases during and after dedifferentiation (Dy et al. 2012; Caron et al. 2012; Ma et al. 2013).

To investigate cellular morphology, the degree of circularity was analyzed in chondrocytes and dedifferentiated cells. To achieve this, the samples were imaged using epifluorescent and bright field microscopy. From the bright-field images, a degree of circularity was measured in the cells, where 1 defines a perfect circle. In order to assess the expression of the transcription factor SOX9, freshly harvested chondrocytes were seeded in monolayer and stained with an anti-SOX9 antibody. The samples were imaged using epifluorescence and bright field imaging, and the intensity from the epifluorescent images were normalized to the highest values measured on each sample.

Circularity was plotted against the intensity of SOX9 immunofluorescence (Figure 8A). Round cells (chondrocytes) displayed circularity values closer to 1 and higher SOX9 intensity in comparison to dedifferentiated cells, which also showed a lower degree of circularity (Figure 8A). Therefore, chondrocytes with circular morphology exhibit a higher intensity of the transcription factor SOX9 and dedifferentiated cells display lower intensity of SOX9 and a fibroblast-like morphology.

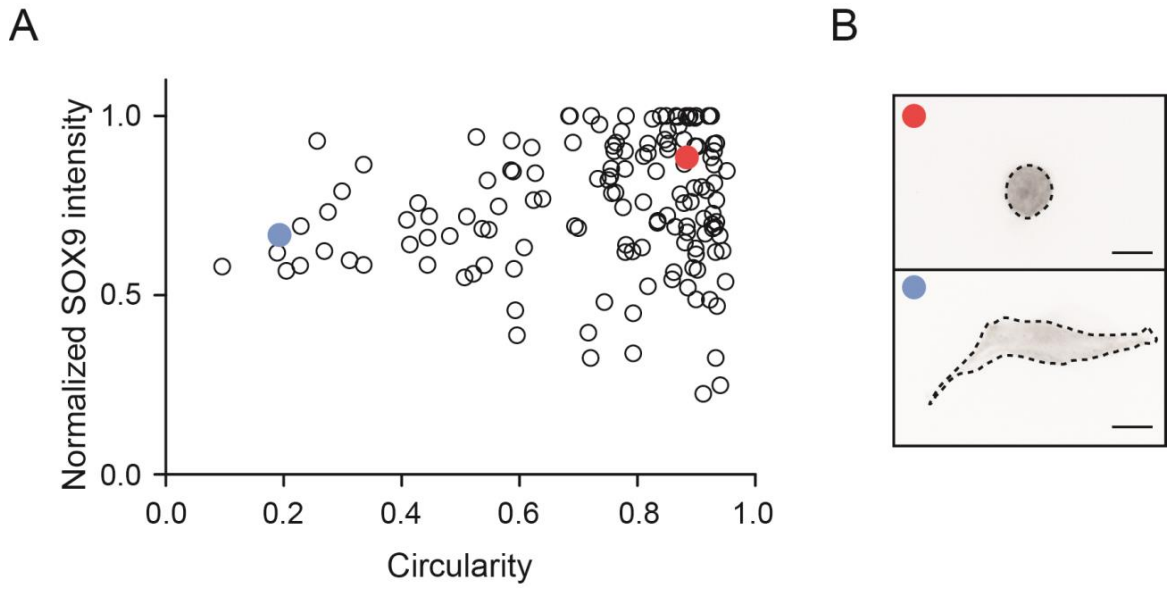

Figure 8. Chondrocytes and dedifferentiated cells exhibit distinct morphologies.
A) Chondrocytes with circular morphology exhibit a higher SOX9 intensity. After redifferentiation in alginate, chondrocytes were recovered from the 3D culture, seeded on glass coverslips, fixed and labeled with anti-SOX9 antibody. Samples were imaged using epifluorescece and bright-field microscopy. The circularity of the cells was measured (from bright-field images), here 1 defines a perfect circle. The circularity was plotted against the SOX9 signal, which was derived from epifluorescece imaging where intensity was normalized to the highest values measured for each sample. Data are displayed as individual values of intensity and circularity. n=144 cells. **B**) Example images of round and fibroblast-like cells. Cells corresponding to the red and blue marked points within the graph are displayed in an inverted fluorescence image (based on anti-SOX9 intensity). On the basis of morphology and SOX9 signal, the round cells are classified chondrocytes (red point) and the fibroblast-like cells are classified as dedifferentiated cells (blue point). Scale bar 10 µm.

As shown in (Figure 8B), primary and dedifferentiated cells displayed different shapes. Chondrocytes showed a round morphology with average diameter of 11.7 ± 2.0 µm (mean ± s.d., n=77 cells). In contrast, the dedifferentiated cells lack a round shape therefore no diameter could be measured (Figure 8B).

These results indicate that round cells possess a higher SOX9 expression, which agrees with known chondrocyte characteristics. Therefore, based on morphology and SOX9 signal, the round cells are referred to as chondrocytes and the fibroblast-like cells as dedifferentiated cells.

9.1.2 Gene expression in chondrocytes and dedifferentiated cells

In addition to morphological changes occurring during dedifferentiation, an alteration in the expression of chondrocyte gene markers occurs. Important genes such as *Sox9*, *aggrecan*, *collagen II* and *collagen X* are highly expressed in chondrocytes, however, after dedifferentiation the transcript levels of these genes decrease (Oldershaw et al. 2010). To study these changes in gene expression, RNA was extracted from freshly isolated chondrocytes and from cells cultured in monolayer (up to three passages). RNA was reverse-transcribed to produce cDNA, and subsequently used to analyze the expression of specific candidates.

The expression of *Sox9*, *aggrecan* and *collagen X* significantly decreased after the cells were cultured as a monolayer for just one passage, this tendency prevailed for further passages (Figure 9) (Two-way ANOVA with Bonferroni post-hoc test). However, the expression of *collagen II* remained stable during the monolayer culture in comparison with freshly isolated chondrocytes (Figure 9). Additionally, cells were only kept until P3 because cells lose their ability to redifferentiate when passaged further (Ma et al. 2013).

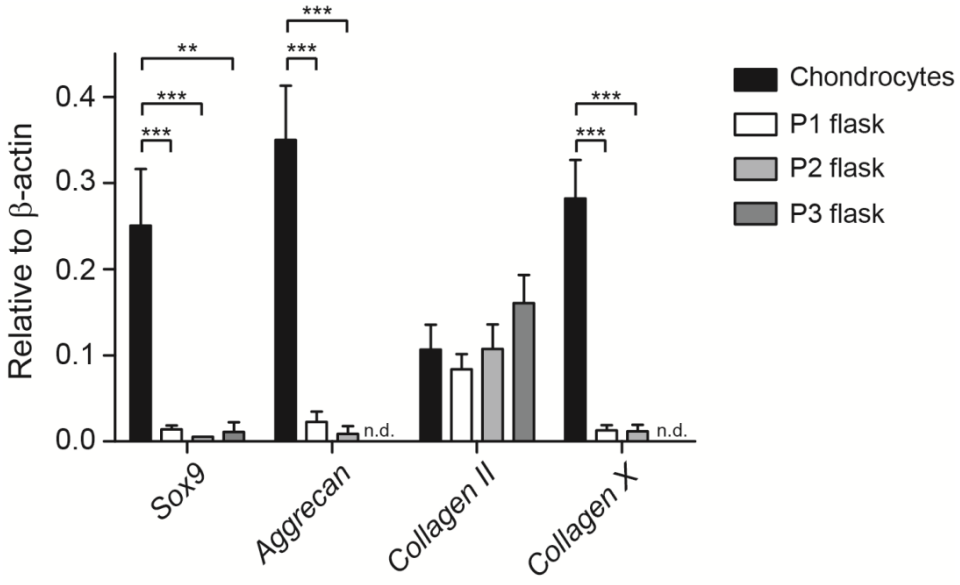

Figure 9. Dedifferentited chondrocytes show decreased expression of chondrocyte marker genes after monolayer culture.
Levels of the transcription factor *Sox9* and the extracellular matrix proteins *aggrecan*, *collagen II* and *collagen X* are displayed for freshly harvested chondrocytes and dedifferentiated cells that were kept in monolayer for up to three passages. Data were normalized taking as a reference the housekeeping gene *β-actin* and displayed as mean, s.e.m. Two-way ANOVA with Bonferroni post-hoc test. $^{**}P<0.01$; $^{***}P<0.001$; n≥3 preparations (one preparation corresponds to the tissue recovered from 1 litter of mice which can range from 4-9 pups). Transcripts that were not detected are labeled as n.d.

This transcript level characterization corroborated previous work which showed that chondrocyte dedifferentiation is accompanied by an alteration in gene regulation (Caron et al. 2012; Minegishi et al. 2013; Ma et al. 2013). These results demonstrate the dramatic decrease in chondrocyte marker expression after monolayer culture. In particular, *Sox9* an important transcription factor regulating the chondrogenesis (Lefebvre et al. 2001; Dy et al. 2012) of the cells was changed, suggesting that when *Sox9* expression decreases other important chondrocytes markers are no longer maintained.

9.1.3 Protein characterization of chondrocytes and dedifferentiated cells

To further characterize the differences between chondrocytes and dedifferentiated cells at the protein level, immunostainings with antibodies against SOX9 and collagen X were performed in freshly isolated chondrocytes and dedifferentiated cells. Figure 10 shows the immunofluorescence signal for the transcription factor SOX9 in chondrocytes and dedifferentiated cells. In the case of the chondrocytes SOX9 is located inside the cell. The immunofluorescence signal decreased in dedifferentiated cells (Figure 10, lower panel). In addition, the ECM protein, collagen X is localized at the border of the chondrocytes and its expression also decreased after dedifferentiation (see lower panel of Figure 10). There is a reduced expression of chondrocyte markers in dedifferentiated cells compared to primary chondrocytes.

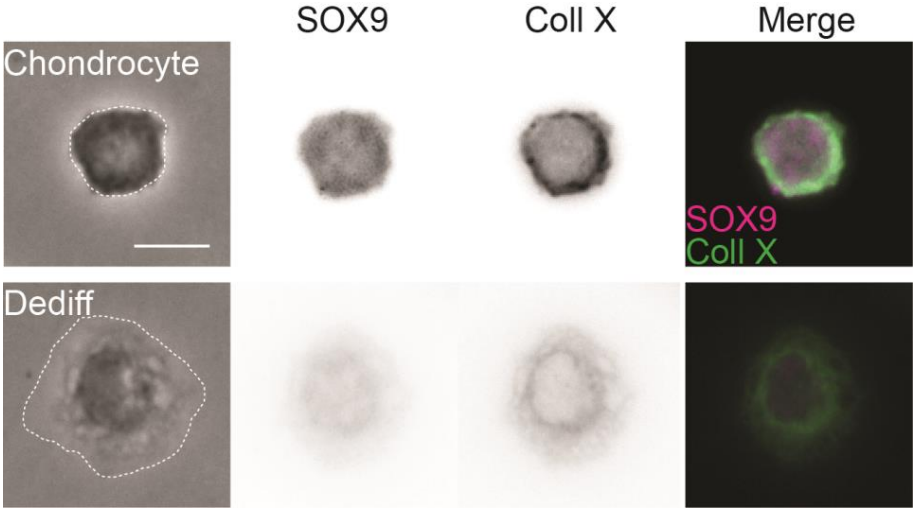

Figure 10. Dedifferentiated chondrocytes show decreased protein expression of chondrocyte markers after monolayer culture.
Phase-contrast (left), epifluorescent inverted (middle images) and merged images (right) of chondrocytes and dedifferentiated cells are shown. SOX9 and collagen X were detected in chondrocytes and detected signal decreased in dedifferentiated cells. SOX9 is represented in magenta and collagen X in green in the merged image. Scale bar 10 µm.

Additionally, it is important to note that the dedifferentiated cells display a flattened and spread-out morphology. Therefore, dedifferentiated cells, besides displayed a different morphology compared to the chondrocytes, also exhibit a different gene expression profile that is reflected by lower expression of classical chondrocytes markers such as SOX9.

9.1.4 Cellular redifferentiation by alginate encapsulation

It is known that dedifferentiated cells can be redifferentiated back into chondrocytes through several available protocols. The most common is to perform a 3D cell culture in a gel matrix, using alginate or agarose (Brand et al. 2012; Guo et al. 1989; Caron et al. 2012). In order to redifferentiate fibroblast-like cells into chondrocytes, cells were encapsulated in alginate and maintained with the growth factors TGF-*β,* insulin and transferrin. Alginate is a polysaccharide originated from brown algae that when mixed with water, forms a jelly-like structure. The alginate forms a 3D porous environment hence nutrients can flow inside the matrix and cultured cells have a suitable environment for cellular maintenance.

In order to assess redifferentiation efficacy, chondrocytes cultured as monolayers from different passages were kept in 3D cultures for 7 or 14 days, then cells were released from alginate, and RNA collected. To evaluate the differentiation status of the cells, an assessment of transcript levels was performed. Figure 11A shows transcript levels of *Sox9* in freshly harvested chondrocytes, in dedifferentiated cells from passage 1 (P1) to passage 3 (P3) and redifferentiated cells from P1 to P3 that remained in alginate for 7 days. *Sox9* transcripts significantly decreased after monolayer culture in comparison to freshly isolated chondrocytes (one-way ANOVA with Tukey's multiple comparison test). In addition, dedifferentiated cells from P1, P2 and P3 that were kept in alginate encapsulation for 7 days to redifferentiate them into chondrocytes, showed a recovery of *Sox9* transcript levels compared to freshly harvested chondrocytes.

Cells that were kept in alginate for 7 days (meaning, redifferentiated chondrocytes) showed positive staining for SOX9 and collagen X similar to freshly harvested chondrocytes (Figure 11B**,** lower panel), indicating a positive redifferentiation towards the chondrocyte phenotype. As it was previously shown, dedifferentiated cells showed low signal intensities for SOX9 and collagen X, and had a spread-out and flattened morphology (Figure 11B**,** middle panel).

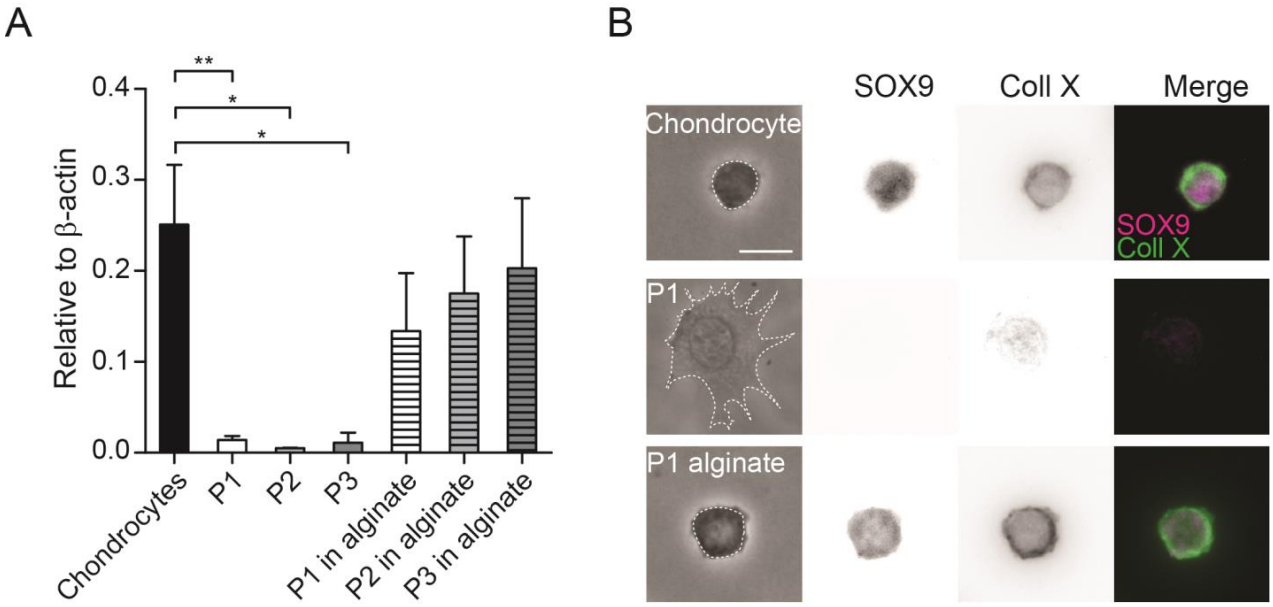

Figure 11. Redifferentiated chondrocytes recapitulate the characteristics of the freshly harvested chondrocytes.
A) Relative expression of *Sox9* transcript relative to *β-actin*, the expression of *Sox9* was compared in the freshly harvested chondrocytes, to the levels of dedifferentiated cells (cultured in monolayer P1 to P3, significant differences) and the redifferentiated cells (alginate for 7 days from P1 to P3, no significant differences). One-way ANOVA with Tukey's multiple comparison test **P*<0.05; ***P*<0.01; n≥3 preparations. B) Protein detection in chondrocytes dedifferentiated cells and redifferentiated chondrocytes. Phase-contrast (left), epifluorescence inverted (center) and merged images (right) are shown. SOX9 and collagen X were detected in chondrocytes and redifferentiated chondrocytes, the signal decreased in dedifferentiated cells. SOX9 is represented in magenta and collagen X in green in the merged image. Scale bar 10 µm.

To summarize, primary chondrocytes display a round morphology with a diameter of 11.7 ± 2.0 µm (mean ± s.d.), and a high expression of SOX9 and collagen X. In contrast, dedifferentiated cells present a flattened morphology similar to fibroblasts and SOX9 expression was significantly lower compared to primary chondrocytes. However, the dedifferentited cells can be redifferentiated back to chondrocytes so that redifferentiated cells recapitulate the morphology, transcript and protein expression of primary chondrocytes.

Achievement of redifferentiation is important to study physiologically relevant cells. In the following sections of this thesis, the morphological parameters described here were used to discriminate chondrocytes from dedifferentiated cells. An additional hypothesis, that these cells display differential functional characteristics, was tested using electrophysiology.

9.2 Assessing mechanoelectrical transduction in chondrocytes

Chondrocytes respond to mechanical stimulation by activating a gene expression program to synthesize ECM proteins such as collagens and proteoglycans (Quinn et al. 1998; Grodzinsky et al. 2000; Fitzgerald et al. 2004; Guilak et al. 1994; Buschmann et al. 1995). However, the mechanisms that are activated after mechanical stimulation are not completely understood and the sensors of the mechanical forces are not known. Therefore, to study the role of mechanosensitive ion channels in chondrocyte mechanotransduction, two different types of mechanical stimulation techniques were used. On one hand, cells were studied using High-Speed Pressure Clamp (HSPC) to analyze responses to membrane stretch using outside-out membrane patches. The second method used cells seeded onto elastomeric pillar arrays to stimulate the cell substrate interface by pilus deflection, while simultaneously measuring currents using whole-cell patch clamp.

The HSPC in outside-out mode allows the study of channels exclusively sensitive to membrane stretch. For instance, HSPC has been used to study Piezo1 and the bacterial channels MscL and MscS (Lewis & Grandl 2015; Cox et al. 2016; Coste et al. 2010; Gnanasambandam et al. 2015; Nomura et al. 2012). On the other hand, using pillar arrays to deflect the substrate allows the stimulation of proteins within the cellular environment, avoiding the disruption of the cytoskeleton and maintaining contacts with ECM proteins as well as proteins involved in attachment to the substrate. Pillar arrays were previously used to study mechanosensitive responses in DRG neurons, as well as to study Piezo1 and Piezo2 in a heterologous expression system (Poole et al. 2014).

In the following sections I will introduce work performed to study the mechanoelectrical response of chondrocytes and dedifferentiated cells in response to different mechanical stimuli. Section 9.2.1 contains results obtained when cells were stimulated at the cell-substrate interface with substrate deflections. Subsequently, section 9.2.2 contains the results regarding the response to membrane stretch using HSPC.

9.2.1 Using pillar arrays as force transducers

Pillar arrays are elastic microcolumns that are used as a cell substrate. The arrays were made out of PDMS with curing conditions that result in an elasticity of 2.1 MPa, which is similar to the elasticity of cartilage (McGloughlin 2011). The elements within the array have defined dimensions (radius: 1.79 µm; length: 5.87 µm) and a spring constant of 251 pN/nm (Poole et al. 2014). They behave as a spring following the Hooke´s law. Substrate deflection by moving a single pilus allows the activation of mechanosensitive ion channels.

In order to study the contribution of ion channels in chondrocyte mechanotransduction, encapsulated cells were released from alginate and seeded onto PLL-coated pillar arrays. Substrate deflections from a single pilus were performed while recording the current activity in whole-cell patch clamp configuration (Figure 12A). In order to deflect a single pilus, a sealed glass probe driven by a piezo-electric element was used. The glass probe was used to apply a series of fine deflection stimuli to cells directly at the cell-substrate interface (Figure 12). An image was taken before, during and after deflection (Figure 12B), and the magnitude of each stimulus was subsequently calculated from the difference between the coordinates of the center of the pilus in successive images (Figure 12B, right). Each individual pilus acts as a light guide, therefore the center can be calculated from a 2D Gaussian fit of light intensity values from a bright-field image (du Roure et al. 2005). Post-processing, the deflection distance was correlated with the current amplitude to obtain current amplitude-stimulus graphs.

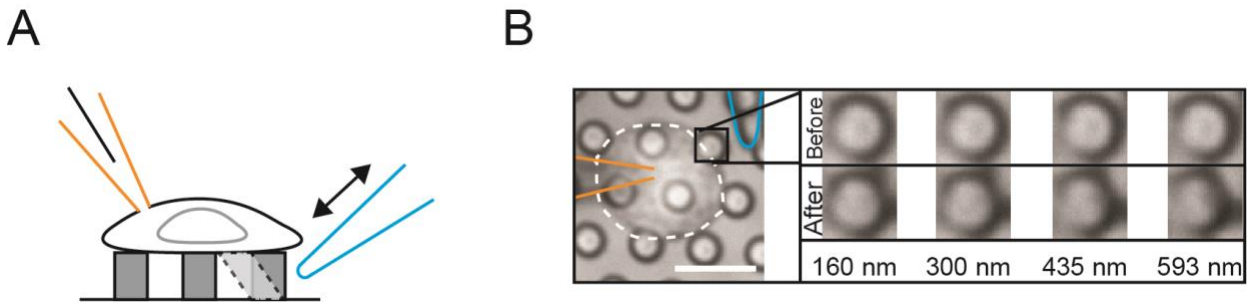

Figure 12. Using pillar arrays as force transducers to study chondrocyte mechanoelectrical transduction.
A) Schematic of a cell seeded on top of a pillar array during an electrophysiology experiment. The orange pipette represents the patch-clamp electrode and the blue pipette represents the mechanical stimulator connected to the piezo-electric element, which is used to move a single pilus to perform substrate deflections. B) Micrograph of a chondrocyte over the pillar array (scale bar 10 µm), and micrographs of consecutive pictures taken before and after deflection. Note that the magnitude of the deflection is represented below the zoomed-in micrographs.

After seeding the chondrocytes, the cells attached within 1 hr and exhibited a spherical morphology characteristic of chondrocytes (as was previously characterized in the first section of results Figure 8), however within 3 hr the morphology of a subset of cells started to change towards a more elongated shape like that observed in fibroblasts or dedifferentiated cells (Figure 13A-B). Cells were stimulated with pillar deflections nominally covering a range of 1 to1000 nm. Healthy cells were stimulated at two different pili in the same deflection range. The application of stimuli to chondrocytes triggered deflection-gated inward currents in 88.9% of these cells (24/27) and in 88.2% (15/17) of dedifferentiated cells (Figure 13C), indicating that both cell types display mechanically activated currents.

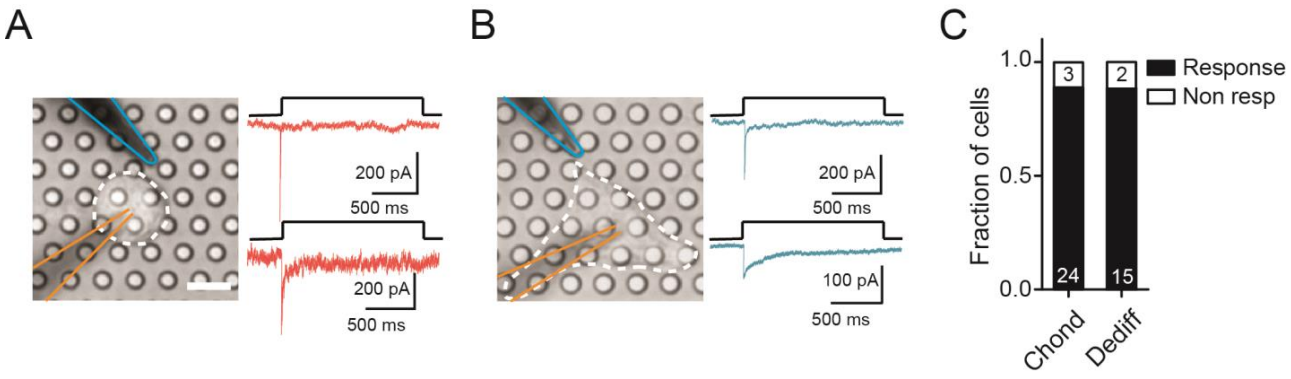

Figure 13. Chondrocytes and dedifferentiated cells respond to substrate deflections.
A) Representative image of a chondrocyte seeded over a pillar array and example traces are displayed in red. B) Bright-field image of a dedifferentiated cell seeded over an array and examples traces of the currents triggered by pillar deflections (blue traces). C) Fraction of cells that responded to pillar deflections, 88.9% of chondrocytes (24/27) and 88.2% of dedifferentiated cells (15/17) display mechanically gated currents in response to substrate deflections. Scale bar indicates 10 μm.

Cells that responded with a change in membrane current to at least one stimulus between 1 to 1000 nm were used to generate deflection-response graphs (Figure 14A). The current amplitude was measured, and data was binned by stimulus size and averaged across cells for each bin.

In chondrocytes and dedifferentiated cells larger current amplitudes were observed with increasing deflection steps (Figure 14A). The overall response of chondrocytes and dedifferentiated cells was compared using the deflection-response graph, the responses of dedifferentiated cells were larger, and significantly different (Figure 14A) (two-way ANOVA P=0.03; 24 chondrocytes vs. 15 dedifferentiated cells). Additionally, when comparing the bins of chondrocytes and dedifferentiated cells in every corresponding pair, significant differences were found in the range from 10 to 50 nm and from 250 to 500 nm, where dedifferentiated cells possessed larger currents compared to those in chondrocytes (Figure 14A) (Mann-Whitney test, for the range 10 nm to 50 nm P=0.02 and for 100 nm to 250 nm P=0.004).

Additionally, when the percentage of response per pilus deflection was quantified (percentage of triggered currents/the total number of stimuli), chondrocytes responded 22.2% ± 10% (mean ± s.d., 24 cells) and dedifferentiated cells 56.0% ± 19 %, (mean ± s.d., 15 cells) of the stimulations (unpaired t test with Welch's correction P <0.0001) (Figure 14B). When the average threshold of activation (smallest deflection that induced mechanically-gated currents in a cell) was measured, chondrocytes needed significantly larger deflections (252 ± 68 nm, 24 cells) compared to dedifferentiated cells (59 ± 13 nm, 15 cells) (Mann-Whitney test P=0.028), (Figure 14C). These results strongly suggest that dedifferentiated cells are more sensitive to pillar deflections than chondrocytes.

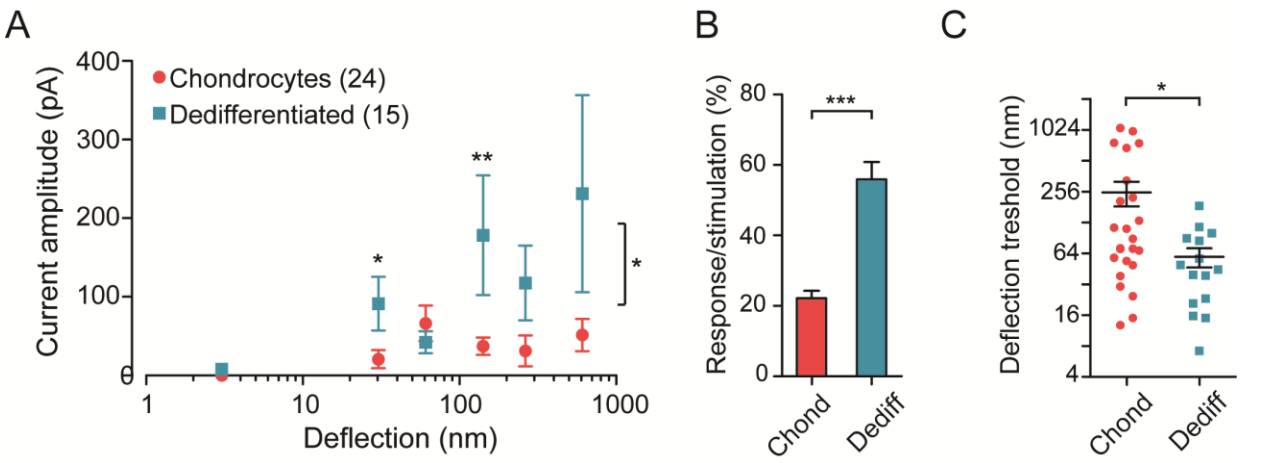

Figure 14. Chondrocytes and dedifferentiated cells display deflection-sensitive currents with different sensitivity. A) Current amplitude-deflection graph that represents the response of chondrocytes (red) and dedifferentiated cells (blue) to pillar deflections. The response of chondrocytes was significantly different from dedifferentiated cells (two-way ANOVA **P*=0.03; 24 chondrocytes vs. 15 dedifferentiated cells). Stimuli in the range of 10-50 nm and 250-500 nm produced significantly larger currents in the differentiated cells compared to chondrocytes (Mann-Whitney test, 10 nm to 50 nm **P*=0.02 and for 100 nm to 250 nm ***P*=0.004). B) Comparison of the percentage of response per total number of stimulations, chondrocytes respond 22.2 % on average ± 10 % (s.d.) from the total range of stimulations, in comparison to dedifferentiatiated cells which are more responsive (56 % on average (± 19 %, s.d.)), (unpaired t test with Welch's correction ****P*<0.0001). C) Deflection threshold needed to activate the deflection-gated currents in chondrocytes and dedifferentiated cells. Chondrocytes need on average 252 ± 68 nm (mean ± s.e.m., 24 cells) and dedifferentiated cells 59 ± 13 nm (15 cells) (Mann-Whitney test, **P*<0.05).

Furthermore, the current kinetics were measured in chondrocytes and dedifferentiated cells. The mean latency for a mechanosensitive current in chondrocytes was 3.6 ± 0.3 ms, and for dedifferentiated cells was 3.1 ± 0.3 ms (Figure 15B). Note that the short latency (shorter than 5 ms) suggests a channel directly gated by mechanical stimuli according to the criteria proposed by Christensen & Corey 2007. The mean activation time (τ_1) for chondrocytes was 1.7 ± 0.3 ms and for dedifferentiated cells was 1.4 ± 0.3 ms (Figure 15B). The mean inactivation time (τ_2) for chondrocytes was 46.7 ± 8.3 ms and for dedifferentiated cells was 125.3 ± 24.5 ms, in this case no significant differences were found however, the variance of the currents was significantly different in the τ_2 values (F test, *P*<0.0001) (n=99 currents measured across 24 chondrocytes and n=109 currents measured across 15 dedifferentiated cells) (Figure 15). Interestingly, τ_1 and τ_2 presented skewed distributions and the median of τ_1 for chondrocytes was 0.7 ms and for dedifferentiated cells was 0.5 ms. The τ_2 median for chondrocytes was 16.7 ms and for dedifferentited cells was 30.8 ms.

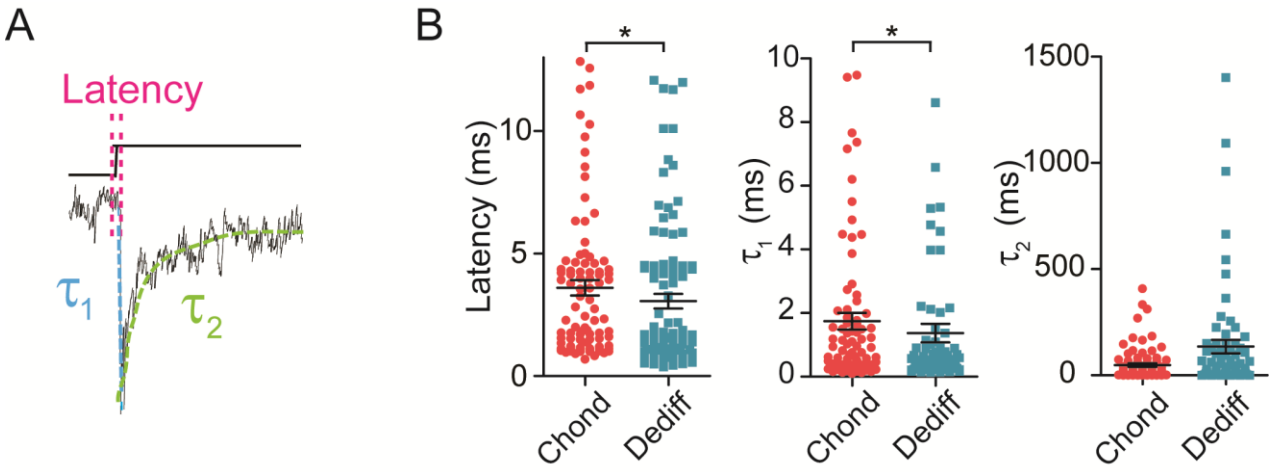

Figure 15. Current kinetics of chondrocytes and dedifferentiated cells.
A) Scheme of kinetics parameters (left), latency: time between the stimulus and the beginning of a current, τ_1: activation time and τ_2: inactivation time. B) Kinetics of mechanically gated currents from chondrocytes and dedifferentiated cells. Latency for chondrocytes: 3.6 ± 0.3 ms and for dedifferentiated cells: 3.1± 0.3 ms (Mann-Whitney test, **P*=0.018); chondrocyte τ_1 = 1.7 ± 0.3 ms and for dedifferentiated cells τ_1 = 1.4 ± 0.3 ms (Mann-Whitney test, **P*= 0.04); chondrocyte τ_2 = 46.7 ± 8.3 ms and for dedifferentiated cells τ_2 = 125.3 ± 24.5 ms (n=99 currents measured across 24 chondrocytes and 109 currents measured across 15 dedifferentiated cells).

In summary, these results characterize the activity of mechanosensitive ion channels in chondrocytes and dedifferentiated cells. Current activity was measured in whole-cell patch clamp configuration and triggered by substrate deflection using pillar arrays. So far, electrophysiological evidence for mechanosensitive currents in chondrocytes and dedifferentiated cells has proven extremely difficult to obtain (Lee, et al. 2014); thus, this is the first experimental evidence confirming the presence of mechanically activated currents in chondrocytes. In addition, the short activation latencies suggest that mechanosensitive channels expressed in chondrocytes may have a direct activation mechanism. Interestingly, chondrocytes and dedifferentiated cells appeared to be functionally different, for instance the dedifferentiated cells displayed mechanoelectrical activity triggered by substrate deflection with a smaller activation threshold and with larger current amplitudes. Therefore, dedifferentiated cells appear to be more sensitive to substrate deflections than chondrocytes.

9.2.2 Using High-Speed Pressure Clamp to stretch the plasma membrane

Many cell types extracted from primary tissue such as renal tubular epithelial cells (Peyronnet et al. 2013) exhibit stretch-activated ion channel activity when negative pressure is applied to membrane patches. To investigate the stretch sensitive response in primary chondrocytes, outside-out patches were pulled from chondrocytes and dedifferentiated cells, and stimulated with increasing steps of pressure (10 to 150 mmHg).

After generating a stimulus-response curve for the membrane stretch of chondrocytes and dedifferentiated cells, curves were fit to a Boltzmann equation and the P_{50} (amount of pressure that gives half-maximal response) was calculated. The P_{50} for chondrocytes (87.1 ± 6.0 mmHg) and dedifferentiated cells (78.7 ± 7.4 mmHg) did not present any significant differences Figure 16. Figure 16B shows example traces obtained after membrane stretch in membrane patches pulled from chondrocytes and dedifferentiated cells. It is important to note that the stretch-sensitive currents from chondrocytes and dedifferentiated cells do not appear to have a different sensitivity as was observed for deflection-sensitive currents.

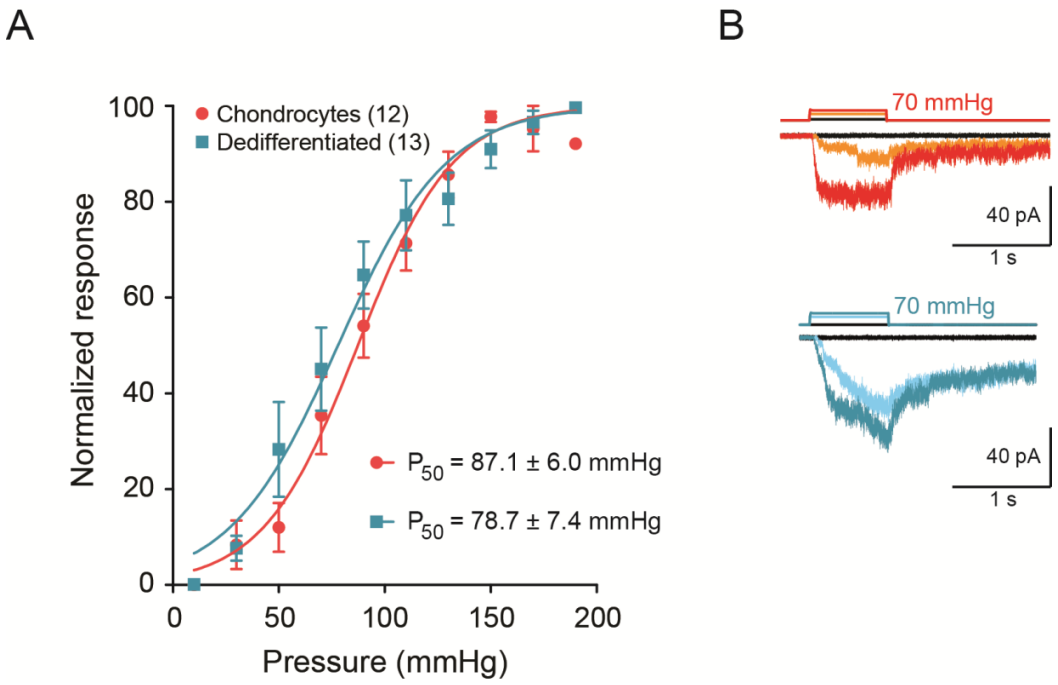

Figure 16. Chondrocytes and dedifferentiated cells display stretch-sensitive currents.
A) Stretch-response curve of chondrocytes and dedifferentiated cells stimulated by membrane stretch in out-side out patches. P_{50} values were obtained with a Boltzmann equation fitting from chondrocytes and dedifferentiated cell data. The P_{50} for chondrocytes was 87.1 ± 6.0 mmHg and for dedifferentiated cells 78.7 ± 7.4 mmHg. 12 chondrocytes (red) and 13 dedifferentiated cells (blue). B) Example traces of stretch sensitive currents from chondrocytes and dedifferentiated cells. Stretch activation experiments were performed with help of Dr. Mirko Moroni.

These data suggest that the stretch-sensitive mechanoelectrical transduction in membrane patches is a separable phenomenon from deflection-gated currents observed when stimuli are applied at cell-substrate contact points. Due to the significant differences in mechanoelectrical transduction in response to deflection stimuli in chondrocytes versus dedifferentiated cells all further experiments were conducted on cells exhibiting a chondrocyte phenotype.

9.3 Identifying mechanosensitive ion channels in chondrocytes

9.3.1 Molecules involved in chondrocyte mechanoelectrical transduction

To identify molecules that are participating in chondrocyte mechanoelectrical transduction, we assayed for the expression of particular candidates. Based on the literature, we looked for ion channels that have been proposed to be mechanosensitive (such as TRPV4 and TRPM7) and that have been proven to be mechanosensitive (Piezo1 and Piezo2).

RNA was extracted from isolated chondrocytes, reverse-transcribed to cDNA and RT-qPCR was used to determine if *Piezo1*, *Piezo2*, *Trpv4* and *Trpm7* transcripts are expressed in murine chondrocytes. *Trpv4* and *Piezo1* transcripts are expressed in murine chondrocytes, however *Piezo2* and *Trpm7* transcript signal was very low and was not detected in all the samples (Figure 17). These results suggest that TRPV4 and Piezo1 may be involved in the mechanosensitive response of chondrocytes.

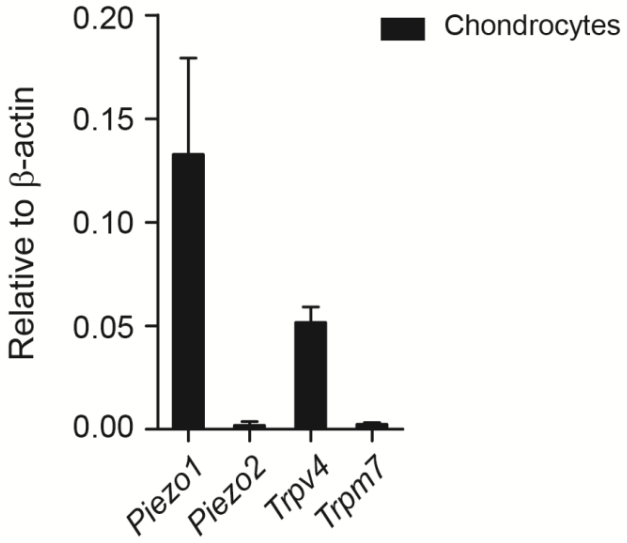

Figure 17. Murine chondrocytes express mechanosensitive ion channels.
Transcript levels of *Trpv4* were detected in chondrocytes as well as *Piezo1*. *Piezo2* and *Trpm7* were not reliably detected in samples. Data were normalized taking as a reference the housekeeping gene *β-actin*. n≥3 preparations (a single preparation corresponds to the tissue recovered from 1 litter of mice which can range from 4-9 pups).

9.3.2 Confirming the functional activation of TRPV4 and Piezo1 in mouse articular chondrocytes

In order to confirm the functional expression and activation of the ion channels TRPV4 and Piezo1, WT chondrocytes were loaded with a Ca^{2+} sensitive dye and challenged with agonists that activate either TRPV4 or Piezo1.

Cultured chondrocytes were released from alginate beads, seeded onto PLL coverglass and loaded with Cal520 dye to assess Ca^{2+} influx. First, chondrocytes were challenged with ATP (10 µM) which stimulates purinergic receptors expressed in viable cells, subsequently cells were stimulated with Yoda1 (10 µM) to activate Piezo1, and finally cells were challenged with GSK1016790A (50 nM) to activate TRPV4 (Figure 18). All cells that responded to ATP also responded to Yoda1 and GSK1016790A (400 cells, from two separate chondrocyte preparations).

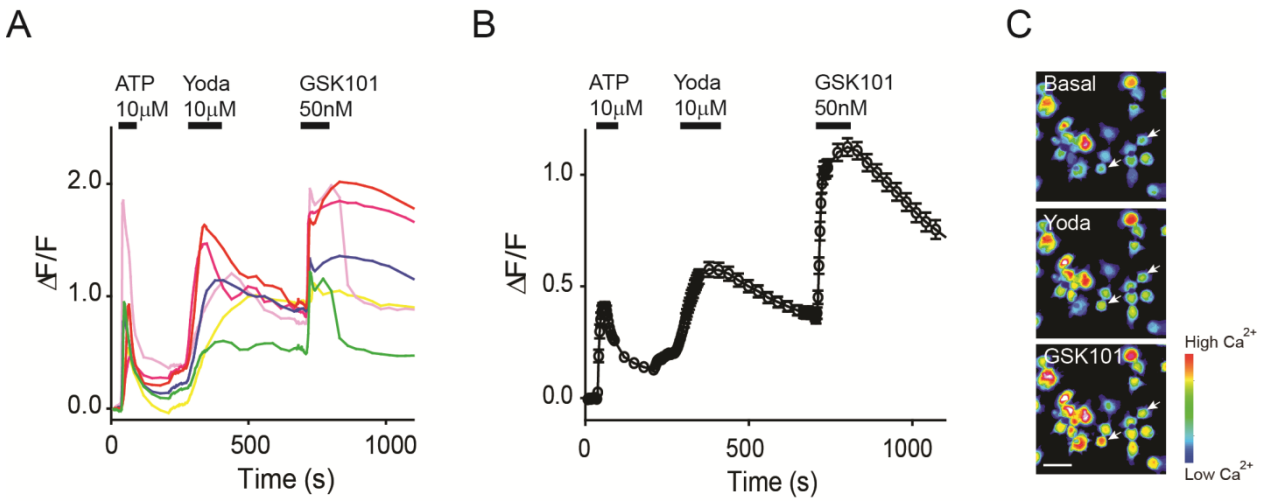

Figure 18. Chondrocytes express functional TRPV4 and Piezo1.
A) Fluorescence intensity of chondrocytes loaded with Cal520, a Ca^{2+} sensitive dye. Cells were challenged with ATP (10 µM), then washed, then stimulated with Yoda1 (10 µM) to activate Piezo1 and subsequently with GSK1016790A (50 nM) to activate TRPV4. Data was normalized according to the formula $\Delta F/F = (F-F_0)/F_0$, where F_0 is the basal fluorescence. Every color represents a single chondrocyte. B) Average intensity of all the imaged chondrocytes (400 cells, from two separate chondrocyte preparations). C) Representative images of chondrocytes before the stimulation (top image), after the Yoda1 (middle image) and GSK1016790A stimulation (bottom image). The white arrowheads point to responsive chondrocytes. The pseudocolor scale is represented on the low-right side of the image. Scale bar 20 µm. Experiments done in collaboration with Dr. Mirko Moroni.

These results suggest that all chondrocytes that respond to ATP are able to respond to Yoda1 and GSK1016790A, which specifically activate Piezo1 and TRPV4 respectively. This is a corroboration of

the TRPV4 functional expression in murine chondrocytes and the first description of the functional expression of Piezo1 in these cells.

9.3.3 Assessing mechanoelectrical transduction in chondrocytes lacking the TRPV4 ion channel

In order to test the individual role of the mechanosensitive ion channels expressed in chondrocytes, the role of Piezo1 and TRPV4 was studied separately. To study the role of TRPV4 in chondrocyte mechanotransduction, a *Trpv4*$^{-/-}$ mouse was used to extract articular chondrocytes from knees and femoral heads. Subsequently, to assess the mechanosensitive response, *Trpv4*$^{-/-}$ chondrocytes were stimulated with substrate deflections and with membrane stretch.

9.3.3.1 Assessment of the mechanoelectrical response of chondrocytes lacking TRPV4 using substrate deflections

To study the role of TRPV4 in chondrocyte mechanotransduction, chondrocytes were extracted from knees and femoral heads from *Trpv4*$^{-/-}$ mice. Chondrocytes were released from alginate and seeded on elastomeric pillar arrays. A range of deflections (1 to 1000 nm) was applied to stimulate the cells. Only 46.2% (6/13) of *Trpv4*$^{-/-}$ chondrocytes responded at least once to pillar deflections, this is a significantly smaller response in comparison to wild type (WT) chondrocytes (88.9%, 24/27 cells, Fisher's exact test, P=0.03) (Figure 19A). In addition, the average current amplitude displayed by the *Trpv4*$^{-/-}$ chondrocytes was significantly smaller compared to WT chondrocytes (two-way ANOVA, P=0.04) (Figure 19B). Furthermore, when the current amplitude of the cells was averaged either with the zero responses or without the zero responses, the mean current amplitude in the *Trpv4*$^{-/-}$ chondrocytes was reduced. This suggests that TRPV4 is partially contributing to the mechanosensitive response evoked by substrate deflection. It is important to note that *Trpv4*$^{-/-}$ chondrocyte currents were observed in response to the full range of deflections (Figure 19B).

Additionally, the kinetic parameters of the remaining currents found in *Trpv4*$^{-/-}$ chondrocytes were calculated and compared to the WT kinetics. However due to the decreased response of the *Trpv4*$^{-/-}$ chondrocytes, fewer currents were obtained. For instance, the average latency of the *Trpv4*$^{-/-}$ currents (7.8 ± 1.6 ms) was significantly longer compared to WT currents (3.6 ± 0.3 ms) (Figure 19C) (Mann-Whitney test, P=0.015, *Trpv4*$^{-/-}$ currents: 12 and WT currents: 99). Therefore, when TRPV4 is not expressed in

chondrocytes, the latency of activation was increased, which supports the idea that TRPV4 can be directly gated by mechanical stimuli.

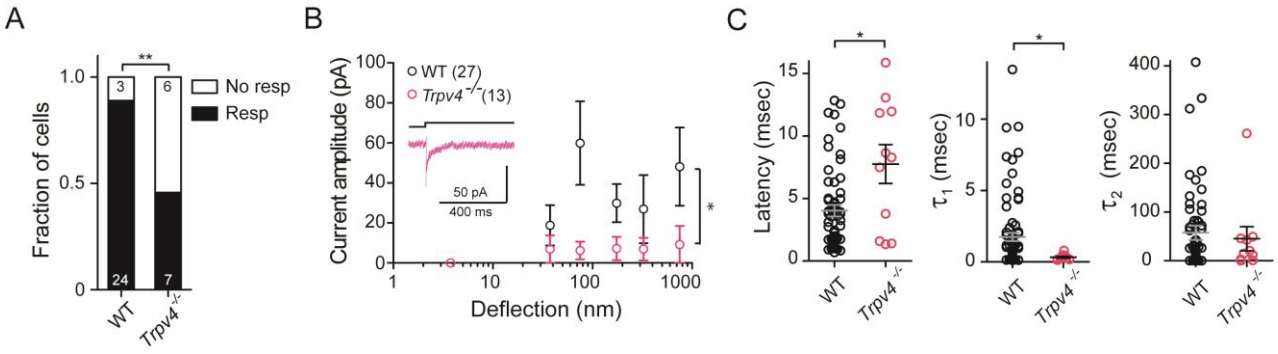

Figure 19. Chondrocytes lacking TRPV4 show an impaired response to substrate deflections.
A) *Trpv4*$^{-/-}$ chondrocytes respond less to substrate deflections. Only 46.2% (6/13) of *Trpv4*$^{-/-}$ chondrocytes respond to deflections, which is significantly less in comparison to WT chondrocytes (88.9%, 24/27 cells) (Fisher's exact test, ***P*=0.03). The fraction of responsive cells is shown in black and the non-responsive cells in white. B) Current amplitude-deflection graph that represents the response to substrate deflections from WT (black) and *Trpv4*$^{-/-}$ chondrocytes (pink) (27 and 13 cells respectively). The average current amplitude displayed by *Trpv4*$^{-/-}$ chondrocytes is smaller in comparison to WT chondrocytes (two-way ANOVA, **P*=0.04). The inset has an example current trace of a *Trpv4*$^{-/-}$ chondrocyte stimulated with substrate deflection. C) Kinetic comparison of WT and *Trpv4*$^{-/-}$ chondrocytes. The latency of the *Trpv4*$^{-/-}$ currents (7.8 ± 1.6 ms) was significantly smaller in comparison to WT currents (3.6 ± 0.3 ms) (n=12 and 99 currents, respectively, Mann-Whitney test, **P*=0.015). The τ_1 for *Trpv4*$^{-/-}$ chondrocytes was 0.3 ± 0.06 ms and for WT was 1.7 ± 0.3 ms (Mann-Whitney test, **P*=0.012). The τ_2 for *Trpv4*$^{-/-}$ chondrocytes was 45.1 ± 24.7 ms and for WT cells 47.7 ± 8.6 ms.

When the activation time constant was measured, *Trpv4*$^{-/-}$ chondrocytes displayed a faster τ_1 (0.3 ± 0.06 ms) compared to WT chondrocytes (1.7 ± 0.3 ms) (Figure 19C) (Mann-Whitney test, *P*=0.012, n=12 and 99 currents from *Trpv4*$^{-/-}$ and WT respectively). For τ_2, there was not a significant difference in the τ_2 between *Trpv4*$^{-/-}$ chondrocytes (45.1 ± 24.7 ms) and WT chondrocytes (47.7 ± 8.6 ms) (Figure 19C).

These results indicate that TRPV4 is important because 53.8% (7/13) of *Trpv4*$^{-/-}$ chondrocytes are not able to respond to pillar deflections, which was significantly different than WT chondrocytes. However, there was a subset of *Trpv4*$^{-/-}$ cells that responded to substrate deflections (46.2%, 6/13) but smaller current amplitudes were observed in these cells. These results suggest that there are other channels compensating for the loss of mechanosensitive function in the cell, and that TRPV4 is important for the mechanical response but not indispensable for currents activated by substrate deflections.

9.3.3.2 The deflection-sensitive current is inhibited by a TRPV4 antagonist

In order to test the *in-situ* role of TRPV4 in WT isolated chondrocytes, a TRPV4 specific antagonist named GSK205 was used. WT chondrocytes were released from the alginate matrix and seeded onto pillar arrays, after which substrate deflections were applied. After obtaining a current control response from WT chondrocytes activated by substrate deflections, GSK205 was applied in the extracellular solution of the WT chondrocytes for 3 min, then deflections were repeated, and the antagonist was washed for 5 min with extracellular solution (Figure 20B). The acute application of GSK205 (10 µM) inhibited the mechanosensitive current triggered by pillar deflections by 87% ± 6 compared to control. In addition, GSK205 can be washed out and the mechanosensitive current can be recovered to 97% ± 28 of pretreatment values (Figure 20A) (one-way ANOVA, matched measures with Dunnett's post-hoc test for multiple comparisons. *P*=0.01 treated vs. pre-treated).

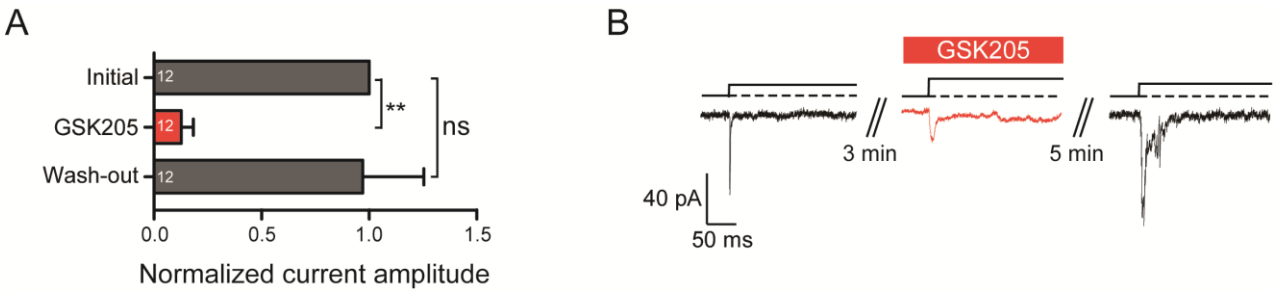

Figure 20. A TRPV4-specific antagonist (GSK205) inhibits the deflection-sensitive currents in WT chondrocytes. A) Quantification of the current amplitude normalized with the pre-treated control. The application of GSK205 reduces 87% ± 6 of the response in comparison with the pre-treatment condition, after 5 min of washing out the current is recovered 97% ± 28 in comparison to the pre-treatment (one-way ANOVA, matched measurements with Dunnett's post-hoc test, ns = not significant, ***P*= 0.01, 12 chondrocytes). B) Example traces of deflection-sensitive currents triggered by substrate deflections before, during and after the washout of GSK205 (10 µM).

The experiments performed using *Trpv4*$^{-/-}$ chondrocytes suggest that other channels are compensating the TRPV4 mechanosensitive function. However, the results obtained using GSK205 indicate that TRPV4 is directly mediating 87% of the deflection-activated currents in WT chondrocytes. The pharmacological experiments are quite remarkable compared to the *Trpv4*$^{-/-}$ experiment. One explanation may be that following genetic ablation of the channel, changes in gene regulation may affect the expression of other channels, like Piezo1.

9.3.3.3 Mechanoelectrical response of chondrocytes lacking TRPV4 assessed with membrane stretch

There is controversial evidence concerning the stretch sensitivity of TRPV4. Indeed Loukin and colleagues observed that when TRPV4 channels were expressed in Xenopus oocytes there was a small current activated by membrane stretch (Loukin et al. 2010). However, no stretch activated current were observed by other studies after the channel was overexpressed in HEK-293 cells (Strotmann et al. 2000). Therefore, more research is needed to elucidate the mechanical response of TRPV4. To further study the role of TRPV4 to membrane stretch in chondrocytes, outside-out patches were pulled from WT and *Trpv4*$^{-/-}$ chondrocytes, and membrane patches were stimulated with increasing pressure steps (10 to 150 mmHg). Interestingly, there was no difference in the pressure-response curve in patches from WT and *Trpv4*$^{-/-}$ chondrocytes (Figure 21A). In addition, the maximal current amplitude was not significantly different, and the current kinetics were very similar in both conditions (Figure 21B-C). The P_{50} for WT chondrocytes was 87.1 ± 6.0 mmHg and for *Trpv4*$^{-/-}$ chondrocytes was 88.2 ± 9.3 mmHg (Figure 21A). These data indicate that TRPV4 is not involved in the stretch-sensitive response of chondrocytes.

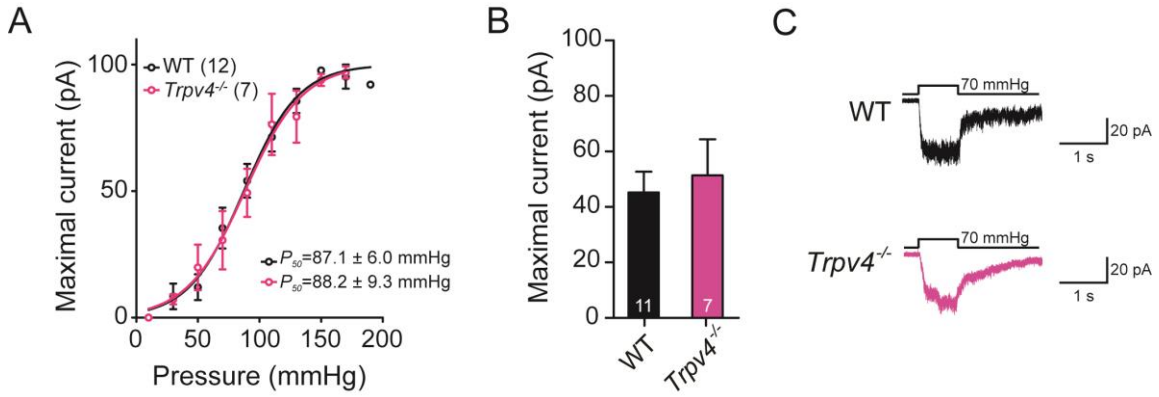

Figure 21. TRPV4 is not involved in the stretch-sensitive response of chondrocytes.
A) Current amplitude graph of WT and *Trpv4*$^{-/-}$ chondrocytes in response to membrane stretch, the P_{50} for chondrocytes (black) is 87.1 ± 6.0 mmHg and for *Trpv4*$^{-/-}$ (magenta) 88.2 ± 9.3 mmHg. B) Comparison of the maximal current amplitude displayed by WT and *Trpv4*$^{-/-}$ chondrocytes. C) Example traces of WT and *Trpv4*$^{-/-}$ chondrocyte currents elicited by membrane stretch. Stretch activation experiments performed with the help of Dr. Mirko Moroni.

9.3.4 Assessing mechanoelectrical transduction in chondrocytes with reduced expression of Piezo1 (knockdown experiments)

It is known that the Piezo1 ion channel is a *bona fide* mechanosensitive channel that responds to cellular indentation (Coste et al. 2010; Coste et al. 2012), membrane stretch (Coste et al. 2010; Coste et al. 2012),

substrate deflections (Poole et al. 2014), ultrasound (Loynaz Prieto 2016), and lipid bilayer perturbations (Syeda et al. 2016). In order to study whether Piezo1 is involved in chondrocyte mechanotransduction, a previously validated siRNA directed against *Piezo1* was used to decrease the channel expression (Poole et al. 2014). Subsequently, the mechanical responses were assessed with membrane stretch and substrate deflection.

9.3.4.1 Mechanoelectrical response of chondrocytes with reduced expression of Piezo1 assessed with substrate deflections

To study the role of Piezo1 in the mechanoelectrical response of chondrocytes by substrate deflection, dedifferentiated cells were transfected with a miRNA designed against *Piezo1* or with a scrambled construct as a control. The cells were recovered from culture flask and redifferentiated in alginate beads (at least 3 days). The cells were recovered from alginate beads after redifferentiation and seeded onto pillar arrays. Only chondrocytes expressing the GFP marker were selected to perform electrophysiological analysis.

Reducing the expression of *Piezo1* was associated with a significant decrease in cells responding to pillar deflections, only 50% (6/12 cells) of *Piezo1*-KD chondrocytes showed mechanosensitive currents, which is a smaller percentage compared to cells transfected with the scrambled miRNA control (86%, 19/22 cells, Fisher's exact test, P=0.04) (Figure 22A). These results show that reducing the expression levels of Piezo1 decreases the likelihood of evoking deflection-gated currents when compared to WT chondrocytes; this was additionally reflected in a reduction in current amplitude measured from *Piezo1*-KD chondrocytes compared to WT chondrocytes (Figure 22B). In addition, the subset of responding cells presented currents in the complete deflection range (1 to 1000 nm) but again with reduced current amplitudes.

When kinetic parameters were measured, the latency of *Piezo1*-KD (8.1 ± 1.9 ms) tended to be longer than currents from chondrocytes transfected with the scrambled miRNA (4.3 ± 0.7 ms) but no significant differences were found (Figure 22C). The activation time for the control was 1.1 ± 0.3 ms and 1.3 ± 0.2 ms for the *Piezo1*-KD chondrocytes (Figure 22C). The inactivation time for the control was 67.8 ± 13.5 ms and 26.3 ± 16.6 ms for the *Piezo1*-KD chondrocytes (Figure 22C). It is important to note that the number of currents was reduced due to the effect of the knockdown (64 and 15 currents, scrambled and *Piezo1*-KD respectively).

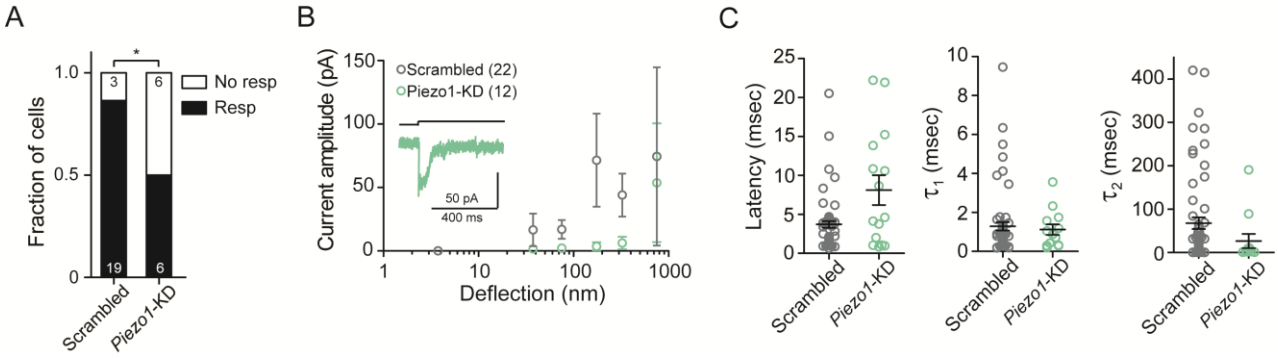

Figure 22. *Piezo1*-knockdown chondrocytes show a reduced mechanosensitive response to substrate deflections. A) Only 50% (6/12 cells) of Piezo1-KD chondrocytes respond to substrate deflections, which is significantly less compared to control chondrocytes (scrambled) (86.4%, 19/22 cells) (Fisher's exact test, **P*=0.04). The fraction of responsive cells is shown in black and the non-responsive cells in white. B) Current amplitude-deflection graph that represents the response to substrate deflections from control (gray) and *Piezo1*-KD chondrocytes (green) (22 and 12 cells respectively). The inset has an example trace of a current from a *Piezo1*-KD chondrocyte. C) Kinetics comparison of scrambled compared to *Piezo1*-KD chondrocytes. The average latency of the *Piezo1*-KD currents (7.8 ± 1.6 ms) tends to be longer than for the scrambled (4.3 ± 0.7 ms) however it was not significant (n=64 and 15 currents, scrambled and *Piezo1*-KD respectively). τ_1 and τ_2 did not show any significant difference between scrambled control and the *Piezo1*-KD chondrocytes (τ_1 control: 67.8 ± 13.5 ms and 26.3 ± 16.6 ms for the *Piezo1*-KD chondrocytes; τ_2 control: 67.8 ± 13.5 ms and 26.3 ± 16.6 ms for *Piezo1*-KD chondrocytes).

These results indicate that the ion channel Piezo1 is necessary but not indispensable for the substrate deflection response in WT chondrocytes. Therefore, it seems likely that the response induced by substrate deflection in chondrocytes depends on both TRPV4 and Piezo1. Taken together with the results from WT chondrocytes using GSK205 to block TRPV4, the mechanically gated current obtained after pillar deflections mostly depends on TRPV4 activation. To test that GSK205 is acting specifically on TRPV4 and not on Piezo1, N2a cells were transfected with Piezo1 and stimulated with cellular indentation (data not shown). A control response was obtained and subsequently GSK205 was perfused into the extracellular solution for 3 min, then the cell was stimulated again and Piezo1 currents were observed. These currents were also observed after the GSK205 washout (data not shown). These results confirm the specificity of GSK205 for TRPV4, thus supporting TRPV4 as the major contributor to mechanosensitive currents activated by substrate deflections in chondrocytes.

9.3.5 Mechanoelectrical response of chondrocytes cells with reduced expression of *Piezo1* assessed by membrane stretch

As previously mentioned, Piezo1 is a true mechanically gated ion channel; in particular the channel can respond to membrane stretch by detecting differential tension in the lipid bilayer (Lewis & Grandl 2015;

Cox et al. 2016; Syeda et al. 2016). Additionally, in RT-qPCR analysis we found expression of Piezo1 in mouse chondrocytes. Therefore, to study the role of Piezo1 in the response to membrane stretch of chondrocytes, a miRNA against *Piezo1* was used to decrease the expression of the channel.

Membrane patches were pulled from scrambled and *Piezo1*-KD chondrocytes, followed by stimulation with increasing pressure steps. The response in both conditions was extremely different, so much that *Piezo1*-KD chondrocytes did not show enough response before the membrane patch was broken to generate a pressure-response curve (Figure 23A). Hence, only the maximal current amplitude obtained per membrane patch was compared, the current from *Piezo1*-KD chondrocytes was reduced significantly in comparison with the control cells (transfected with the scrambled miRNA).

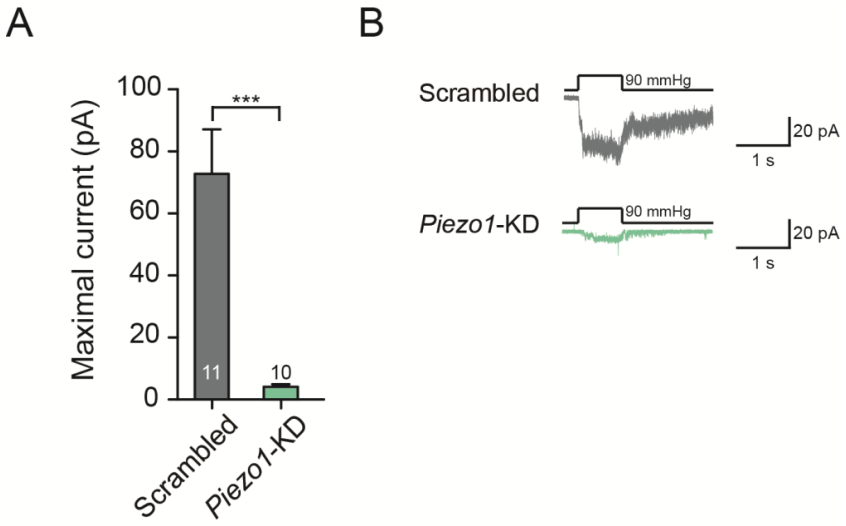

Figure 23. Piezo1 is required for the stretch sensitive response in chondrocytes.
A) Comparison of the maximal current amplitude in response to membrane stretch between control (transfected with a scrambled miRNA) and *Piezo1*-KD membrane patches. Note the significantly smaller amplitude observed in *Piezo1*-KD membrane patches (unpaired Student's t test, ***P=0.0002, 10 *Piezo1*-KD and 11 scrambled membrane patches). B) Examples traces of stretch-sensitive currents from control (gray) and *Piezo1*-KD membrane patches (green). Stretch activation experiments performed with help of Dr. Mirko Moroni.

These results indicate that the stretch-sensitive currents found in WT chondrocytes depend on the expression of Piezo1. These observations suggest the activation of parallel mechanoelectrical transduction pathways in chondrocytes, which are differentially mediated by membrane stretch and substrate deflection.

9.3.6 Assessing mechanoelectrical transduction of *Trpv4*$^{-/-}$-*Piezo1* knockdown chondrocytes with substrate deflection and membrane stretch

The previous results indicate that when the expression of TRPV4 or Piezo1 is reduced chondrocytes display a decreased response to substrate deflections, indicating that both channels are required for normal mechanoelectrical transduction in chondrocytes, in response to substrate deflections. It is important to note that the Ca^{2+} imaging data shows that all WT chondrocytes are able to respond to the TRPV4 agonist and the Piezo1 agonist, meaning that there is a homogenous population of chondrocytes expressing both functional channels.

To further test that these channels are both required for the normal mechanosensitive response in chondrocytes, a knockdown of the *Piezo1* channel was performed in chondrocytes lacking TRPV4. To achieve this, a miRNA directed against *Piezo1* was transfected into *Trpv4*$^{-/-}$ dedifferentiated cells and cells were then redifferentiated. The *Trpv4*$^{-/-}$-*Piezo1*-KD chondrocytes responded significantly less (2/11) to substrate deflections compared to WT chondrocytes and WT chondrocytes transfected with scrambled miRNA (Fisher's exact test, P=0.0002) (Figure 24A). Moreover, the stimulus-response plot of the *Trpv4*$^{-/-}$-*Piezo1*-KD chondrocytes was significantly different to that of scrambled miRNA-treated WT chondrocytes (two-way ANOVA, P=0.04), the current amplitude significantly decreased in *Trpv4*$^{-/-}$-*Piezo1*-KD chondrocytes and no response to substrate deflection was observed in the bin ranges of 1 to 100 nm and 250 to 1000 nm (Figure 24B). One explanation for the residual currents is that they could result from an incomplete knockdown of the *Piezo1* transcript.

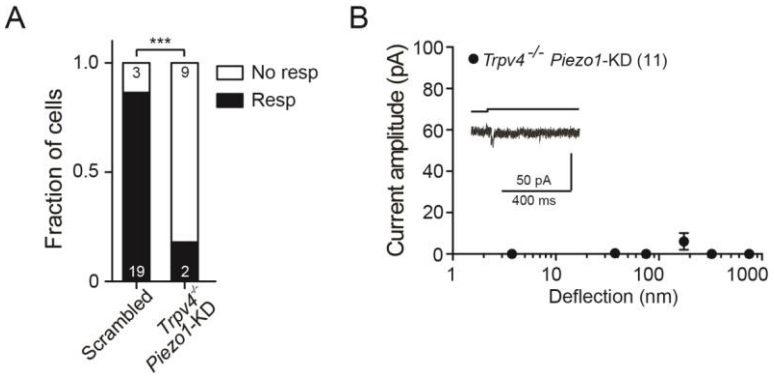

Figure 24. Both TRPV4 and Piezo1 are necessary for the substrate deflection response in chondrocytes.
A) Comparison of responding cells to substrate deflections, only 2 out of 11 *Trpv4*$^{-/-}$-*Piezo1*-KD chondrocytes responded to deflections, which is significantly less in comparison with the scrambled chondrocytes (86.4%, 19/22 cells) (Fisher's exact test, ***P=0.0002). B) Current amplitude-deflection graph of *Trpv4*$^{-/-}$-*Piezo1*-KD chondrocytes in response to substrate deflections, note the decrease in current amplitude, which is significantly different in comparison to WT cells treated with the scrambled control. The inset shows a representative trace of a *Trpv4*$^{-/-}$-*Piezo1*-KD current.

On the other hand, when membrane patches from *Trpv4*$^{-/-}$-Piezo1-KD chondrocytes were pulled and assessed with membrane stretch, no current activation was observed as expected from the *Piezo1*-knockdown experiments (Figure 25). Again, the maximal current amplitude was measured instead of the dose-response curve because there was not enough current activation found to membrane stretch; therefore, no dose-response curve was generated.

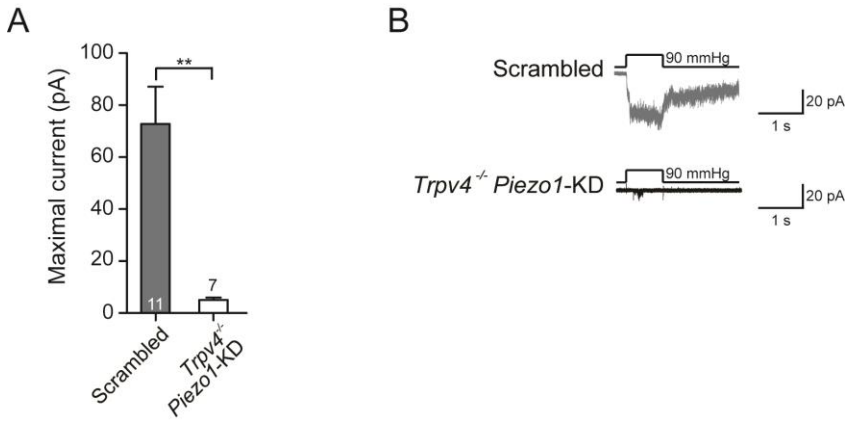

Figure 25. The expression of Piezo1 but not TRPV4 is required for the stretch-sensitive response in chondrocytes.
A) Comparison of the maximal current amplitude elicited by membrane stretch in membrane patches pulled from WT cells transfected with a scrambled (gray bar) control and *Trpv4*$^{-/-}$-*Piezo1*-KD patches (white bar). The patches from *Trpv4*$^{-/-}$-*Piezo1*-KD chondrocytes showed smaller current amplitude in comparison to the scrambled (unpaired Student's t test, ***P*=0.002, n=7 scrambled and 11 *Trpv4*$^{-/-}$-*Piezo1*-KD membrane patches). B) Example traces of stretch-sensitive currents, in gray the scrambled trace, in black *Trpv4*$^{-/-}$-*Piezo1*-KD. Stretch activation experiments performed with the help of Dr. Mirko Moroni.

Taken together the results obtained from the *Trpv4*$^{-/-}$ chondrocytes, *Piezo1* knockdown chondrocytes and *Trpv4*$^{-/-}$-*Piezo1*-KD chondrocytes, indicate that both channels: TRPV4 and Piezo1 are needed for the appropriate response to substrate deflections in primary chondrocytes. On the other hand, the response to membrane stretch exclusively depends on the expression of Piezo1, and TRPV4 does not play a role in the activation of these currents.

9.4 Investigation of Piezo1 and TRPV4 mechanosensitivity in a heterologous expression system

A mechanosensitive ion channel is considered as one when 1) the current latency is shorter than 5 ms (Christensen & Corey 2007), 2) the channel is present in mechanosensitive cells and its ablation eliminates the mechanosensitive response and 3) the channel produces mechanically gated currents in heterologous expression system (Árnadóttir & Chalfie 2010).

TRPV4 participates in diverse mechanosensitive functions such as stretch sensing in the bladder wall (Gevaert et al. 2007), osteoclast differentiation (Masuyama et al. 2008), osmotic regulation in endothelia, lungs, intestinal sensory innervation (Liedtke & Friedman 2003; Liedtke 2008; Phan et al. 2009; Lechner et al. 2011; Mizuno et al. 2003), endothelial function (Marrelli et al. 2007; Loot et al. 2008; Sonkusare et al. 2012; Vriens et al. 2005), hearing (Tabuchi et al. 2005), pressure sensation (Suzuki, Mizuno, et al. 2003), and pain sensing (Everaerts et al. 2010; Cortright et al. 2007). However, the mechanism that allows the mechanical activation of the channel remains elusive. To investigate whether TRPV4 is directly gated by mechanical stimulation, the TRPV4 ion channel was overexpressed in a heterologous system. Such an experiment is important because some putative mechanosensitive ion channels, when overexpressed in a heterologous system, do not display currents. For instance, the *C. elegans* mechanosensitive proteins MEC-4 and MEC-10 do not form functional mechanosensitive ion channels possibly because they lack a required subunit (Kellenberger & Schild 2002). As a control in our system, we used Piezo1, which is a *bona fide* mechanosensitive ion channel as it can be activated by membrane stretch (Coste et al. 2010; Coste et al. 2012), substrate deflection (Poole et al. 2014) and cellular indentation (Coste et al. 2010; Coste et al. 2012) when expressed heterologously.

9.4.1 Piezo1 is activated by different mechanical stimuli

Initially, to confirm the robust activation of the Piezo1 channel, mousePiezo1 (mPiezo1) was overexpressed in HEK-293 cells. These cells were tested with three different mechanical stimulation techniques: substrate deflection, membrane stretch and cellular indentation, and currents were monitored with patch clamp.

When outside-out patches were pulled from HEK-293 cells overexpressing mPiezo1, robust currents were found in response to increasing pressure steps (Figure 26A) as was previously reported (Gottlieb & Sachs 2012; Lewis & Grandl 2015; Cox et al. 2016). Moreover, activation of mPiezo1 by cellular indentation was also confirmed and robust activation was detected (Figure 26B) as has been previously described (Coste et al. 2010; Coste et al. 2012). Additionally, when mPiezo1 was overexpressed in HEK-293 cells and cells stimulated with substrate deflections, robust current activation was observed as was previously reported (Poole et al. 2014) (Figure 26C).

As these results show, the activation of mPiezo1 by different mechanical stimuli demonstrates that mPiezo1 is a true mechanosensitive ion channel that can be gated by membrane stretch, substrate deflection and cellular indentation. In addition, our systems successfully activate the channels as was previously reported.

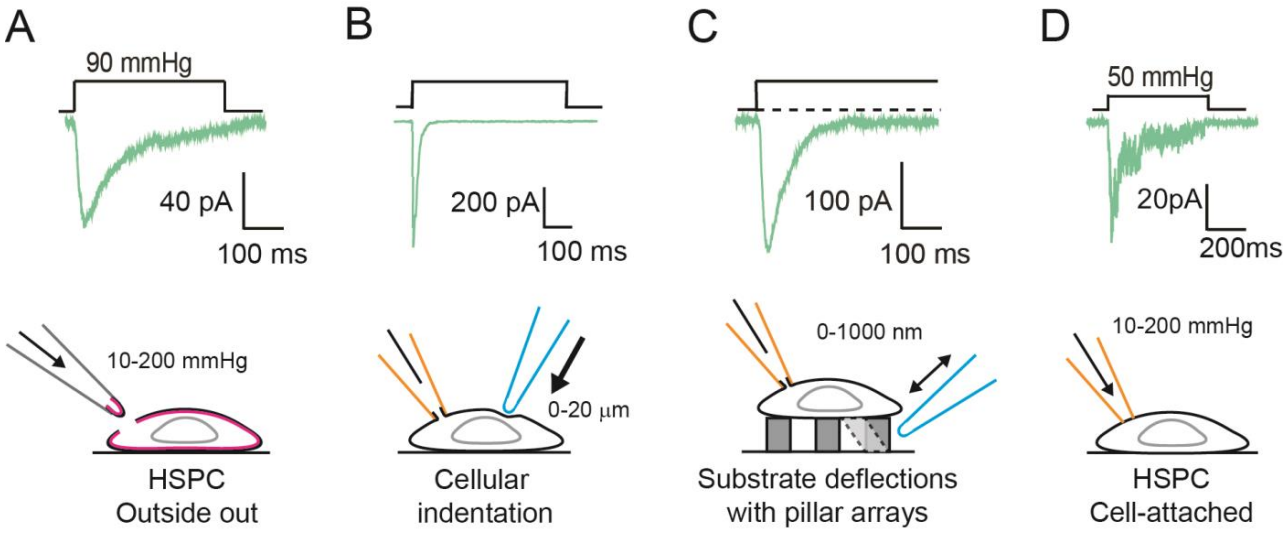

Figure 26. Piezo1 is a true mechanosensitive ion channel.
A) Current trace elicited in outside-out membrane patches pulled out from HEK-293 cells overexpressing mPiezo1 in response to membrane stretch; the lower panel shows a representation of the membrane-stretch setup using HSPC. B) mPiezo1 current in response to cellular indentation in whole-cell patch clamp mode, the lower panel shows a schematic of the cellular indentation. C) Deflection-sensitive current elicited in HEK-293 cells overexpressing mPiezo1, the lower panel has a schematic of the pillar array setup. D) Example trace of a HEK-293 cell overexpressing mPiezo1 in response to membrane stretch in cell-attached mode. The lower panel has a schematic of the setup. Note that in cell-attached mode the experiment is performed over the cell, in contrast to the outside-out mode in which membrane patches are detached from the cells. Stretch activation experiments performed with the help of Dr. Mirko Moroni.

9.4.2 TRPV4 is activated by cell-substrate deflection

After confirming the activation of mPiezo1, mouseTRPV4 (mTRPV4) was overexpressed in HEK-293 cells to study the response to mechanical stimulation with membrane stretch, substrate deflection and cellular indentation.

As mentioned before, TRPV4 responds to membrane stretch only when it is overexpressed in *Xenopus* oocytes (Loukin et al. 2010), yet this response was not observed when the channel was overexpressed in HEK-293 cells (Strotmann et al. 2000). To study the response of mTRPV4 to membrane stretch, again membrane patches from HEK-293 cells overexpressing the channel were pulled out and challenged with increasing pressure steps (10-150 mmHg).

A small current was found in membrane patches containing mTRPV4 in response to membrane stretch (Figure 27A). This weak activation was found only in a subset of membrane patches (55%, 5/9 patches). The responsive patches broke down before reaching a robust activation; therefore, the P_{50} was not determined. On the other hand, when mTRPV4 was assessed with cellular indentation in the range of 0.5-11 µm, no response was observed (12 cells) (Figure 27B). The response of mTRPV4 was indistinguishable from the negative control where HEK-293 cells were transfected with a plasmid encoding LifeAct. When mTRPV4 was overexpressed in HEK-293 cells and the cells were stimulated with substrate deflections, robust current activation was observed (Figure 27C).

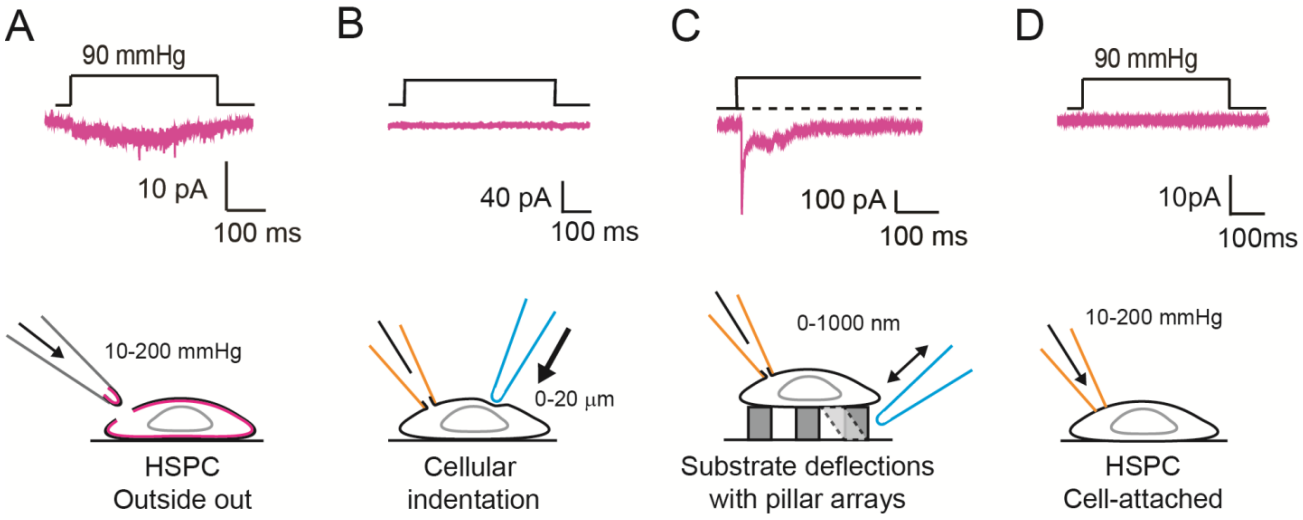

Figure 27. TRPV4 is specifically gated by substrate deflections.
A) Current trace elicited in outside-out from membrane patches detached from HEK-293 cells overexpressing mTRPV4 in response to membrane stretch (only 5/9 patches showed this weak activation); the lower panel shows a representation of the membrane-stretch setup using HSPC. B) mTRPV4 is not activated by cellular indentation, the lower panel shows a schematic of the cellular indentation. C) Robust activation of mTRPV4 stimulated by substrate deflection in HEK-293 cells overexpressing the channel, the lower panel has a schematic of the pillar array setup. D) mTRPV4 is not gated by membrane stretch in cell-attached mode. The lower panel has a schematic of the setup. Stretch activation experiments performed with the help of Dr. Mirko Moroni.

Additionally, it is known that TRPV4 is a polymodal ion channel that can be activated by warm temperatures. However, the channel is no longer responsive to warm temperatures in cell free patches (Watanabe, Vriens, et al. 2002), suggesting that TRPV4 needs additional molecular components for some modes of activation. Therefore, we tested whether mTRPV4 was activated by membrane stretch in cell-attached patches. In this type of experiment the cytoskeleton is not disrupted as happens when pulling the membrane patch for the outside-out mode. Similar to the results obtained applying membrane stretch to outside-patches, mTRPV4 did not display any current activation (Figure 27D), in contrast to the positive activation of mPiezo1 in cell-attached mode (Figure

26D). These data demonstrate that mPiezo1 is more efficiently gated by membrane stretch in comparison with mTRPV4 in a heterologous expression system and that the cytoskeleton is not playing a role in the activation by membrane stretch.

When mTRPV4 was overexpressed in HEK-293 cells and stimulated with substrate deflections, 87% (39/45 cells) of the stimulated cells showed inward currents; this was in contrast to the lack of response observed with cellular indentation or membrane stretch. In order to confirm the identity of the deflection-gated currents, the specific TRPV4 antagonist: GSK205 (10 µM) was used. When GSK205 was added to HEK-293 cells overexpressing mTRPV4, the current amplitude was decreased compared to the control without the antagonist (Figure 28A). Additionally, when GSK205 was acutely used, currents were inhibited and restored to pre-treatment levels after washout of the antagonist (Figure 28B). These data indicate that the TRPV4 channel mediates the deflection-gated current in HEK-293 cells overexpressing mTRPV4.

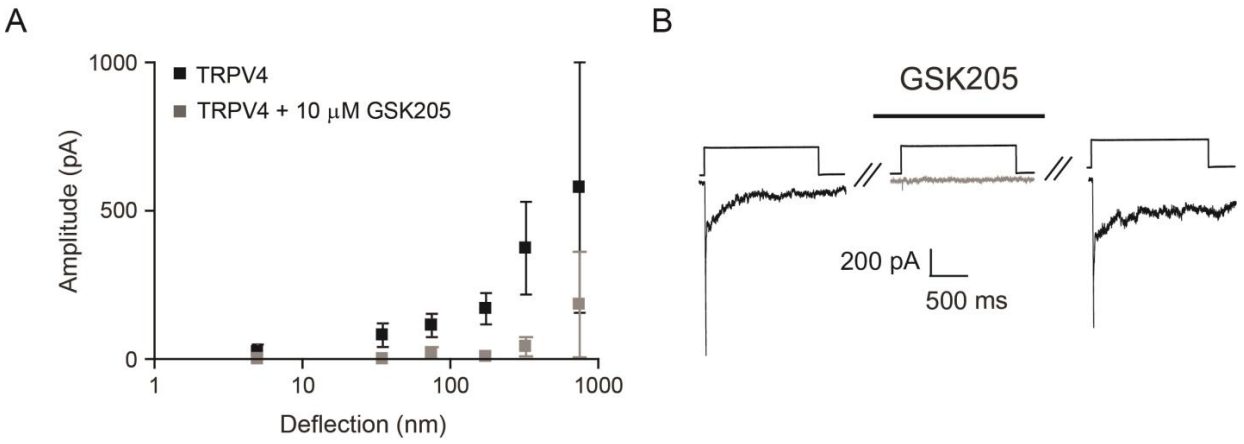

Figure 28. mTRPV4 is gated by substrate deflection in a heterologous expression system.
A) Current amplitude-deflection graph of the response of mTRPV4 to substrate deflection (black) and the channel in the presence of the GSK205 antagonist (gray). B) Example traces of deflection-sensitive currents triggered by substrate deflections before, during and after the washout of GSK205 (10 µm). Experiments performed by Dr. Kate Poole.

In addition, the current kinetics of mPiezo1 and mTRPV4 were measured. Figure 29 shows a direct comparison between the current amplitude, latency, activation and inactivation of mPiezo1 and mTRPV4 currents. mTRPV4 showed a higher current amplitude in response to substrate deflections compared to the cells overexpressing mPiezo1 (Figure 29A). Interestingly, the latencies for activation of mTRPV4 (1.5 ± 0.2 ms) and mPiezo1 (1.5 ± 0.2 ms) were not significantly different. Comparison of activation time, showed that mTRPV4 (0.48 ± 0.05 ms) was significantly faster than mPiezo1 (1.2 ± 0.25 ms) (Student's t test, P=0.04). The inactivation time of mPiezo1 was 76 ± 31 ms and 16 ± 7 ms for mTRPV4, mTRPV4 was significantly faster than mPiezo1 (Student's t test, P=0.005). The mean latency was similar for both ion

channels (Figure 29B). Therefore, the comparison between the latency of mPiezo1 (a *bona fide* mechanically gated ion channel) and mTRPV4 (a putative mechanosensitive channel) strongly suggests a direct activation of mTRPV4 currents by substrate deflections.

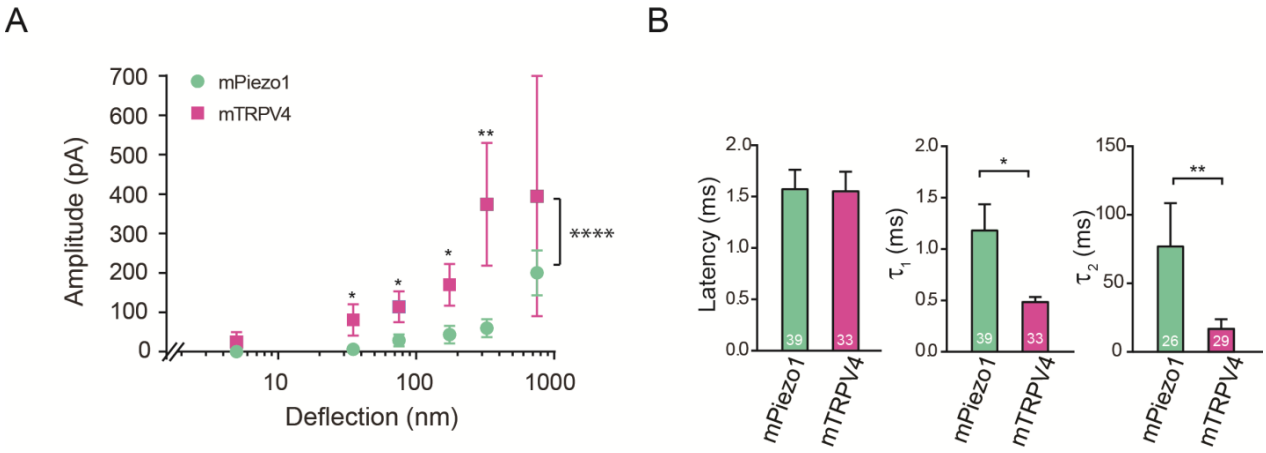

Figure 29. Comparing the deflection-sensitive response obtained by mPiezo1 and mTRPV4.
A) Current amplitude-deflection graph comparing the current amplitude of mPiezo1 and mTRPV4, note that the cells overexpressing mTRPV4 (magenta squares) displayed larger current amplitude in the stimulus ranges 10-20 nm, 50-100 nm, 100-250 nm and 250-500 nm. In addition, the mTRPV4 response is significantly different from mPiezo1 (two-way ANOVA, ****P<0.0001). B) Kinetic parameters of mPiezo1 and mTRPV4 currents triggered by substrate deflections. No differences were observed in the latency (of mTRPV4 1.5 ± 0.2 ms and mPiezo1 1.5 ± 0.2 ms), however τ_1 (mPiezo1 displayed 1.2 ± 0.25 ms and mTRPV4 0.48 ± 0.05 ms) and τ_2 (mPiezo1 was 76 ± 31 ms and 16 ± 7 ms for mTRPV4) were significantly faster in mTRPV4 (Student's t test, *P=0.04; **P=0.005). Experiments performed by Dr. Kate Poole.

The mechanical activation of mTRPV4 by substrate deflections has not been described before. To investigate whether the mechanical response can be modulated by voltage, as has been observed for the TRPV4 activation by 4αPDD (a TRPV4 agonist), cell swelling and warm temperature (Lechner et al. 2011; Nilius et al. 2003; Vriens et al. 2004; Nilius et al. 2004), experiments holding the cell at +60 mV and -60 mV were performed (Figure 30).

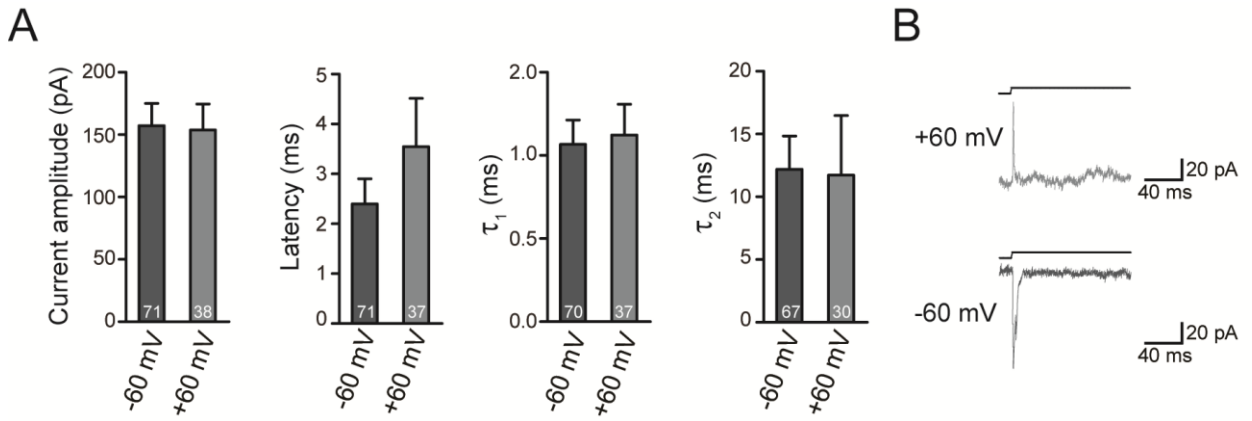

Figure 30. The mechanosensitive response of mTRPV4 is not voltage modulated.
A) Kinetic parameters of the mechanosensitive response of mTRPV4 at +60 mV and -60mV. Current amplitude at +60mV is 153.7 ± 20.9 pA and at -60 mV is 157.2 ± 17.9 pA. The latency at +60 mV is 153.7 ± 20.9 ms and at -60 mV 157.2 ± 17.9 ms). τ_1 (for +60 mV: 1.1 ± 0.2 ms and for – 60 mV: 1.1 ± 0.1 ms) and τ_2 (for +60 mV: 11.7 ± 4.8 ms and for – 60 mV: 12.2 ± 2.7 ms). B) Example traces of the mTRPV4 mechanosensitive currents in response to substrate deflections at +60 mV and -60 mV.

When the current kinetic parameters were measured and compared, no significant difference was found in the average current amplitude elicited at +60 mV and -60 mV (153.7 ± 20.9 pA and 157.2 ± 17.9 pA respectively). The mean latency obtained at +60 mV and -60 mV (3.6 ± 1 ms and 2.4 ± 0.5 ms respectively) did not show any significant difference, as well as the τ1 (for +60 mV was 1.1 ± 0.2 ms and for – 60 mV was 1.1 ± 0.1) and τ_2 (for +60 mV was 11.7 ± 4.8 ms and for – 60 mV was 12.2 ± 2.7 ms). Therefore, the different voltages did not modulate the mechanical response of the channel as was shown with other mTRPV4 activators.

9.4.3 Role of the actin cytoskeleton in the TRPV4 response to substrate deflections

Due to the previous set of results, one possibility is that the cytoskeleton is involved in the particular activation of TRPV4 by substrate deflection. To test if the cytoskeleton is involved in the transduction of the mechanical signal to the TRPV4 channel, we used an agent that causes depolymerization of the actin modules in the intracellular solution, cytochalasin D.

When cytochalasin D (10 μM) was used in the recording pipette, and cells stimulated with substrate deflection, the current amplitude did not change in comparison to the response of HEK-293 cells overexpressing mTRPV4. However, a tendency was observed in which mTRPV4 overexpressing cells elicited smaller current amplitude in the presence of cytochalasin D, mainly in the largest deflection range 500 to 1000 nm (Figure 31A). When, pooling together all responses and comparing the mean current

amplitudes obtained from cells overexpressing mTRPV4 (56.6 pA ± 6.1) against mTRPV4 in the presence of cytochalasin D (25.8 pA ± 6.9), the presence of this agent was associated with significantly smaller currents (Mann Whitney test $P<0.0001$) (Figure 31B). Even though the fraction of responsive cells did not show a significant difference, there is a tendency for a decreased cellular response in the presence of cytochalasin D (Figure 31B, right).

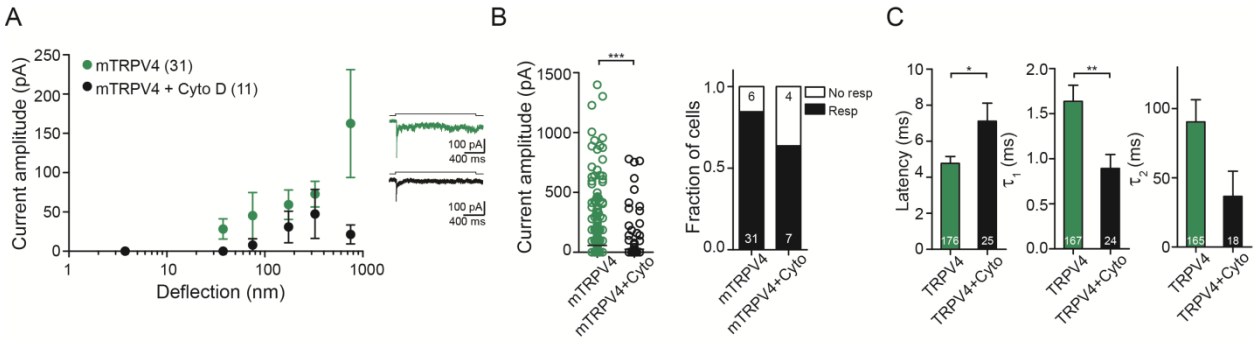

Figure 31. The cytoskeleton partially contributes to the mechanosensitive response of mTRPV4 by susbtrate deflections.
A) Current amplitude-deflection graph of the effect of cytochalasin D on the mechanosensitive response of mTRPV4. The inhibition of the actin cytoskeleton by cytochalasin D partially decreases the response to substrate deflection, mainly in the last bin. Example traces are shown on the right side of the graph. B) Average current amplitude of mTRPV4 alone and in the presence of cytochalasin D. Overexpression of mTRPV4 (56.6 pA ± 6.1) results in significantly higher current amplitude in comparison with mTRPV4 in the presence of cytochalasin D (25.8 pA ± 6.9) (cytochalasin D, 10 µM, Mann Whitney test, ***$P<$ 0.0001). C) Fraction of cells that respond to mTRPV4 and mTRPV4 in the presence of cytochalasin D. 31 out of 37 cells overexpressing mTRPV4 responded to substrate deflections, in contrast to when cytochalasin D is present in the intracellular solution only 7 out of 11 cells responded D) Cytochalasin D affects the latency and τ_1 time of mTRPV4 mechanical response. The latency displayed by mTRPV4: 4.8 ± 0.4 ms is significantly shorter in the presence of cytochalasin D: 7.1 ± 1.0 ms (Mann Whitney test, *P=0.016). The τ_1 for mTRPV4 with cytochalasin D is significantly faster (0.9 ± 0.2 ms) than in the absence of the drug (1.6 ± 0.2 ms) (Mann Whitney test, **P=0.009). The τ_2 for mTRPV4 in the presence (36.6 ± 18.2 ms) and absence of cytochalasin D (90.44 ± 16.2 ms) did not show significant differences (Mann Whitney test, P=0.016).

Additionally, when kinetic parameters were measured, a longer mean latency was observed in cells that responded to mechanical stimulation when treated with cytochalasin D (Figure 31C). The mean τ_1 was also significantly shorter in the presence of the drug (Figure 31D). These results suggest a partial contribution of the actin cytoskeleton in the mechanosensitive response of mTRPV4, which is mainly observed in the average current amplitude, in the delayed latency and in the shorter τ_1 in the presence of cytochalasin D.

9.4.4 PLA2 is not involved in the TRPV4 response to substrate deflections

It is known that TRPV4 responds to osmotic challenge, this response was previously characterized, and it is dependent on the activation of phospholipase A2 (PLA2) (Vriens et al. 2004). After a hypotonic change,

PLA2 produces arachidonic acid (AA), which can activate TRPV4. Subsequently, AA is used as a substrate by the P450 epoxygenase to produce 5',6'-EET, which also activates TRPV4 (Vriens et al. 2004). This activation takes place in seconds.

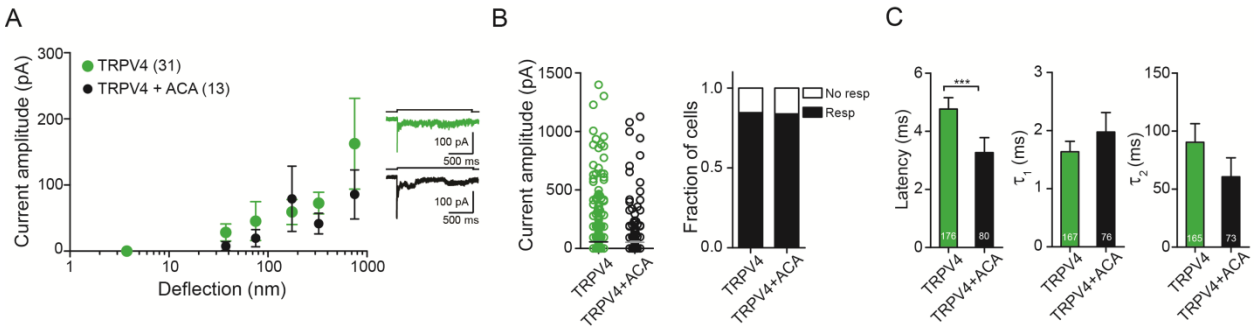

Figure 32. PLA2 is not involved in the mTRPV4 activation by substrate deflections.
A) Current amplitude- deflection graph of the response obtained by cells overexpressing mTRPV4 in the presence (black) and absence of ACA (green), no significant differences were observed. On the right hand, example traces are shown. B) Pulled current amplitude and responding cells. The pulled current amplitude of the response in the presence of the inhibitor (53.2 ± 9.4 pA) did not show any significantly different responses in comparison to the absence of ACA (56.6 ± 6.1 pA). The fraction of responsive cells was the same in the presence and absence of ACA, 31 cells out of 37 responded to the stimulation when overexpressing mTRPV4, and 11 out 13 with mTRPV4 and ACA. C) Current kinetics. The latency of mTRPV4 in the presence of ACA is significantly shorter (3.3 ± 0.5 ms) in comparison to mTRPV4 alone (4.8 ± 0.4 ms) (Mann Whitney test, ***P=0.001). The τ_1 for mTRPV4 (1.6 ± 0.2 ms) and mTRPV4 plus ACA (2.0 ± 0.3 ms) did not show any difference. The τ_2 for mTRPV4 with (60.7 ± 16.3 ms) and without ACA (90.4 ± 16.0 ms) were not significantly different.

In order to study whether this signaling pathway is activated during mechanical activation by substrate deflections, a broad inhibitor of PLA2 was used known as ACA (N-(p-Amylcinnamoyl)anthranilic acid). ACA was added to the intracellular pipette solution. No significant differences were found in the response when mTRPV4 was overexpressed in HEK-293 cells in presence or absence of ACA (Figure 32A). The pooled current amplitude also did not display any significant differences and the same fraction of cells responded to the substrate deflection in the presence and absence of ACA (Figure 32B). There was a change in the mean latency, with mTRPV4 being significantly faster in the presence of the PLA inhibitor (Figure 32C) (mTRPV4 = 4.8 ± 0.4 ms vs mTRPV4 and ACA = 3.3 ± 0.5 ms, Mann Whitney test, P=0.001), however τ_1 and τ_2 did not change in the presence of ACA (Figure 32C). These results strongly suggest that PLA2 is not involved in the mTRPV4 activation by substrate deflections and reinforce the previous results that suggest a direct activation of the channels.

9.5 Effect of TRPV4 on the structure of the cartilage extracellular matrix

Inhibition of mTRPV4 impairs cartilage ECM production when stimulated with cyclical mechanical loading (O'Conor et al. 2014). Additionally there is data showing that TRPV4 increased the activity of the transcription factor SOX9 during chondrogenesis (Muramatsu et al. 2007). We wanted to investigate whether the absence of TRPV4 affects the ECM structure, for instance by changing the ratio of the ECM proteins being deposited in the cartilage or by ECM remodeling. Therefore, we decided to analyze the overall cartilage structure using Second Harmonic Generation (SHG) microscopy which allows a free-label visualization of the tissue.

SHG is a second order coherent process in which two lower energy photons are converted to exactly twice the incident frequency (half the wavelength) of an excitation laser (Campagnola 2011). Fibrillar proteins such as collagen I and collagen II have non-centrosymetric structures which give rise to SHG signals (Cox & Kable 2006).

Taking advantage of the cartilage composition (high amount of fibrillar collagens), we could image the cartilage using SHG microscopy. The technique is applied using a multiphoton microscope, equipped with pulsed infrared lasers. Typical excitation wavelengths are in the range of 700 to 1000 nm, while the SHG signals are detected in between the visible region (400 to 500 nm). This means that SHG imaging can achieve high resolution at depths of several hundred micrometers. In addition, the SHG process involves virtual excitation states, resulting in reduced photobleaching and phototoxicity when compared to fluorescence methods (including multiphoton). Another advantage of imaging tissues rich in fibrillar proteins using SGH microscopy is visualizing real tissue structure because the signal is produced from endogenous proteins and not by addition of exogenous dyes (label-free microscopy). SHG has been used to observe collagen remodeling that occurs in different types of cancers, like ovarian, skin and breast cancer (Provenzano et al. 2006; Conklin et al. 2011; Kirkpatrick et al. 2007; Chen et al. 2010).

In order to compare ECM structure, femoral heads from 4-5 day old pups were taken. This age was chosen because at this point of development the skeleton is not yet calcified, instead it consists of cartilage. Therefore, the cartilage volume is much larger compared to the adult, in which the cartilage would be a very thin layer covering the femur.

The femoral heads were taken from WT and *Trpv4*$^{-/-}$ pups (Figure 7, in Materials and Methods), washed with PBS, immediately immersed in glycerol (80%) and frozen. The femoral heads were thawed and

embedded in LMP agarose. After the acquisition, the images were stitched and reconstructed (see methods). Figure 33 shows two representative images of reconstructed femoral heads from a WT and a *Trpv4*$^{-/-}$ mouse.

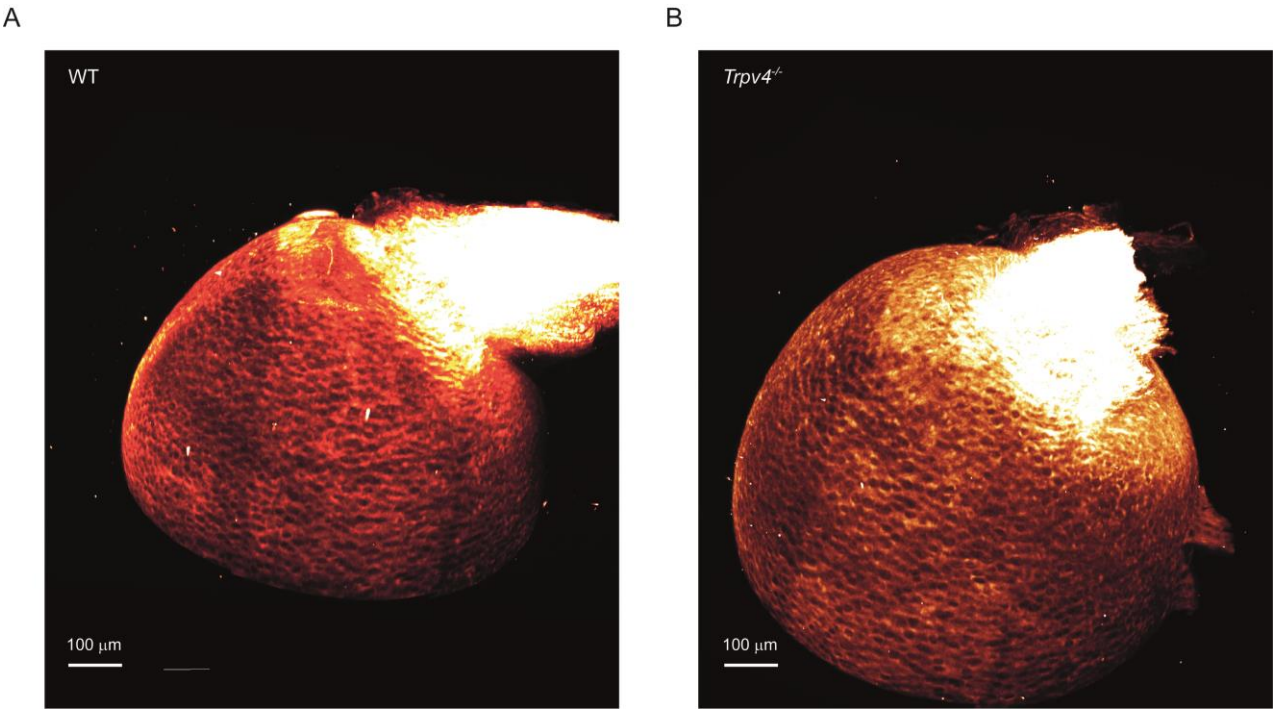

Figure 33. Example images of reconstructed femoral heads.
A) SHG image from a WT femoral head, the brightest section corresponds to the ligament. B) *Trpv4*$^{-/-}$ femoral head. Images were stitched and reconstructed with ImageJ/Fiji and Imaris. Scale bar corresponds to 100 µm. Images acquired with help from Dr. Anca Margineanu.

Images transversal to the longest axis were analyzed at different depths: 200 µm, 300 µm and 400 µm below the end of the ligament (data below 400 µm not used for the analysis, as the SHG signal was too low) (Figure 34A). A ring with high intensity was observed on the border of the cartilage (Figure 34B), which is related to the accumulation of fibrillar proteins. Taking advantage of the almost perfect circles obtained with the transversal planes from the femoral heads, the "radial profile" plugin from ImageJ/Fiji was used for analysis (Figure 34B). The "radial profile" produces a plot of integrated intensities as a function of distance from the center of a circle defined around the cartilage structure (Figure 34C). These plots were normalized according to the highest intensity value on each plot. The radial plots have an intensity peak at the border of the tissue; therefore, it is possible to estimate the width of the peak to investigate whether some differences arise between WT and *Trpv4*$^{-/-}$ femoral heads. Taking the normalized intensity plots, widths of 25%, 50% and 75% from the peak were measured taking as a reference the point with the highest intensity value (Figure 34C, right).

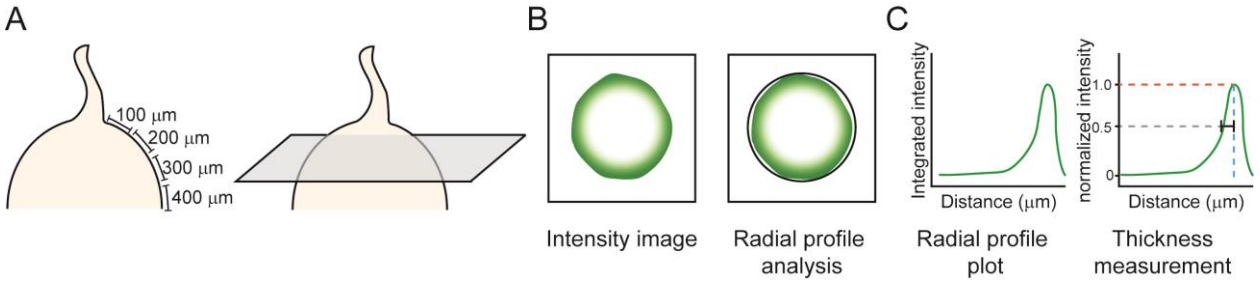

Figure 34. Scheme of image analysis.
A) Scheme of femoral head. The complete femoral head was imaged but only at 200 µm, 300 µm and 400 µm where the transversal images analyzed. B) The transversal images showed a ring pattern in which the highest intensity was observed at the borders of the tissue (left). The "Radial Profile" plugin from ImageJ/Fiji was used to analyze the intensity of the images (right). C) The "Radial Profile" analysis results in a plot with integrated intensities as a function of distance from the center of the circle (left). The radial profile plot was normalized, and the width of the peak was measured (black solid line) at 75%, 50% (gray dash line) and 25% from the distance with the maximum intensity (blue dashed line) (right); therefore, the right side of the curve was not included (everything on the right side of the blue dashed line), because the femoral head is not a perfect circle.

When WT and *Trpv4*$^{-/-}$ widths were analyzed at 200 µm, 300 µm and 400 µm below the end of the ligament no significant differences were observed (Figure 35A). This suggests that the width of the cartilage ring was comparable in both conditions throughout the tissue.

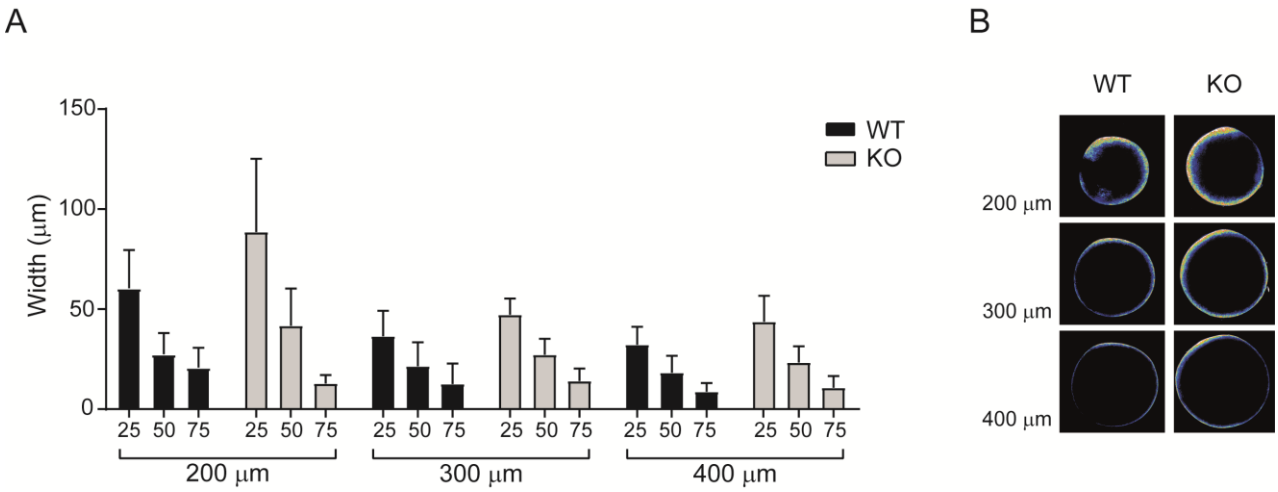

Figure 35. Width of femoral head intensity in WT and *Trpv4*$^{-/-}$ samples.
A) The widths were measured at 200 µm, 300 µm and 400 µm and at 25%, 50% and 75% from the maximum intensity peak. No significant differences were found WT (black) and *Trpv4*$^{-/-}$ (gray) samples. B) Representative pseudocolored images from WT and *Trpv4*$^{-/-}$ femoral heads at 200 µm, 300 µm and 400 µm.

However, the width of the peak measured relative to the highest intensity value does not quantitate the whole area under the plot (Figure 34C, area on the left side of the blue dashed line). Therefore, the integrated area under the curve (AUC), that represents the surface with SHG signal, was measured in WT and *Trpv4*$^{-/-}$. The

AUC from radial profiles at 200 µm, 300 µm and 400 µm below the end of the ligament, lacked significant differences between WT and *Trpv4*$^{-/-}$ mice (Figure 36). Meaning that WT and WT and *Trpv4*$^{-/-}$ cartilages have comparable intensities values that come from the signal from fibrillar proteins.

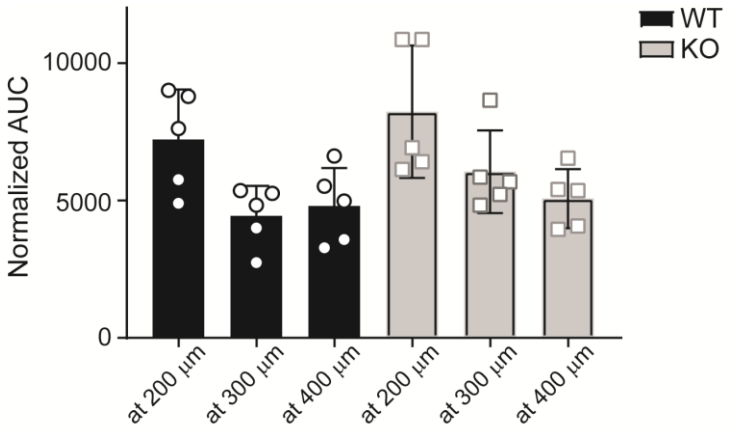

Figure 36. Area under the curve (AUC) from intensity radial profile plot corresponding to WT and *Trpv4*$^{-/-}$ femoral heads.
The AUC of WT (black) and *Trpv4*$^{-/-}$ (gray) was quantified and no significant differences were found.

In summary, we successfully imaged the cartilage structure from the complete femoral head using SHG microscopy. We observed that the cartilage from 4-5 day old does not display significant differences between the WT and *Trpv4*$^{-/-}$ conditions. This means that at this age, TRPV4 does not play a role in structuring of the cartilage, however imaging of the cartilage at other ages could be analyzed to further test this hypothesis.

10 Discussion

The present study provides experimental evidence for the expression of mechanosensitive ion channels in primary chondrocytes, and showed that mechanically activated currents can be recorded in these cells. The ion channels TRPV4 and Piezo1 were identified as the molecules mediating these currents. Furthermore, mechanisms required for activation of mechanosensitive ion channels in these cells were elucidated by means of a multi-technical approach.

10.1 Chondrocytes vs. dedifferentiated cells, importance of using the right cells

Differentiated chondrocytes and dedifferentiated cells, which develop when chondrocytes are cultured in monolayer, displayed different morphology, protein expression and current properties. The dedifferentiated cells were more sensitive when tested with substrate deflections, showing a smaller distance of activation and a higher percentage of responses per stimulation (see pili experiments, Figure 14). This might be due to the fact that chondrocytes and dedifferentiated cells express different proteins. Importantly, both differentiated chondrocytes and the non-physiologically dedifferentiated cells display mechanically-activated inward currents in response to membrane stretch and substrate deflection. These results demonstrate a functional difference between these cell types. This is relevant because studies performed to understand chondrocyte biology have most often used dedifferentiated cells.

The dedifferentiated cells showed an increased sensitivity only to substrate deflections, which suggests a particular regulation of proteins involved in cell-substrate interaction. Possibly proteins are up regulated or trafficked differentially to the membrane, like mechanosensitive ion channels or proteins involved in the cell-substrate response.

10.2 Importance of mechanical activation techniques to elucidate the activation mode of mechanosensitive ion channels

In general two mechanisms have been proposed to explain how mechanosensitive ion channels detect force (Martinac et al. 1990; Katta et al. 2015). First, force transduced through the lipid bilayer, known as "*force-*

from-lipids" mechanism. Here no cytoskeletal or tether components are required for the force transduction to the channel. Only ion channels and lipids would be necessary for force detection and pore opening. Second, force transduced through accessory proteins attached to the channels, known as "*force-from-tethers"* mechanism. Here, proteins that connect the channels to the cytoskeleton or ECM are needed to efficiently transfer the force and gate the channels. Both mechanisms enable rapid mechanoelectrical transduction responses in the order of milliseconds.

The most common techniques that have been used to study mechanosensitive ion channels are membrane stretch and cellular indentation. However, in recent years more techniques have been developed to study the mechanical response of such channels. For instance, elastomeric pillar arrays to deflect the cell-substrate interface (Poole et al. 2014); the coupling of magnetic nanoparticles to different sites of Piezo1 to activate different domains of the channel (Wu et al. 2016); ultrasound stimulation of Piezo1 (Prieto et al. 2017); and substrate indentation in soft matrixes (i.e. PDMS) to stimulate DRG neurons (Lin et al. 2016). These large efforts to develop new techniques are very important for the study of mechanosensitive ion channels; since these channels do not share sequence or structural domains, they evolved and acquired different activation mechanisms. To date there is no common technique that can activate all types of mechanosensitive ion channels. Thus, diverse techniques convey force to cells in different forms. As a consequence, certain mechanical stimulation modes will evoke channel gating in some mechanosensitive ion channels, while other mechanosensitive ion channels will not be gated. This is the case for TRPV4, in this study it was found that TRPV4 was successfully opened in response to substrate deflections, while membrane stretch and cellular indentation failed to activate the channel in the same cellular context.

In addition, different techniques provide a broad range in force manipulation that go from the molecular to the cellular scale. For instance, magnetic nanoparticles were attached to different amino acids on the extracellular side of Piezo1. To activate the channel, a magnetic field that pulled the nanoparticle was used, this resulted in a differential activation of Piezo1 depending on the domain to which the nanoparticle was attached (Wu et al. 2016). Instead, other studies have used membrane patches excised from cells and stimulated these with increasing pressure steps to stretch the membrane using a high-speed pressure clamp device (Gottlieb et al. 2012; Bae et al. 2011; Levina et al. 1999; Honoré et al. 2006). In these studies, researchers focused on lipid bilayers and ion channels, and detected gating of stretch-activated ion channels. Another example is when cells are stimulated with substrate deflections using pillar arrays (Poole et al. 2014). This preparation includes the ion channels within their cellular environment: lipids, ECM and cytoskeleton. Therefore, more complexity can be added with these techniques, which can affect the response of the channels. While only the stretch-activated ion channels are able to respond to membrane stretch

because they follow the force-from-lipids mechanism, the mechanosensitive ion channels that require a tether will be able to respond to methods like pillar array deflection or substrate indentation. The pillar array technique also potentially stimulates the force-from-lipids channels because it locally perturbs the plasma membrane.

It is important to note that channels that follow the force-from-lipids principle such as Piezo1, is also sensitive to other types of mechanical stimulation such as cellular indentation, which produces membrane deformation that activates these channels (Coste et al. 2010). Thus, the different techniques used to manipulate forces have an impact on the channel response that depends on its mode of activation (lipid or tether). Thus, it is extremely important to know which type of technique targets specific activation modes.

To address the different types of mechanosensitive-ion-channel activation, we used three types of techniques, cellular indentation that perturbs and deforms the complete cell; membrane stretch in outside-out membrane patches that stretches the plasma membrane; and substrate deflections using elastomeric pillar arrays which cause local displacement at the cell-substrate interface of a pilus. The use of three techniques was necessary to show different modes of activation of the ion channels involved in chondrocyte mechanotransduction.

10.3 Piezo1 is involved in the chondrocyte response to membrane stretch

Piezo1 has been found in mechanosensitive tissues that are exposed to constant physical forces, such as the endothelium where it has an important role in vasculature development (Ranade et al. 2014); as well as in tubular epithelial cells where stretch-activated currents were recorded (Peyronnet et al. 2013). Additionally, Lee and colleagues found *Piezo1* and *Piezo2* transcripts expressed at similar levels in human and in porcine chondrocytes (Lee, et al. 2014). However in murine cartilage the expression of *Piezo2* was 90% lower in comparison with that of *Piezo1* (4-week-old) (Lee, et al. 2014).

In this thesis, robust *Piezo1* transcript expression was detected in primary murine chondrocytes, but not of *Piezo2*. To validate the functional presence of the Piezo1 channel, WT chondrocytes were challenged with Yoda1, a synthetic Piezo1 agonist (Syeda et al. 2015). All the WT chondrocytes responded with a robust calcium influx, suggesting that Piezo1 is functionally expressed in WT murine chondrocytes. Importantly, Piezo2 is not activated by Yoda1 (Syeda et al. 2015).

With the use of high-speed pressure clamp, one can stimulate channels that follow the force-from-lipid principle by excising membrane patches from cells and stimulating them with increasing pressure steps. When membrane patches from primary chondrocytes were challenged with stretch, WT cells responded with inward currents. However, when *Piezo1* was knockdown in WT chondrocytes, no stretch response was found in membrane patches excised from these cells (see pressure experiments, Figure 23). These data indicate that Piezo1 is necessary for this response and that murine chondrocytes have mechanosensitive ion channels that are activated by membrane stretch. These results are relevant because this is the first time that the functional response of Piezo1 was shown in chondrocytes both with electrophysiology and calcium imaging recordings.

Interestingly, mutations in the *Piezo2* gene cause different forms of arthrogryposis, which are diseases characterized by congenital contractures in joints (Haliloglu et al. 2016; Coste et al. 2013; McMillin et al. 2014). Depending on the severity of the disease, this phenotype is often accompanied by proprioception defects (Haliloglu et al. 2016). *Piezo2* transcript expression was not reliable detected in chondrocytes used in this thesis, possibly the mRNA was below our detection level. Another explanation for the different mRNA expression in our study and Liedtke´s study (Lee, et al. 2014) is that there may be a differential expression of the Piezo channels depending on the species. Similar expression levels of *Piezo1* and *Piezo2* transcripts were observed in porcine and human chondrocytes (Lee, et al. 2014), in contrast to higher expression of *Piezo1* compared to *Piezo2* in murine chondrocytes (see RT-qPCR experiments, Figure 17 and Lee et al. 2014).

10.4 Piezo1 and TRPV4 mediate the response to substrate deflection in chondrocytes

TRPV4 has a known role in chondrocyte physiology functioning as an osmosensor and by regulating the transcription factor SOX9 (Dy et al., 2012; Lefebvre et al, 2001; Phan et al., 2009). In the current study, *Trpv4* transcripts were found in chondrocytes as was previously reported (Andrea et al, 2010; O'Conor, Leddy et al, 2014; Phan et al., 2009). To confirm the functional expression of TRPV4 in WT chondrocytes, a specific agonist (GSK1016790A) was used in calcium imaging. All WT chondrocytes responded with a robust calcium influx, this confirms a functional expression of TRPV4 channel in WT murine chondrocytes (see calcium imaging experiments, Figure 18).

The pillar array technique relies on performing the stimulation at the cell matrix interface without disrupting the cytoskeleton. This technique, in contrast to pressure clamp, can successfully stimulate mechanosensitive ion channels that follow the force-from-tethers principle. Using primary chondrocytes, we observed inward currents in response to the substrate deflections. We hypothesized that TRPV4 might mediate these currents. Therefore, substrate deflection experiments were performed in *Trpv4*$^{-/-}$ chondrocytes, which showed a decreased response to pili deflection. In addition, *Piezo1*-knockdown chondrocytes also presented a reduced response to substrate deflections. Furthermore, the *Piezo1*-knockdown in *Trpv4*$^{-/-}$ chondrocytes practically led to a loss in currents activated by substrate deflections. The minimal response obtained in these experiments (only 2% of responding cells) may be due to an incomplete knockdown of *Piezo1*. This data strongly suggests that TRPV4 and Piezo1 together mediate the response to substrate deflections.

When a TRPV4 specific antagonist (GSK205) was used in WT chondrocytes, 87% of the mechanically gated current was abolished, indicating that TRPV4 has a significant acute role in mediating this response *in situ*. This is relevant because ours is the first report of TRPV4 directly mediating mechanically gated currents in chondrocytes.

Both *Trpv4*$^{-/-}$ and *Piezo1*-knockdown chondrocytes respectively showed an impaired response to substrate deflections. The decreased response was observed from 1 to 1000 nm, yet with smaller current amplitudes in both conditions. This observation means that there is an overlap in the sensitivity of TRPV4 and Piezo1. However, differences in sensitivity may appear in ranges that were not tested in this study.

Liedtke and colleagues observed a differential contribution of TRPV4 and Piezo channels depending on the magnitude of the applied force. For instance, Piezo1 and Piezo2 mediated-calcium signals were shown to respond to non-physiological compression forces (in the range of injuries) (Lee, et al. 2014). While TRPV4 regulated the chondrocyte metabolic response to low-level physiological loading (O'Conor et al. 2014). Thus, concluding that TRPV4 modulates low mechanical inputs and Piezos modulate response to harmful forces. This conclusion differs from the findings of this thesis, in which an overlap of sensitivity was observed in pillar array experiments. One idea to explain the different conclusions is that studies by Lee and O'Conor measured effects downstream of the activated mechanosensitive currents. For instance, to evaluate the role of TRPV4 in chondrocytes they quantified protein synthesis after cyclical mechanical compression (O'Conor et al. 2014). To evaluate the role of Piezo1 and Piezo2 they used calcium imaging after compressing with an AFM cantilever N2a cells overexpressing the channels (Lee, et al. 2014). Thus, these studies focused in downstream effects (protein quantification and calcium imaging) to the direct activation of the channel. In contrast, in this thesis electrophysiological techniques were used to record direct activation

of mechanically activated ion channels. In addition, the type of mechanical stimulation performed in the previous studies (cyclical mechanical compression (O'Conor et al. 2014) and compression with an AFM cantilever (Lee, et al. 2014)), as well as the scale of forces differed to this thesis, which may also account for some of these discrepancies.

Experiments performed in chondrocytes with substrate deflections may explain the reason why young *Trpv4*$^{-/-}$ mice have no obvious bone or joint phenotype. The *Trpv4*$^{-/-}$ chondrocytes have a decreased response to substrate deflection that is probably compensated by Piezo1 activation. The residual current in the *Trpv4*$^{-/-}$ chondrocytes is smaller than in WT chondrocytes, and was activated within the complete deflection range used here (1 to 1000 nm). This suggests that the remaining mechanosensitivity is sufficient to keep the homeostasis of the tissue under normal conditions (without degeneration that comes during ageing and without the extra loading resulting from obesity (Andrea et al., 2010; O'Conor et al, 2013)).

Additionally, TRPV4 is a channel in which mutations can cause several channelopathies in humans. Interestingly three main diseases arise from mutations in TRPV4 that can be grouped as peripheral neuropathies, skeletal dysplasias and arthropathies. The mutations that affect the channel function (gain of function, loss of function, trafficking) are located throughout the entire channel sequence and the ankyrin repeat domain is a hot spot for such mutations. For instance, mutations in the inner part of the ankyrin repeat cause skeletal dysplasias, and mutations in the outer face cause arthropathies and peripheral neuropathies (Lamandé et al. 2011a). These mutations affect the function of the channel (gain of function, loss of function, or trafficking defects), which highlight the importance of TRPV4 in cartilage physiology (Nilius & Voets 2013; Nilius & Owsianik 2010).

A contrasting channelopathy example comes from a cat breed known as Scottish fold cat, these cats have osteochondrodysplasias that affect cartilage and bone development, presenting degenerative joint diseases. This breed is quite popular because its ears are bent forward and downward and this results in an unusual and cute appearance of these cats. This phenotype is caused by a mutation in the *Trpv4* gene from Valine to Phenylalanine in position 342, causing decreased membrane localization and a gain of function in the channel (Gandolfi et al. 2016). This mutation is also present in humans causing a skeletal dysplasia (Lamandé et al. 2011a) and therefore breeding these animals for aesthetic purposes is ethically questionable.

10.5 Mechanosensitive ion channels are functionally expressed in chondrocytes

As mentioned before, two mechanisms have been proposed to explain force detection in mechanosensitive ion channels, *force-from-lipids* and *force-from-tethers* (Martinac et al. 1990; Katta et al. 2015). Additionally, through the study, discovery and description of new mechanosensitive ion channels some criteria have been established to classify channels as mechanosensitive (Christensen & Corey 2007; Árnadóttir & Chalfie 2010; Ernstrom & Chalfie 2002). These are: 1) the proteins have to be expressed in a mechanosensitive tissue. 2) Ablation of the channel impairs the mechanosensitive properties of the tissue. 3) When the channel is expressed in a heterologous system, mechanosensitive currents have to be observed and the latency of activation should be shorter than 5 ms, which is a time that allows direct activation of the channel without the initiation of intermediate signaling pathways.

The first mechanosensitive ion channels were discovered in bacteria. The MscL and MscS are pore forming subunits that bacteria use as a survival mechanism against osmotic stress (Sukharev et al. 1994; Häse et al. 1995; Levina et al. 1999). These channels are experimentally activated by membrane stretch, which is a characteristic of the channels that follow the force-from-lipids principle. Although, it has been more difficult to identify and characterize mechanosensitive ion channel in eukaryotes, in 2010, Coste and colleagues discovered the Piezo channels (Coste et al. 2010). Piezos are large transmembrane proteins that form homotrimers, in which one subunit has at least 14 transmembrane segments (Ge et al. 2015). Piezo1 is activated by a variety of mechanical stimuli such as cellular indentation (Coste et al. 2010; Coste et al. 2012), ultrasound (Prieto et al. 2017), substrate deflection (Poole et al. 2014), shear stress (Ranade et al. 2014), membrane stretch (Coste et al. 2010; Coste et al. 2012). Lewis, Cox and Syeda have shown with different approaches that the channel detects the tension in the lipid bilayer, strongly suggesting that Piezo1 follows the force-from-lipids mechanism (Lewis & Grandl 2015; Cox et al. 2016; Syeda et al. 2016). So far, experimental evidence has shown that Piezo2 can be activated by cellular indentation (Coste et al. 2010; Coste et al. 2012) and substrate deflection (Poole et al. 2014), however demonstrating activation by non-symmetrical lipid bilayers or membrane tension to test the force-from-lipids principle remains elusive. In addition, the potassium channels TREK and TRAAK, members of the two-pore domain family are transmembrane proteins characterized by K^+ selectivity, each pore is formed by two subunits, and each subunits has a two-pore domain (Brohawn et al. 2012). These channels are expressed in DRG neurons as well as the central nervous system (Medhurst et al. 2001; Kang & Kim 2006). These ion channels respond to different stimuli such as polyunsaturated fatty acids, temperature changes, and mechanical deformation

of the plasma membrane via the force-from-lipid principle (Brohawn et al. 2014; Brohawn et al. 2012; Noel et al. 2009; Kang et al. 2005; Maingret et al. 2000; Patel et al. 2001).

Ion channels from the TRP family, which consist of 7 subfamilies respond to a variety of physical (temperature, light, osmolarity) and chemical stimuli (synthetic and plant derived compounds such as menthol or capsaicin) (Venkatachalam & Montell 2007; Zheng 2013). TRP members are considered as integrators of multiple signals and are truly relevant to physiological processes (Venkatachalam & Montell 2007). They respond to more than one agonist that often binds to different sites in the channel, thereby modifying the protein to promote channel gating. Some of the members of the TRP family have been proposed to be mechanosensitive, for instance PKDs, NOMPC, TRPM7, TRPV4, TRPC6 however, the activation mechanism remains elusive and controversial. An exception is the TRP channel NOMPC, which is expressed in neurons from the fruit fly *Drosophila melanogaster*. Zhang and colleagues showed that NOMPC is involved in touch sensation and that and interaction between microtubules and the ankyrin repeat domain is necessary to transduce force to open the channel pore (Zhang et al. 2015). This ankyrin-repeat-domain association with microtubules is an example of the force-from-tether mechanism that conveys mechanical stimuli into biological signals in the touch receptor neurons of *Drosophila* (Zhang et al. 2015).

In the current study, the ion channels TRPV4 and Piezo1 were found to be expressed in murine primary chondrocytes. TRPV4 has been associated with a variety of mechanotransduction processes and it was proposed to be a mechanosensitive ion channel, while Piezo1 is a true mechanosensitive ion channel activated by membrane stretch. Therefore at least one mechanism of activation is known for Piezo1 (force-from-lipids), however the mechanism for TRPV4 mechanical activation is controversial. Thus, in the following sections I will elaborate on each of the proposed characteristics that a mechanosensitive ion channel has to accomplish in order to analyze the response of TRPV4 to mechanical stimuli. Additionally, these characteristics will be compared to that of Piezo1.

10.5.1 Expression of TRPV4 and Piezo1 in chondrocytes

The cartilage is a known mechanosensitive tissue, because chondrocytes are able to induce the remodeling of the cartilage ECM in response to changing mechanical loads (static or dynamic). In previous studies was observed that the addition of a broad inhibitor of mechanosensitive ion channels, gadolinium, impairs the synthesis of ECM proteins (Roberts et al. 2001; Pingguan-Murphy et al. 2006), suggesting a functional role of ion channels in cartilage mechanotransduction. This role is hypothesized to be at the force detection level.

TRPV4 has been implicated in chondrocyte physiology as an activator of SOX9 (transcription factor in chondrogenesis) (Dy et al. 2012; Lefebvre et al. 2001). Moreover, TRPV4 functions as an osmosensor in chondrocytes, which supports the idea of the mechanosensitive role of the channel. Yet, electrophysiology evidence has been missing to corroborate the function of TRPV4 as a mechanosensor. This work identified transcript expression of the ion channels TRPV4 and Piezo1, functional activity using Ca^{2+} imaging together with specific agonist for TRPV4 and Piezo1 channels respectively, and electrophysiological measurements using mechanical stimulation.

10.5.2 Ablation of the channels impairs the mechanosensitive currents in chondrocytes

To test the importance of TRPV4, a mouse with a genetic ablation in the *Trpv4* gene was used (Mizuno et al. 2003). These mice live well and express a series of mild phenotypes some of which are related to mechanosensitive tissues such as in nociceptive fibers (Alessandri-Haber et al. 2005; Alessandri-Haber et al. 2003), in skin mechanosensors (Suzuki, Mizuno, et al. 2003; Suzuki, Watanabe, et al. 2003), and in the auditory system (Tabuchi et al. 2005). In the case of cartilage, the *Trpv4*$^{-/-}$ mouse has a higher tendency to develop age-related and obesity-induced osteoarthritis (Andrea et al. 2010; O'Conor et al. 2013).

In *Trpv4*$^{-/-}$ chondrocytes, the response to substrate deflections was diminished and a similar effect was observed when *Piezo1* was knocked down in chondrocytes. The response to substrate deflections was only abolished when the chondrocytes lacked both channels. In addition, when WT chondrocytes were stimulated with substrate deflections in the presence of a TRPV4 antagonist, the mechanical current was decreased by 87% and recovered after washout, indicating that TRPV4 plays an important role in chondrocyte mechanotransduction *in situ*.

In addition, the stretch-sensitive response was completely abolished when *Piezo1* was knocked down in chondrocytes, but unchanged in the absence of TRPV4. These data indicate that Piezo1 is necessary to produce the stretch sensitive response in chondrocytes.

In summary, these results indicate that the loss of TRPV4 partially abolishes the sensitivity of chondrocytes to substrate deflections. The knockdown of *Piezo1* has the same effect and removal of both channels ablates the mechanosensitive response to substrate deflections. In addition, the loss of Piezo1 completely abolishes the response of chondrocytes to membrane stretch, indicating the role of both ion channels in the

mechanosensitive response of chondrocytes. These data also suggest that there are separable mechanotransduction pathways that can be activated solely by membrane stretch and on the other hand by deformations at the cell-substrate interface.

10.5.3 Heterologous expression of TRPV4 and Piezo1 give rise to mechanosensitive current activation.

About TRPV4 mechanosensitivity

Cellular indentation did not trigger any mechanically-gated currents in HEK-293 cells overexpressing TRPV4. The stretch response was inefficient (small responses in half of the tested patches) and only substrate deflection triggered robust current activation in TRPV4-overexpressing cells (model in Figure 37). A possible reason for lack of response to cellular indentation is that the stimulation is performed on the top of the cell, in contrast to pillar array stimulation that takes place at the interface of the basal membrane and the substrate, where attachment proteins are expressed. This protein environment may be required for the efficient mechanical response of TRPV4. Another option is that TRPV4 is not homogenously distributed in the cells. For instance, instead of being evenly expressed throughout the cell surface, the channel may be mainly located in the basal section; therefore, an apical indentation would not be sufficient for its activation. On the other hand, in the case of TRPV4-homogeneous expression throughout the cell, the channel would not be able to respond when it is not interacting with its tether. That in the case of cell-matrix localization, the channels would be only located at the attachment sites.

Regarding the response to membrane stretch, one study reports small currents obtained from TRPV4 overexpression in *Xenopus* oocytes. The content of the solution might explain the activation of stretch-sensitive currents because elements (20 mM citrate) and conditions (pH of 4.5, holding potential of 50 mV) that promote gating were used in the experiments (Loukin et al. 2010). This study suggests a lipid mechanism of gating (Loukin et al. 2010). It is known that diverse amphipaths, such as arachidonic acid and its derivatives activate TRPV4 (Watanabe et al. 2003), which as well support the lipid activation hypothesis. However, it is not known if these compounds directly act on the channel or if they change the lipid bilayer environment to activate the channel. It is likely that only particular conditions in the TRPV4 environment explain the possible lipid-gating mechanism. 1) TRPV4 would have to be surrounded by lipids. 2) Low concentration of agonist needs to be bound to the channel, such that the agonist in low concentration or the

surrounding lipids sensitize the channel to promote a transition to an open state. Thus, when TRPV4 encounters stretch or any other agonist, it can be more readily gated.

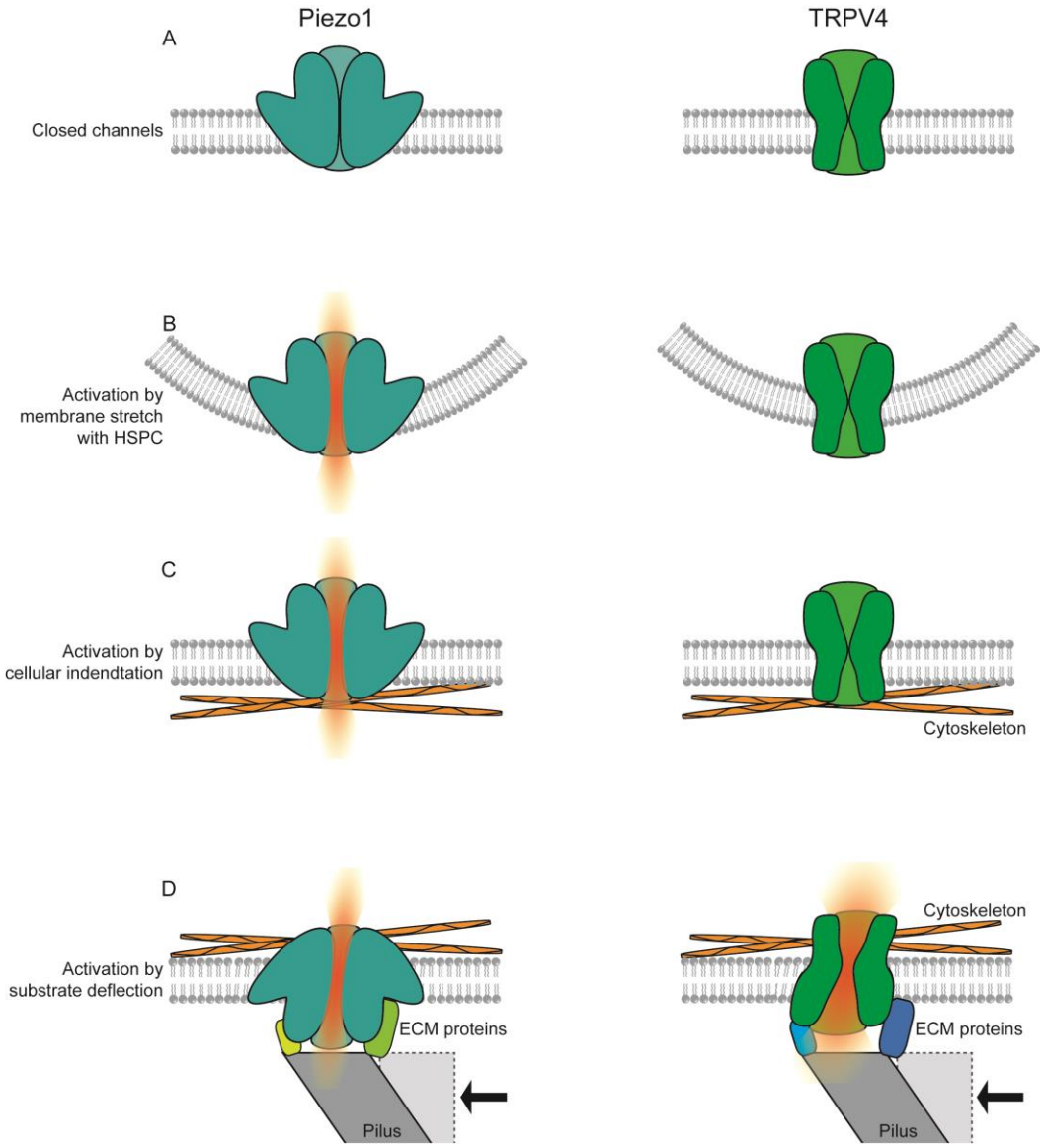

Figure 37. Activation modes by mechanical activation for Piezo1 and TRPV4.
A) Schematic representation of closed channels. B) The membrane stretch induced by HSPC activates Piezo1 currents, but this activation is not efficient for TRPV4. C) Piezo1 is activated by cellular indentation but not TRPV4, note that in this mode the cytoskeleton may be important for this activation. D) In the stimulation by substrate deflection, Piezo1 is gated as well as TRPV4. Note that in this mode, the cytoskeleton and ECM proteins may play a role in the gating.

The idea that the channel can be sensitized with agonists to respond to stretch also suggests substrates of conformational changes that eventually lead to an efficient gating. This process might happen in a

physiological context when TRPV4-expressing cells encounter different types of stimuli at the same time (some of which would be agonists for the channel). This would ease the channel opening in response to stretch. However, more research is needed to characterize consecutive agonist responses in polymodal TRP channels.

Interestingly, Gao and colleagues reported that TRPV4 overexpressed in HEK-293 cells has a modest response to shear stress measured with calcium imaging. When the temperature was raised to 37 °C, the calcium influx due to shear stress increased significantly (Gao et al. 2003). These results again suggest that TRPV4-activating stimuli can sensitize the channel to facilitate the pore opening; in this example, first a weak activator is used (shear stress) and this response was enhanced by the dual activation of shear stress and warm temperature (a stronger activator). In addition, the activation by heat in TRPV4 has been successfully observed in cell attached patches but not in excised inside-out patches (Watanabe, Vriens, et al. 2002). This strongly suggests the need of additional components to open the pore with warm temperatures. However, further research is needed to investigate whether changing the TRPV4 lipid environment or stimulating with temperature or chemical agonist can push the channel to a force-from-lipid activation mechanism.

On the other hand, 87% of the HEK-293 cells overexpressing TRPV4 exhibited mechanically gated currents when stimulated with substrate deflections but not to cellular indentation and we observed a slight activation by membrane stretch in half of our membrane patches. This strongly suggests that TRPV4 lacks the ability to sense changes in the lipid bilayer tension (force-from-lipid principle) as Piezo1 or the bacteria channels MscL and MscS. However, so far there is no evidence regarding the detection of membrane tension by TRPV4, for example in lipid bilayer reconstitution.

The substrate deflection activation indicates that in this particular setting (cell-substrate interface), TRPV4 is able to respond to a mechanical stimulus. Suggesting a direct activation of TRPV4 through a tether mechanism, like NOMPC channel. The current study additionally demonstrates that PLA2 is not required for TRPV4 activation by substrate deflections (Figure 32 in Results), in contrast to TRPV4 response to osmotic stress (Vriens et al. 2004; White et al. 2016; Vriens et al. 2007). Furthermore, the mechanosensitive response observed by substrate deflections is not affected by voltage (Figure 30 in Results) as other responses in which TRPV4 is involved, such as activation by 4αPDD (Watanabe, Vriens, et al. 2002; Watanabe, Davis, et al. 2002) or by arachidonic acid (Watanabe et al. 2003).

These data answer the long-standing question of whether TRPV4 is a mechanically gated ion channel, evaluating the criteria for considering a channel mechanosensitive (Christensen & Corey 2007), we observed that 1) TRPV4 is expressed in the cells that produce cartilage, which is a mechanosensitive tissue. 2) Ablation of TRPV4 impairs the substrate deflection response of cartilage and a specific antagonist inhibits 87% of the mechanically gated current in WT chondrocytes. 3) When TRPV4 is expressed in a heterologous system and stimulated with substrate deflections, inward mechanosensitive currents were observed. 4) The TRPV4 latency is shorter than 5 ms (1.5 ± 0.2 ms for mTRPV4 in comparison with 1.5 ± 0.2 ms for mPiezo1).

An important question remains: Why is TRPV4 specifically activated by substrate deflections? One explanation is that in this particular context the channel can encounter a proper molecular environment to respond, meaning that the channel is able to associate with the tether that allows it to detect and transmit force to the pore. For instance, it seems important that the cytoskeleton is not disrupted (contrary to the outside-out configuration in membrane stretch). This is supported by experiments performed with cytochalasin D in TRPV4-overexpressing HEK-293 cells (see Figure 31). There the latency of activation increased, suggesting that the connection with the actin cytoskeleton might be necessary for an efficient force transfer. However, the cells still displayed mechanosensitive currents, possibly because other components are participating in the response (microtubules, ECM proteins, transmembrane proteins, focal adhesion components or lipids). All these hypotheses need further research. More inhibitors can be used to study the individual contribution of microtubules (colchicine) or other cytoskeleton components. Additionally, knowing the interaction partners of the channel would provide insights into the role of the channel in the mechanosensitive response of chondrocytes. Also, the isolation of interaction partners of the channel would help to test the force-through-tethers hypothesis.

On the other hand, integrins have been implicated in diverse mechanosensitive pathways, and forces applied to β1 integrins resulted in calcium influx through TRPV4 (Matthews et al. 2010). Coupling of β1 integrins with extracellular magnetic beads was used to apply mechanical force to endothelial cells that were loaded with a calcium-sensitive dye. The activation of β1 integrins led to a calcium influx mediated by TRPV4 with a latency of 4 ms (Matthews et al. 2010). Additionally, TRPV4 has been shown to co-immunoprecipitate with β1 integrin in mouse fibroblasts (Arora et al. 2017). Together this evidence suggests that β1 integrin may function as a tether to mediate the force transfer that gates TRPV4. However, more research is needed to test whether β1 integrin blockade impairs the TRPV4 mechanical response to substrate deflection.

There is now a large amount of information about genetic diseases caused by mutations in the *Trpv4* gene is available. For instance, mutations in *Trpv4* cause gain of function, loss of function or trafficking problems (Landouré et al. 2010; Lamandé et al. 2011b; Inada et al. 2012; Nilius & Voets 2013). It would be interesting to know if some of these mutations, in particular mutations causing different type of chondroplasias or skeletal diseases differentially modulate the mechanosensitive response of TRPV4. Analysis of these mutations in the context of the tether model may also provide insights into how tethering works.

About Piezo1 mechanosensitivity

The mechanosensitive ion channel Piezo1 responds to cellular indentation, membrane stretch and to substrate deflections as was confirmed in our experiments (see overexpression experiments, Figure 26). Piezo1 is an exquisite mechanosensor that can be gated by lipid bilayer asymmetry (Coste et al. 2012; Syeda et al. 2016), and modulated by proteins such as Stoml3 (Poole et al. 2014) or ECM proteins like collagen IV (Gaub & Müller 2017), and the cytoskeleton (Cox et al. 2016) (model in Figure 37).

To test whether the cytoskeleton modulates Piezo1 gating, cell swelling was used to detach the plasma membrane from cytoskeleton. This leads to the formation of a membrane bubble without cytoskeleton (membrane bleb). Less tension was required to gate Piezo1 in membrane blebs (P_{50} = 4.5 mN/m) in comparison to the tension required in cell attached experiments that retain connections with the cytoskeleton (P_{50} = 5.1 mN/m) (Cox et al. 2016). Meaning that the actin cytoskeleton and microtubules have a constraining effect on Piezo1.

In the case of modulation by ECM, Gaub and colleagues performed experiments compressing Piezo1-overexpressing HEK-293 cells with an AFM cantilever (Gaub & Müller 2017). The authors observed that when the AFM probe was coated with an ECM protein, such as collagen IV, the Piezo1-dependent Ca^{2+} influx was observed with less pulling forces, suggesting that collagen IV sensitizes Piezo1-overexpressing HEK-293 cells (Gaub & Müller 2017).

In addition, scaffolding proteins such as Stoml3 also sensitize Piezo1 and Piezo2. In overexpression experiments it was shown that when Piezo1 and Stoml3 are co-expressed, Piezo1 is gated with smaller deflection in comparison to when Piezo1 is overexpressed alone (Poole et al. 2014). This together with a recent finding in neurons showing that Stoml3 association with cholesterol-rich domains modulates Piezos activity (Qi et al. 2015). All these data strongly suggest that Piezo channels have different modulation layers through their immediate environment, and the pillar array stimulation is a powerful technique that offers an

integration of the different complexity levels in a cell, including lipids, ECM proteins, cytoskeleton and modulatory proteins like Stoml3.

Currently, extensive information is known about the gating mechanism of Piezo1 within the lipid bilayer. However, it is necessary to broaden these studies to identify the channel modulators required for Piezo1 functions. These functions range from early vasculature development to cancer migration (Li et al. 2014; Ranade et al. 2014). Along this line, a new review by Nourse and Pathak, proposed an integrative view of the role of Piezo1 in which the channel can detect forces that come from the external environment as well as from inside the cell, for instance forces that are generated in microenvironments such as focal adhesions or during cell migration (Nourse et al 2017). This is a very interesting and integrative idea that highlights the role of Piezos as mechanosensors in excitable and non-excitable cells where mechanotransduction does not have to be extremely fast. Instead, Piezo mechanotransduction has a role in the maintenance of homeostasis and not only in the modulation and transmission of fast responses as happens in the generation of action potentials in neurons.

Every family of mechanosensitive ion channels has a different structure, which points to a convergent evolution to gain mechanosensitivity: different sequence, different structure, same function (as the wings in birds and bats). The different structure also promotes different interactions of each of these channels with its environment. However, structural and functional information about mechanosensitive channels have led Cox and Martinac to postulate a unifying principle for gating. Here they propose that even though there is a lack of sequence conservation, there is a minimal common structure in all mechanosensitive channels. The common denominator is a helix that appears horizontally to other helices that are coupled with the membrane which in turns interact with a pore-lining helix. This common structure can be a small or large helix that together with its location and the mechanical force from the bilayer can be converted into a conformational rearrangement to open the pore (Cox et al. 2016).

As we learned in this study, TRPV4 behaves as a mechanosensitive ion channel only in the proper environment, showing the defining characteristics of a mechanosensitive channel such as Piezo1 (Figure 29B). However, when TRPV4 is not in the proper location, no mechanosensitive response is observed, and the channel appears silent (as for cellular indentation, Figure 27B). This is incredibly relevant because the pillar array technique offers an environment that keeps the cellular component ensemble as in a physiological condition, and this can help us to better understand cellular mechanotransduction.

11 Conclusions

This thesis showed that the mechanosensitive ion channels Piezo1 and TRPV4 are expressed and active in primary murine chondrocytes. Chondrocytes are able to respond to different types of mechanical activation. In this study, currents triggered by membrane stretch and substrate deflections were observed in chondrocytes. In particular, the mechanical gated currents activated by membrane stretch require the expression of Piezo1. Both Piezo1 and TRPV4 mediate the currents activated by substrate deflections in chondrocytes. Therefore, an interesting finding is that Piezo1 and TRPV4 are activated by different yet overlapping mechanical stimuli in chondrocytes. Furthermore, this phenomenon can be tested in other cell types where these two channels show overlapping expression, such as bladder urothelium (Ihara, Mitsui, Nakamura, Kanda, et al. 2017; Ihara, Mitsui, Nakamura, Kira, et al. 2017; Miyamoto et al. 2014) or astrocytes in optic nerve (Choi et al. 2015) .

The ion channel TRPV4 is gated by substrate deflections and the results of this thesis support a force-through-tethers mechanism of activation. Further validation of this hypothesis may be confirmed via identification of interaction partners (i.e. tethers) of TRPV4 with immunoprecipitation and mass spectrometry analysis. Experiments using blockers of cytoskeleton components may in addition be used to determine the contribution of individual components, such as actin cytoskeleton or microtubules, to the activation of the channel.

In this thesis, a combination of techniques to stimulate mechanosensitive ion channels was used. This was proven to be a powerful method because we could understand why two unrelated proteins, Piezo1 and TRPV4 that function as mechanosensitive ion channels are differentially activated.

For the mechanosensitive ion channel field, the use of multiple techniques to compare and study the activation mechanisms was very important to elucidate different pathways of mechanoelectrical transduction in chondrocytes. Therefore, this approach could be used and extended by other groups to study these channels and gain a broader understanding about the activation mode of these specialized proteins. This is important because mechanosensitive ion channels have converged through evolution only in function but not in sequence or channel structure and they found different strategies for the activation mode.

12 References

Adams, M. a, 2006. The mechanical environment of chondrocytes in articular cartilage. *Biorheology*, 43(3–4), pp.537–545.

Adapala, R.K. et al., 2013. TRPV4 channels mediate cardiac fibroblast differentiation by integrating mechanical and soluble signals. *Journal of Molecular and Cellular Cardiology*, 54(1), pp.45–52.

Adelman, J.P., Maylie, J. & Sah, P., 2012. Small-Conductance Ca 2 + -Activated K + Channels : Form and Function.

Aigner, T. et al., 2007. Mechanisms of Disease : role of chondrocytes in the pathogenesis of osteoarthritis — structure , chaos and senescence REVIEW CRITERIA. , 3(7), pp.391–399.

Alessandri-Haber, N. et al., 2003. Hypotonicity induces TRPV4-mediated nociception in rat. *Neuron*, 39(3), pp.497–511.

Alessandri-Haber, N. et al., 2008. Interaction of transient receptor potential vanilloid 4, integrin, and SRC tyrosine kinase in mechanical hyperalgesia. *The Journal of neuroscience : the official journal of the Society for Neuroscience*, 28(5), pp.1046–1057.

Alessandri-Haber, N. et al., 2005. TRPV4 mediates pain-related behavior induced by mild hypertonic stimuli in the presence of inflammatory mediator. *Pain*, 118(1–2), pp.70–79.

Alvarez, D.F. et al., 2006. Transient receptor potential vanilloid 4-mediated disruption of the alveolar septal barrier: A novel mechanism of acute lung injury. *Circulation Research*, 99(9), pp.988–995.

Andolfo, I. et al., 2013. Multiple clinical forms of dehydrated hereditary stomatocytosis arise from mutations in PIEZO1. *Blood*, 121(19).

Andrea, P.D., 1996. GaD iunctions mediate intercellular cakbn signalling in cultured articular chondrocytes.

Andrea L., C. et al., 2010. Chondroprotective role of the osmotically-sensitive ion channel TRPV4: Age- and sex-dependent progression of osteoarthritis in Trpv4 deficient mice. *Arthritis Rheum*, 62(10), pp.2973–2983.

Araldi, E. & Schipani, E., 2010. Hypoxia, HIFs and bone development. *Bone*, 47(2), pp.190–196.

Árnadóttir, J. & Chalfie, M., 2010. Eukaryotic Mechanosensitive Channels. *Annual Review of Biophysics*, 39(1), pp.111–137. Available at: http://www.annualreviews.org/doi/10.1146/annurev.biophys.37.032807.125836.

Arora, P.D. et al., 2017. TRPV4 mediates the calcium influx required for Flightless-non-muscle myosin interaction and collagen remodeling. *Journal of Cell Science*, p.jcs.201665. Available at: http://www.ncbi.nlm.nih.gov/pubmed/28526784%0Ahttp://jcs.biologists.org/lookup/doi/10.1242/jcs.201665.

Bae, C., Sachs, F. & Gottlieb, P.A., 2011. The mechanosensitive ion channel Piezo1 is inhibited by the peptide GsMTx4. *Biochemistry*, 50(29), pp.6295–6300.

Barczyk, M. & Carracedo, S., 2010. At-a-glance article. , pp.269–280.

Benya, P.D. & Shaffer, J.D., 1982. Dedifferentiated Chondrocytes Reexpress the Differentiated Collagen Phenotype When Cultured in Agarose Gels. , 30(August), pp.215–224.

Brand, J.A., Mcalindon, T.E. & Zeng, L., 2012. A 3D System for Culturing Human Articular Chondrocytes in Synovial Fluid. , 4(January), pp.4–9.

Brohawn, S.G., del Mármol, J. & MacKinnon, R., 2012. Crystal structure of the human K2P TRAAK, a lipid- and mechano-sensitive K+ ion channel. *Science (New York, N.Y.)*, 335(6067), pp.436–41. Available at: /pmc/articles/PMC3329120/?report=abstract.

Brohawn, S.G., Su, Z. & MacKinnon, R., 2014. Mechanosensitivity is mediated directly by the lipid membrane in TRAAK and TREK1 K+ channels. *Proceedings of the National Academy of Sciences of the United States of America*, 111(9), pp.3614–9. Available at: http://www.pubmedcentral.nih.gov/articlerender.fcgi?artid=3948252&tool=pmcentrez&rend

ertype=abstract.
Buckwalter, J. a, Mankin, H.J. & Grodzinsky, A.J., 2005. Articular cartilage and osteoarthritis. *Instructional course lectures*, 54, pp.465–480. Available at: https://vpn2.uio.no/+CSCO+0h756767633A2F2F6A726F2E7A76672E727168++/cortiz/www/3.052/3.052CourseReader/26_BuckwalterArticularCartilage.pdf.
Burton-wurster, N. et al., 1993. Effect of Compressive Loading and Unloading on the Synthesis of Total Protein , Proteoglycan , and Fibronectin by Canine Cartilage Explants.
Buschmann, M.D. et al., 1995. Mechanical compression modulates matrix biosynthesis in chondrocyte/agarose culture. *J Cell Sci*, 108 (Pt 4, pp.1497–1508. Available at: http://www.ncbi.nlm.nih.gov/pubmed/7615670.
Cahalan, S.M. et al., 2015. Piezo1 links mechanical forces to red blood cell volume. *eLife*, 4(MAY).
Campagnola, P., 2011. Second harmonic generation imaging microscopy: Applications to diseases diagnostics. *Analytical Chemistry*, 83(9), pp.3224–3231.
Cao, D.-S., Yu, S.-Q. & Premkumar, L.S., 2009. Modulation of transient receptor potential Vanilloid 4-mediated membrane currents and synaptic transmission by protein kinase C. *Molecular pain*, 5, p.5.
Caron, M.M.J. et al., 2012. Redifferentiation of dedifferentiated human articular chondrocytes: Comparison of 2D and 3D cultures. *Osteoarthritis and Cartilage*, 20(10), pp.1170–1178.
Cescon, M. et al., 2015. Collagen VI at a glance. *Journal of cell science*, 128(19), pp.3525–31. Available at: http://www.ncbi.nlm.nih.gov/pubmed/26377767.
Chen, S.Y. et al., 2010. In vivo virtual biopsy of human skin by using noninvasive higher harmonic generation microscopy. *IEEE Journal on Selected Topics in Quantum Electronics*, 16(3), pp.478–492.
Chesler, A.T. et al., 2016. The Role of {PIEZO2} in Human Mechanosensation. *New Engl J Medicine*, 375(14), pp.1355–1364.
Choi, H.J., Sun, D. & Jakobs, T.C., 2015. Astrocytes in the optic nerve head express putative mechanosensitive channels. *Molecular vision*, 21(January), pp.749–66. Available at: http://www.pubmedcentral.nih.gov/articlerender.fcgi?artid=4502055&tool=pmcentrez&rendertype=abstract.
Christensen, A.P. & Corey, D.P., 2007. TRP channels in mechanosensation: direct or indirect activation? *Nature Reviews Neuroscience*, 8(7), pp.510–521. Available at: http://www.nature.com/doifinder/10.1038/nrn2149.
Clark, A.L. et al., 2010. Chondroprotective role of the osmotically sensitive ion channel transient receptor potential vanilloid 4: Age- and sex-dependent progression of osteoarthritis in Trpv4-deficient mice. *Arthritis and Rheumatism*, 62(10), pp.2973–2983.
Cohen, N.P., Foster, R.J. & Mow, V.C., 1998. Composition and dynamics of articular cartilage: structure, function, and maintaining healthy state. *The Journal of orthopaedic and sports physical therapy*, 28(4), pp.203–15. Available at: http://www.ncbi.nlm.nih.gov/pubmed/9785256.
Conklin, M.W. et al., 2011. Aligned collagen is a prognostic signature for survival in human breast carcinoma. *American Journal of Pathology*, 178(3), pp.1221–1232.
Conor, C.J.O. et al., 2014. TRPV4-mediated mechanotransduction regulates the metabolic response of chondrocytes to dynamic loading. , 111(4), pp.1–6.
Cortright, D.N., Krause, J.E. & Broom, D.C., 2007. TRP channels and pain. *Biochimica et Biophysica Acta - Molecular Basis of Disease*, 1772(8), pp.978–988.
Coste, B., Houge, G., Murray, M.F., Stitziel, N., Bandell, M. & Giovanni, M.A., 2013. Gain-of-function mutations in the mechanically activated ion channel PIEZO2 cause a subtype of Distal Arthrogryposis. , 110(12).
Coste, B., Houge, G., Murray, M.F., Stitziel, N., Bandell, M., Giovanni, M.A., et al., 2013. Gain-of-function mutations in the mechanically activated ion channel PIEZO2 cause a subtype of Distal Arthrogryposis. *Proceedings of the National Academy of Sciences of the United States of America*,

110(12), pp.4667–72. Available at: http://www.pubmedcentral.nih.gov/articlerender.fcgi?artid=3607045&tool=pmcentrez&rendertype=abstract.
Coste, B. et al., 2010. Piezo1 and Piezo2 are essential components of distinct mechanically activated cation channels. *Science (New York, N.Y.)*, 330(6000), pp.55–60. Available at: http://www.pubmedcentral.nih.gov/articlerender.fcgi?artid=3062430&tool=pmcentrez&rendertype=abstract.
Coste, B. et al., 2012. Piezo proteins are pore-forming subunits of mechanically activated channels. *Nature*, 483, pp.176–181.
Cox, C.D. et al., 2016. Removal of the mechanoprotective influence of the cytoskeleton reveals PIEZO1 is gated by bilayer tension. *Nature Communications*, 7, pp.1–13. Available at: http://dx.doi.org/10.1038/ncomms10366.
Cox, C.D., Bavi, N. & Martinac, B., 2016. Origin of the Force: The Force-From-Lipids Principle Applied to Piezo Channels. *Current Topics in Membranes*.
Cox, G. & Kable, E., 2006. Second-harmonic imaging of collagen. *Methods in molecular biology (Clifton, N.J.)*, 319(1), pp.15–35.
D'Andrea, P. et al., 2000. Intercellular Ca ^2+ waves in mechanically stimulated articular chondrocytes. *Biorheology*, 37(1), pp.75–83.
Degala, S., Zipfel, W.R. & Bonassar, L.J., 2011. Chondrocyte calcium signaling in response to fluid flow is regulated by matrix adhesion in 3-D alginate scaffolds. *Archives of Biochemistry and Biophysics*, 505(1), pp.112–117.
Dreier, R., 2010. Hypertrophic diff erentiation of chondrocytes in osteoarthritis : the developmental aspect of degenerative joint disorders.
Dy, P. et al., 2012. Sox9 Directs Hypertrophic Maturation and Blocks Osteoblast Differentiation of Growth Plate Chondrocytes. *Developmental Cell*, 22(3), pp.597–609.
Earley, S. et al., 2009. TRPV4-dependent dilation of peripheral resistance arteries influences arterial pressure. *American journal of physiology. Heart and circulatory physiology*, 297(3), pp.H1096–H1102.
Ernstrom, G.G. & Chalfie, M., 2002. Genetics of sensory mechanotransduction. *Annual review of genetics*, 36, pp.411–53. Available at: http://www.ncbi.nlm.nih.gov/pubmed/12429699.
Everaerts, W., Nilius, B. & Owsianik, G., 2010. The vanilloid transient receptor potential channel TRPV4: From structure to disease. *Progress in Biophysics and Molecular Biology*, 103(1), pp.2–17.
Filosa, J.A., Yao, X. & Rath, G., 2013. TRPV4 and the regulation of vascular tone. *Journal of cardiovascular pharmacology*, 61(2), pp.113–9. Available at: http://www.pubmedcentral.nih.gov/articlerender.fcgi?artid=3564998&tool=pmcentrez&rendertype=abstract.
Fitzgerald, J.B. et al., 2004. Mechanical Compression of Cartilage Explants Induces Multiple Time-dependent Gene Expression Patterns and Involves Intracellular Calcium and Cyclic AMP. *Journal of Biological Chemistry*, 279(19), pp.19502–19511.
Gandolfi, B. et al., 2016. A dominant TRPV4 variant underlies osteochondrodysplasia in Scottish fold cats. *Osteoarthritis and Cartilage*, 24(8), pp.1441–1450.
Gao, X., Wu, L. & O'Neil, R.G., 2003. Temperature-modulated diversity of TRPV4 channel gating: Activation by physical stresses and phorbol ester derivatives through protein kinase C-dependent and -independent pathways. *Journal of Biological Chemistry*, 278(29), pp.27129–27137.
Garcia, M. & Knight, M.M., 2010. Cyclic loading opens hemichannels to release ATP as part of a chondrocyte mechanotransduction pathway. *Journal of Orthopaedic Research*, 28(4), pp.510–515.
Gaub, B.M. & M??ller, D.J., 2017. Mechanical Stimulation of Piezo1 Receptors Depends on Extracellular

Matrix Proteins and Directionality of Force. *Nano Letters*, 17(3), pp.2064–2072.
Ge, J. et al., 2015. Architecture of the mammalian mechanosensitive Piezo1 channel. *Nature*, 527(7576), pp.64–69. Available at: http://dx.doi.org/10.1038/nature15247.
Gevaert, T. et al., 2007. Deletion of the transient receptor potential cation channel TRPV4 impairs murine bladder voiding. *Journal of Clinical Investigation*, 117(11), pp.3453–3462.
Gnanasambandam, R. et al., 2015. Ionic selectivity and permeation properties of human PIEZO1 channels. *PLoS ONE*, 10(5).
Goldring, M.B. & Marcu, K.B., 2009. Cartilage homeostasis in health and rheumatic diseases. *Arthritis research & therapy*, 11(3), p.224. Available at: http://www.ncbi.nlm.nih.gov/pubmed/19519926%5Cnhttp://www.pubmedcentral.nih.gov/articlerender.fcgi?artid=PMC2714092.
Gosset, M. et al., 2008. Primary culture and phenotyping of murine chondrocytes. , 3(8), pp.1253–1260.
Gottlieb, P.A., Bae, C. & Sachs, F., 2012. Gating the mechanical channel Piezo1: a comparison between whole-cell and patch recording. *Channels (Austin, Tex.)*, 6(4), pp.282–289.
Gottlieb, P.A. & Sachs, F., 2012. Piezo1: properties of a cation selective mechanical channel. *Channels (Austin, Tex.)*, 6(4), pp.214–219.
Graff, R.D. et al., 2000. ATP release by mechanically loaded porcine chondrons in pellet culture. *Arthritis and Rheumatism*, 43(7), pp.1571–1579.
Grodzinsky, A.J. et al., 2000. Cartilage tissue remodeling in response to mechanical forces. *Annual review of biomedical engineering*, 2, pp.691–713.
Gudipaty, S.A. et al., 2017. Mechanical stretch triggers rapid epithelial cell division through Piezo1. *Nature*, 543(7643), pp.118–121. Available at: http://www.nature.com/doifinder/10.1038/nature21407.
Guilak, F. et al., 1999. Mechanically induced calcium waves in articular chondrocytes are inhibited by gadolinium and amiloride. *Journal of Orthopaedic Research*, 17(3), pp.421–429.
Guilak, F. et al., 1994. The effects of matrix compression on proteoglycan metabolism in articular cartilage explants. *Osteoarthritis and Cartilage*, 2(2), pp.91–101.
Guo, J., Jourdian, G.W. & I, D.K.M., 1989. CULTURE AND GROWTH CHARACTERISTICS OF CHONDROCYTES ENCAPSULATED IN ALGINATE BEADS. , 19, pp.277–297.
Haliloglu, G. et al., 2016. Recessive PIEZO2 stop mutation causes distal arthrogryposis with distal muscle weakness, scoliosis and proprioception defects. *Journal of Human Genetics*, (August), pp.1–5. Available at: http://www.nature.com/doifinder/10.1038/jhg.2016.153.
Hamanaka, K. et al., 2007. TRPV4 initiates the acute calcium-dependent permeability increase during ventilator-induced lung injury in isolated mouse lungs. *American journal of physiology. Lung cellular and molecular physiology*, 293(4), pp.L923–L932.
Han, L., Grodzinsky, A.J. & Ortiz, C., 2011. Nanomechanics of the Cartilage Extracellular Matrix. *Annual review of materials research*, 41, pp.133–168. Available at: http://www.pubmedcentral.nih.gov/articlerender.fcgi?artid=3392687&tool=pmcentrez&rendertype=abstract.
Han, S.-K. et al., 2012. Mechanically induced calcium signaling in chondrocytes in situ. *Journal of Orthopaedic Research*, 30(3), pp.475–481. Available at: http://doi.wiley.com/10.1002/jor.21536.
Hartmannsgruber, V. et al., 2007. Arterial response to shear stress critically depends on endothelial TRPV4 expression. *PLoS ONE*, 2(9).
Häse, C.C., Le Dain, A.C. & Martinac, B., 1995. Purification and functional reconstitution of the recombinant large mechanosensitive ion channel (MscL) of Escherichia coli. *Journal of Biological Chemistry*, 270(31), pp.18329–18334.
Heino, J., 2007. The collagen family members as cell adhesion proteins. *BioEssays : news and reviews in molecular, cellular and developmental biology*, 29(10), pp.1001–10. Available at:

http://www.ncbi.nlm.nih.gov/pubmed/17876790.
Ho, T.C. et al., 2012. Evidence TRPV4 contributes to mechanosensitive ion channels in mouse skeletal muscle fibers. *Channels (Austin, Tex.)*, 6(4), pp.246–254.
Honoré, E. et al., 2006. Desensitization of mechano-gated K2P channels. *Proceedings of the National Academy of Sciences of the United States of America*, 103(18), pp.6859–6864.
Ihara, T., Mitsui, T., Nakamura, Y., Kira, S., et al., 2017. Clock genes regulate the circadian Expression of Piezo1, TRPV4, Connexin26, and VNUT in an Ex Vivo Mouse Bladder Mucosa. *PLoS ONE*, 12(1).
Ihara, T., Mitsui, T., Nakamura, Y., Kanda, M., et al., 2017. The Circadian expression of Piezo1, TRPV4, Connexin26, and VNUT, associated with the expression levels of the clock genes in mouse primary cultured urothelial cells. *Neurourology and urodynamics*. Available at: http://www.ncbi.nlm.nih.gov/pubmed/28881406.
Ikeda, R. et al., 2014. Merkel cells transduce and encode tactile stimuli to drive aβ-Afferent impulses. *Cell*, 157(3), pp.664–675.
Inada, H. et al., 2012. Structural and biochemical consequences of disease-causing mutations in the ankyrin repeat domain of the human TRPV4 channel. *Biochemistry*, 51(31), pp.6195–6206.
Janssen, D.A.W. et al., 2016. TRPV4 channels in the human urogenital tract play a role in cell junction formation and epithelial barrier. *Acta Physiologica*.
Jian, M.Y. et al., 2008. High vascular pressure-induced lung injury requires P450 epoxygenase-dependent activation of TRPV4. *American Journal of Respiratory Cell and Molecular Biology*, 38(4), pp.386–392.
Kang, D., Choe, C. & Kim, D., 2005. Thermosensitivity of the two-pore domain K + channels TREK-2 and TRAAK. *J Physiol*, 5641, pp.103–116.
Kang, D. & Kim, D., 2006. TREK-2 (K2P10.1) and TRESK (K2P18.1) are major background K+ channels in dorsal root ganglion neurons. *American journal of physiology. Cell physiology*, 291(1), pp.C138–C146.
Katta, S., Krieg, M. & Goodman, M.B., 2015. Feeling Force: Physical and Physiological Principles Enabling Sensory Mechanotransduction. *Annual Review of Cell and Developmental Biology*, 31(1), pp.347–371. Available at: http://www.annualreviews.org/doi/10.1146/annurev-cellbio-100913-013426.
Kaupp, J.A., Weber, J.F. & Waldman, S.D., 2012. Mechanical Stimulation of Chondrocyte-agarose Hydrogels. , (October), pp.1–5.
Kellenberger, S. & Schild, L., 2002. Epithelial Sodium Channel/Degenerin Family of Ion Channels: A Variety of Functions for a Shared Structure. *Physiological Reviews*, 82(3), pp.735–767. Available at: http://physrev.physiology.org/lookup/doi/10.1152/physrev.00007.2002.
Kirkpatrick, N.D., Brewer, M.A. & Utzinger, U., 2007. Endogenous optical biomarkers of ovarian cancer evaluated with multiphoton microscopy. *Cancer Epidemiology Biomarkers and Prevention*, 16(10), pp.2048–2057.
Kono, T. et al., 2006. Spontaneous oscillation and mechanically induced calcium waves in chondrocytes. , (December 2005), pp.103–111.
Koser, D.E. et al., 2016. Mechanosensing is critical for axon growth in the developing brain. *Nature neuroscience*, accepted(September), pp.1–11. Available at: http://dx.doi.org/10.1038/nn.4394%5Cnhttp://www.ncbi.nlm.nih.gov/pubmed/27643431.
Kuettner, K.E., 1992. Biochemistry of articular cartilage in health and disease. *Clinical Biochemistry*, 25(3), pp.155–163.
Lamandé, S.R. et al., 2011a. Mutations in TRPV4 cause an inherited arthropathy of hands and feet. *Nature Genetics*, 43(11), pp.1142–1146. Available at: http://dx.doi.org/10.1038/ng.945.
Lamandé, S.R. et al., 2011b. Mutations in TRPV4 cause an inherited arthropathy of hands and feet. *Nature genetics*, 43(11), pp.1142–6. Available at: http://www.ncbi.nlm.nih.gov/pubmed/21964574.
Landouré, G. et al., 2010. Mutations in TRPV4 cause Charcot-Marie-Tooth disease type 2C. *Nature*

genetics, 42(2), pp.170–174. Available at: http://dx.doi.org/10.1038/ng.512.
Layman, D.L., Sokoloff, L. & Miller, E.J., 1972. Collagen synthesis by articular chondrocytes in monolayer culture. *Experimental Cell Research*, 73(1), pp.107–112.
Lechner, S.G. et al., 2011. The molecular and cellular identity of peripheral osmoreceptors. *Neuron*, 69(2), pp.332–344.
Lee, D.A. et al., 2000. The influence of mechanical loading on isolated chondrocytes seeded in agarose constructs. , 37, pp.149–161.
Lee, H. et al., 2005. Altered Thermal Selection Behavior in Mice Lacking Transient Receptor Potential Vanilloid 4. *The Journal of Neuroscience*, 25(5), pp.1304–1310. Available at: http://www.jneurosci.org/content/25/5/1304.abstract%5Cnhttp://www.jneurosci.org/content/25/5/1304.full.pdf%5Cnhttp://www.jneurosci.org/content/25/5/1304.long.
Lee, H.S. et al., 2000. Integrin and mechanosensitive ion channel-dependent tyrosine phosphorylation of focal adhesion proteins and beta-catenin in human articular chondrocytes after mechanical stimulation. *J Bone Miner Res*, 15(8), pp.1501–1509. Available at: http://www.ncbi.nlm.nih.gov/entrez/query.fcgi?cmd=Retrieve&db=PubMed&dopt=Citation&list_uids=10934648.
Lee, W., Leddy, H.A., et al., 2014. Synergy between Piezo1 and Piezo2 channels confers high-strain mechanosensitivity to articular cartilage. *Proceedings of the National Academy of Sciences*, 111(47), pp.E5114–E5122. Available at: http://www.pnas.org/lookup/doi/10.1073/pnas.1414298111 [Accessed February 9, 2017].
Lee, W., Leddy, H.A., et al., 2014. Synergy between Piezo1 and Piezo2 channels confers high-strain mechanosensitivity to articular cartilage. *Proceedings of the National Academy of Sciences of the United States of America*, 111(47), pp.E5114-22. Available at: http://www.pubmedcentral.nih.gov/articlerender.fcgi?artid=4250098&tool=pmcentrez&rendertype=abstract.
Lefebvre, V., Behringer, R.R. & De Crombrugghe, B., 2001. L-Sox5, Sox6 and SOx9 control essential steps of the chondrocyte differentiation pathway. *Osteoarthritis and Cartilage*, 9(SUPPL. A).
Leung, V.Y.L. et al., 2011. SOX9 governs differentiation stage-specific gene expression in growth plate chondrocytes via direct concomitant transactivation and repression. *PLoS Genetics*, 7(11).
Levina, N. et al., 1999. Protection of Escherichia coli cells against extreme turgor by activation of MscS and MscL mechanosensitive channels: identification of genes required for MscS activity. *The EMBO journal*, 18(7), pp.1730–7. Available at: http://www.pubmedcentral.nih.gov/articlerender.fcgi?artid=1171259&tool=pmcentrez&rendertype=abstract.
Lewis, A.H. & Grandl, J., 2015. Mechanical sensitivity of Piezo1 ion channels can be tuned by cellular membrane tension. *eLife*, 4(December2015).
Li, J. et al., 2014. Piezo1 integration of vascular architecture with physiological force. *Nature*, 515(7526), pp.279–282. Available at: http://www.ncbi.nlm.nih.gov/pubmed/25119035.
Liedtke, W., 2008. Molecular mechanisms of TRPV4-mediated neural signaling. In *Annals of the New York Academy of Sciences*. pp. 42–52.
Liedtke, W. et al., 2000. Vanilloid Receptor–Related Osmotically Activated Channel (VR-OAC), a Candidate Vertebrate Osmoreceptor. *Cell*, 103(3), pp.525–535. Available at: http://linkinghub.elsevier.com/retrieve/pii/S0092867400001434.
Liedtke, W. & Friedman, J.M., 2003. Abnormal osmotic regulation in trpv4-/- mice. *Proceedings of the National Academy of Sciences of the United States of America*, 100(23), pp.13698–13703.
Lin, S.-H. et al., 2016. Evidence for the involvement of ASIC3 in sensory mechanotransduction in proprioceptors. *Nature communications*, 7(May), p.11460. Available at: http://www.nature.com/doifinder/10.1038/ncomms11460%5Cnhttp://www.ncbi.nlm.nih.gov/pubmed/27161260%5Cnhttp://www.pubmedcentral.nih.gov/articlerender.fcgi?artid=PMC4866049.

Litwic, A. et al., 2013. Epidemiology and burden of osteoarthritis. *British Medical Bulletin*, 105(1), pp.185–199.

Loot, A.E. et al., 2008. Role of cytochrome P450-dependent transient receptor potential V4 activation in flow-induced vasodilatation. *Cardiovascular Research*, 80(3), pp.445–452.

Loukin, S. et al., 2010. Wild-type and brachyolmia-causing mutant TRPV4 channels respond directly to stretch force. *Journal of Biological Chemistry*, 285(35), pp.27176–27181.

Lovell-Badge, R.H. et al., 1987. Tissue-specific expression of the human type II collagen gene in mice. *Proc Natl Acad Sci U S A*, 84(9), pp.2803–2807. Available at: http://www.ncbi.nlm.nih.gov/entrez/query.fcgi?cmd=Retrieve&db=PubMed&dopt=Citation&list_uids=3033664.

Lu, X.L. & Mow, V.C., 2008. Biomechanics of articular cartilage and determination of material properties. *Medicine and Science in Sports and Exercise*, 40(2), pp.193–199.

Ma, B. et al., 2013. Gene expression profiling of dedifferentiated human articular chondrocytes in monolayer culture. *Osteoarthritis and Cartilage*, 21(4), pp.599–603. Available at: http://linkinghub.elsevier.com/retrieve/pii/S1063458413000381.

Maingret, F. et al., 2000. Lysophospholipids open the two-pore domain mechano-gated K+ channels TREK-1 and TRAAK. *Journal of Biological Chemistry*, 275(14), pp.10128–10133.

Maksimovic, S. et al., 2014. Epidermal Merkel cells are mechanosensory cells that tune mammalian touch receptors. *Nature*, 509(7502), pp.617–21. Available at: http://www.ncbi.nlm.nih.gov/pubmed/24717432.

Mansour, J.M., 2009. Biomechanics of Cartilage. *Kinesiology: the mechanics and pathomechanics of human movement*, pp.66–79.

Marrelli, S.P. et al., 2007. PLA2 and TRPV4 channels regulate endothelial calcium in cerebral arteries. *American journal of physiology. Heart and circulatory physiology*, 292(3), pp.H1390-7. Available at: http://www.ncbi.nlm.nih.gov/pubmed/17071727.

Martinac, B., 2001. Mechanosensitive channels in prokaryotes. *Cellular Physiology and Biochemistry*, 11(2), pp.61–76.

Martinac, B., Adler, J. & Kung, C., 1990. Mechanosensitive Ion Channels of E. coli activated by amphipaths. *Letters to Nature*, 348, p.261.

Masuyama, R. et al., 2008. TRPV4-Mediated Calcium Influx Regulates Terminal Differentiation of Osteoclasts. *Cell Metabolism*, 8(3), pp.257–265.

Matthews, B.D. et al., 2010. Ultra-rapid activation of TRPV4 ion channels by mechanical forces applied to cell surface β1 integrins. *Integrative Biology*, 2(9), p.435. Available at: http://xlink.rsc.org/?DOI=c0ib00034e.

McGloughlin, T.M., 2011. *Studies in Mechanobiology , Tissue Engineering and Biomaterials*,

McMillin, M.J. et al., 2014. Mutations in PIEZO2 cause Gordon syndrome, Marden-Walker Syndrome, and distal arthrogryposis type 5. *American Journal of Human Genetics*, 94(5), pp.734–744.

Medhurst, A.D. et al., 2001. Distribution analysis of human two pore domain potassium channels in tissues of the central nervous system and periphery. *Molecular Brain Research*, 86(1–2), pp.101–114.

Mendoza, S. et al., 2010. TRPV4-mediated endothelial Ca2+ influx and vasodilation in response to shear stress. *American Journal of Physiology. Heart and Circulatory Physiology*, 298(December 2009), pp.H466-76. Available at: http://www.pubmedcentral.nih.gov/articlerender.fcgi?artid=2822567&tool=pmcentrez&rendertype=abstract.

Millward-sadler, S.J. et al., 2004. ATP in the mechanotransduction pathway of normal human chondrocytes. , 41, pp.567–575.

Millward-Sadler, S.J. et al., 2000. Altered electrophysiological responses to mechanical stimulation and abnormal signalling through α5β1 integrin in chondrocytes from osteoarthritic cartilage. *Osteoarthritis and Cartilage*, 8(4), pp.272–278.

Millward-Sadler, S.J. et al., 1999. Integrin-regulated secretion of interleukin 4: A novel pathway of mechanotransduction in human articular chondrocytes. *Journal of Cell Biology*, 145(1), pp.183–189.

Millward-Sadler, S.J. & Salter, D.M., 2004. Integrin-dependent signal cascades in chondrocyte mechanotransduction. *Annals of Biomedical Engineering*, 32(3), pp.435–446.

Minegishi, Y., Hosokawa, K. & Tsumaki, N., 2013. Time-lapse observation of the dedifferentiation process in mouse chondrocytes using chondrocyte-specific reporters. *Osteoarthritis and Cartilage*, 21(12), pp.1968–1975.

Miyamoto, T. et al., 2014. Functional role for Piezo1 in stretch-evoked Ca^{2+} influx and ATP release in urothelial cell cultures. *The Journal of biological chemistry*, 289(23), pp.16565–75. Available at: http://www.ncbi.nlm.nih.gov/pubmed/24759099.

Mizuno, A. et al., 2003. Impaired osmotic sensation in mice lacking TRPV4. *American journal of physiology. Cell physiology*, 285(1), pp.C96–C101.

Mobasheri, a et al., 2002. Integrins and stretch activated ion channels; putative components of functional cell surface mechanoreceptors in articular chondrocytes. *Cell biology international*, 26(1), pp.1–18.

Mochizuki, T. et al., 2009. The TRPV4 cation channel mediates stretch-evoked Ca2+ influx and ATP release in primary urothelial cell cultures. *Journal of Biological Chemistry*, 284(32), pp.21257–21264.

Mouw, J.K., Imler, S.M. & Levenston, M.E., 2007. Ion-channel regulation of chondrocyte matrix synthesis in 3D culture under static and dynamic compression. *Biomechanics and Modeling in Mechanobiology*, 6(1–2), pp.33–41.

Mow, V.C., Holmes, M.H. & Michael Lai, W., 1984. Fluid transport and mechanical properties of articular cartilage: A review. *Journal of Biomechanics*, 17(5), pp.377–394.

Muramatsu, S. et al., 2007. Functional gene screening system identified TRPV4 as a regulator of chondrogenic differentiation. *Journal of Biological Chemistry*, 282(44), pp.32158–32167.

Nilius, B. et al., 2004. TRPV4 calcium entry channel: a paradigm for gating diversity. *American journal of physiology. Cell physiology*, 286(2), pp.C195–C205.

Nilius, B. & Owsianik, G., 2010. Channelopathies converge on TRPV4. *Nature genetics*, 42(2), pp.98–100. Available at: http://dx.doi.org/10.1038/ng0210-98.

Nilius, B. & Voets, T., 2013. The puzzle of TRPV4 channelopathies. *EMBO reports*, 14(11), pp.152–163.

Nilius, B., Watanabe, H. & Vriens, J., 2003. The TRPV4 channel: structure-function relationship and promiscuous gating behaviour. *Pflügers Archiv : European journal of physiology*, 446(3), pp.298–303. Available at: http://www.ncbi.nlm.nih.gov/pubmed/12715179.

Noel, J. et al., 2009. The mechano-activated K+ channels TRAAK and TREK-1 control both warm and cold perception. *The EMBO journal*, 28(9), pp.1308–1318. Available at: http://www.ncbi.nlm.nih.gov/pubmed/19279663%5Cnhttp://dx.doi.org/10.1038/emboj.2009.57%5Cnhttp://www.nature.com/emboj/journal/v28/n9/full/emboj200957a.html%5Cnhttp://www.nature.com/emboj/journal/v28/n9/pdf/emboj200957a.pdf.

Nomura, T. et al., 2012. Differential effects of lipids and lyso-lipids on the mechanosensitivity of the mechanosensitive channels MscL and MscS. *Proceedings of the National Academy of Sciences*, 109(22), pp.8770–8775. Available at: http://www.pnas.org/cgi/doi/10.1073/pnas.1200051109.

O'Conor, C.J. et al., 2016. Cartilage-Specific Knockout of the Mechanosensory Ion Channel TRPV4 Decreases Age-Related Osteoarthritis. *Scientific Reports*, 6, p.29053. Available at: http://www.nature.com/articles/srep29053.

O'Conor, C.J. et al., 2013. Increased susceptibility of Trpv4-deficient mice to obesity and obesity-induced osteoarthritis with very high-fat diet. *Annals of the rheumatic diseases*, 72(2), pp.300–4. Available at: http://www.pubmedcentral.nih.gov/articlerender.fcgi?artid=3549299&tool=pmcentrez&rend

ertype=abstract.
O'Conor, C.J. et al., 2014. TRPV4-mediated mechanotransduction regulates the metabolic response of chondrocytes to dynamic loading. *Proceedings of the National Academy of Sciences of the United States of America*, 111(4), pp.1316–21. Available at: http://www.ncbi.nlm.nih.gov/pubmed/24474754%5Cnhttp://www.pubmedcentral.nih.gov/articlerender.fcgi?artid=PMC3910592.
Oldershaw, R.A. et al., 2010. Directed differentiation of human embryonic stem cells toward chondrocytes. *Nature Biotechnology*, 28(11), pp.1187–1194. Available at: http://www.nature.com/doifinder/10.1038/nbt.1683.
Patel, A.J., Lazdunski, M. & Honoré, E., 2001. Lipid and mechano-gated 2P domain K+ channels. *Current Opinion in Cell Biology*, 13(4), pp.422–427.
Peyronnet, R. et al., 2013. Piezo1-dependent stretch-activated channels are inhibited by Polycystin-2 in renal tubular epithelial cells. *EMBO reports*, 14(12), pp.1143–8. Available at: http://www.pubmedcentral.nih.gov/articlerender.fcgi?artid=3981085&tool=pmcentrez&rendertype=abstract.
Phan, M.N. et al., 2009. Functional characterization of TRPV4 as an osmotically sensitive ion channel in porcine articular chondrocytes. *Arthritis and Rheumatism*, 60(10), pp.3028–3037.
Pingguan-Murphy, B. et al., 2005. Activation of chondrocytes calcium signalling by dynamic compression is independent of number of cycles. *Archives of Biochemistry and Biophysics*, 444(1), pp.45–51.
Pingguan-Murphy, B. et al., 2006. Cyclic compression of chondrocytes modulates a purinergic calcium signalling pathway in a strain rate- and frequency-dependent manner. *Journal of Cellular Physiology*, 209(2), pp.389–397.
Plant, T.D. & Strotmann, R., 2007. *TRPV4: A Multifunctional Nonselective Cation Channel with Complex Regulation*, Available at: http://www.ncbi.nlm.nih.gov/pubmed/21204492.
Poole, C. a, 1997. Articular cartilage chondrons: form, function and failure. *Journal of anatomy*, 191 (Pt 1, pp.1–13.
Poole, C. a, Ayad, S. & Gilbert, R.T., 1992. Chondrons from articular cartilage. V. Immunohistochemical evaluation of type VI collagen organisation in isolated chondrons by light, confocal and electron microscopy. *Journal of cell science*, 103 (Pt 4, pp.1101–1110.
Poole, K. et al., 2014. Tuning Piezo ion channels to detect molecular-scale movements relevant for fine touch. *Nature communications*, 5, p.3520. Available at: http://www.pubmedcentral.nih.gov/articlerender.fcgi?artid=3973071&tool=pmcentrez&rendertype=abstract.
Preibisch, S., Saalfeld, S. & Tomancak, P., 2009. Globally optimal stitching of tiled 3D microscopic image acquisitions. *Bioinformatics*, 25(11), pp.1463–1465.
Prieto, M.L. et al., 2017. Mechanical Activation Of Piezo1 But Not Nav1.2 Channels By Ultrasound. *bioRxiv*, p.136994. Available at: http://www.biorxiv.org/content/early/2017/08/30/136994.
Prole, D.L. & Taylor, C.W., 2013. Identification and Analysis of Putative Homologues of Mechanosensitive Channels in Pathogenic Protozoa. *PLoS ONE*, 8(6).
Provenzano, P.P. et al., 2006. Collagen reorganization at the tumor-stromal interface facilitates local invasion. *BMC Medicine*, 4(1), p.38. Available at: http://bmcmedicine.biomedcentral.com/articles/10.1186/1741-7015-4-38.
Qi, Y. et al., 2015. Membrane stiffening by STOML3 facilitates mechanosensation in sensory neurons. *Nature Communications*, 6, p.8512. Available at: http://www.nature.com/doifinder/10.1038/ncomms9512.
Quinn, T.M. et al., 1998. Mechanical compression alters proteoglycan deposition and matrix deformation around individual cells in cartilage explants. *Journal of cell science*, 111 (Pt 5, pp.573–83. Available at: http://www.ncbi.nlm.nih.gov/pubmed/9454731.
Ranade, S.S. et al., 2014. Piezo1, a mechanically activated ion channel, is required for vascular

development in mice. *Proceedings of the National Academy of Sciences of the United States of America*, 111(28), pp.10347–52. Available at: http://www.pnas.org/content/111/28/10347.full.

Ranade, S.S. et al., 2014. Piezo2 is the major transducer of mechanical forces for touch sensation in mice. *Nature*, 516(7529), pp.121–125. Available at: http://www.pubmedcentral.nih.gov/articlerender.fcgi?artid=4380172&tool=pmcentrez&rendertype=abstract.

van der Rest, M. & Garrone, R., 1991. Collagen family of proteins. *FASEB journal : official publication of the Federation of American Societies for Experimental Biology*, 5(13), pp.2814–23. Available at: http://www.ncbi.nlm.nih.gov/pubmed/1916105.

Ricard-Blum, S., 2011. The Collagen Family. *Cold Spring Harbor Perspectives in Biology*, 3(1), pp.1–19.

Roberts, S.R. et al., 2001. Mechanical compression influences intracellular Ca2+ signaling in chondrocytes seeded in agarose constructs. *Journal of applied physiology (Bethesda, Md. : 1985)*, 90(4), pp.1385–1391.

du Roure, O. et al., 2005. Force mapping in epithelial cell migration. *Proceedings of the National Academy of Sciences*, 102(7), pp.2390–2395. Available at: http://www.pnas.org/cgi/doi/10.1073/pnas.0408482102.

Schmittgen, T.D. & Livak, K.J., 2008. Analyzing real-time PCR data by the comparative C T method. , 3(6), pp.1101–1108.

Shen, J. et al., 2006. Functional expression of transient receptor potential vanilloid 4 in the mouse cochlea. *Neuroreport*, 17(2), pp.135–9. Available at: http://www.ncbi.nlm.nih.gov/pubmed/16407759.

Sokabe, T. et al., 2010. The TRPV4 channel contributes to intercellular junction formation in keratinocytes. *Journal of Biological Chemistry*, 285(24), pp.18749–18758.

Sonkusare, S.K. et al., 2012. Elementary Ca2+ Signals Through Endothelial TRPV4 Channels Regulate Vascular Function. *Science*, 336(6081), pp.597–601. Available at: http://www.sciencemag.org/cgi/doi/10.1126/science.1216283.

Sophia Fox, A.J., Bedi, A. & Rodeo, S.A., 2009. The basic science of articular cartilage: structure, composition, and function. *Sports health*, 1(6), pp.461–8. Available at: http://www.ncbi.nlm.nih.gov/pubmed/23015907%5Cnhttp://www.ncbi.nlm.nih.gov/pubmed/23015907.

Sophia Fox, A.J., Bedi, A. & Rodeo, S. a, 2009. The basic science of articular cartilage: structure, composition, and function. *Sports health*, 1(6), pp.461–8. Available at: http://www.ncbi.nlm.nih.gov/pubmed/23015907%5Cnhttp://www.ncbi.nlm.nih.gov/pubmed/23015907.

Stokes, D.G. et al., 2001. Regulation of type-II collagen gene expression during human chondrocyte de-differentiation and recovery of chondrocyte-specific phenotype in culture involves Sry-type high-mobility-group box (SOX) transcription factors. *The Biochemical journal*, 360(Pt 2), pp.461–70. Available at: http://www.pubmedcentral.nih.gov/articlerender.fcgi?artid=1222247&tool=pmcentrez&rendertype=abstract.

Strotmann, R. et al., 2000. OTRPC4, a nonselective cation channel that confers sensitivity to extracellular osmolarity. *Nature Cell Biology*, 2(10), pp.695–702.

Sukharev, S.I. et al., 1994. A large-conductance mechanosensitive channel in E. coli encoded by mscL alone. *Nature*, 368(6468), pp.265–268.

Suzuki, M., Mizuno, A., et al., 2003. Impaired pressure sensation in mice lacking TRPV4. *Journal of Biological Chemistry*, 278(25), pp.22664–22668.

Suzuki, M., Watanabe, Y., et al., 2003. Localization of mechanosensitive channel TRPV4 in mouse skin. *Neuroscience Letters*, 353(3), pp.189–192.

Syeda, R. et al., 2015. Chemical activation of the mechanotransduction channel Piezo1. *eLife*, 4(MAY).

Syeda, R. et al., 2016. Piezo1 Channels Are Inherently Mechanosensitive. *Cell Reports*, 17(7), pp.1739–1746.

Tabuchi, K. et al., 2005. Hearing impairment in TRPV4 knockout mice. *Neuroscience Letters*, 382(3), pp.304–308.

Thirion, S. & Berenbaum, F., Culture and Phenotyping of Chondrocytes in Primary Culture. , 100(4), pp.1–14.

Tian, W. et al., 2004. Renal expression of osmotically responsive cation channel TRPV4 is restricted to water-impermeant nephron segments. *Am J Physiol Renal Physiol*, 287(1), pp.F17-24. Available at: http://www.ncbi.nlm.nih.gov/entrez/query.fcgi?cmd=Retrieve&db=PubMed&dopt=Citation&list_uids=15026302%5Cnhttp://ajprenal.physiology.org/content/287/1/F17.full.pdf.

Venkatachalam, K. & Montell, C., 2007. TRP channels. *Annual review of biochemistry*, 76, pp.387–417.

Voets, T. et al., 2002. Molecular determinants of permeation through the cation channel TRPV4. *Journal of Biological Chemistry*, 277(37), pp.33704–33710.

Vriens, J. et al., 2004. Cell swelling, heat, and chemical agonists use distinct pathways for the activation of the cation channel TRPV4. *Proceedings of the National Academy of Sciences of the United States of America*, 101(1), pp.396–401. Available at: http://www.pubmedcentral.nih.gov/articlerender.fcgi?artid=314196&tool=pmcentrez&rendertype=abstract.

Vriens, J. et al., 2007. Determinants of 4 alpha-phorbol sensitivity in transmembrane domains 3 and 4 of the cation channel TRPV4. *The Journal of biological chemistry*, 282(17), pp.12796–12803. Available at: http://www.ncbi.nlm.nih.gov/pubmed/17341586.

Vriens, J. et al., 2005. Modulation of the Ca2+ permeable cation channel TRPV4 by cytochrome P450 epoxygenases in vascular endothelium. *Circulation Research*, 97(9), pp.908–915.

Watanabe, H., Davis, J.B., et al., 2002. Activation of TRPV4 channels (hVRL-2/mTRP12) by phorbol derivatives. *Journal of Biological Chemistry*, 277(16), pp.13569–13577.

Watanabe, H. et al., 2003. Anandamide and arachidonic acid use epoxyeicosatrienoic acids to activate TRPV4 channels. *Nature*, 424(6947), pp.434–438.

Watanabe, H., Vriens, J., et al., 2002. Heat-evoked activation of TRPV4 channels in a HEK293 cell expression system and in native mouse aorta endothelial cells. *Journal of Biological Chemistry*, 277(49), pp.47044–47051.

White, J.P.M. et al., 2016. TRPV4: Molecular Conductor of a Diverse Orchestra. *Physiological Reviews*, 96(3), pp.911–973. Available at: http://physrev.physiology.org/lookup/doi/10.1152/physrev.00016.2015.

Wilusz, R.E., Sanchez-Adams, J. & Guilak, F., 2014. The structure and function of the pericellular matrix of articular cartilage. *Matrix Biology*, 39, pp.25–32.

Wissenbach, U. et al., 2000. Trp12, a novel Trp related protein from kidney. *FEBS Letters*, 485(2–3), pp.127–134.

Woo, S.-H. et al., 2014. Piezo2 is required for Merkel-cell mechanotransduction. *Nature*, 509(7502), pp.622–626. Available at: http://www.ncbi.nlm.nih.gov/pubmed/24717433%5Cnhttp://www.nature.com/doifinder/10.1038/nature13251.

Wright, M. et al., 1996. Effects of Intermittent Pressure-Induced Strain on the Electrophysiology of Cultured Human Chondrocytes: Evidence for the Presence of Stretch-Activated Membrane Ion Channels. *Clinical Science*, 90(1), pp.61–71.

Wright, M.O. et al., 1997. Hyperpolarisation of cultured human chondrocytes following cyclical pressure-induced strain: Evidence of a role for ??5??1 integrin as a chondrocyte mechanoreceptor. *Journal of Orthopaedic Research*, 15(5), pp.742–747.

Wu, J. et al., 2016. Localized force application reveals mechanically sensitive domains of Piezo1. *Nature Communications*, 7, p.12939. Available at:

http://www.nature.com/doifinder/10.1038/ncomms12939.
Wu, Z. et al., 2016. Mechanosensory hair cells express two molecularly distinct mechanotransduction channels. *Nature Neuroscience*, (November). Available at: http://www.nature.com/doifinder/10.1038/nn.4449.
Yellowley, C.E. et al., 1997. Effects of fluid flow on intracellular calcium in bovine articular chondrocytes. *The American journal of physiology*, 273, pp.C30–C36.
Yellowley, C.E., Jacobs, C.R. & Donahue, H.J., 1999. Mechanisms contributing to fluid-flow-induced Ca2+ mobilization in articular chondrocytes. *Journal of Cellular Physiology*, 180(3), pp.402–408.
Yin, J. et al., 2008. Negative-feedback loop attenuates hydrostatic lung edema via a cGMP-dependent regulation of transient receptor potential vanilloid 4. *Circulation Research*, 102(8), pp.966–974.
Zarychanski, R. et al., 2012. Mutations in the mechanotransduction protein PIEZO1 are associated with hereditary xerocytosis. *Blood*, 120(9), pp.1908–1915.
Zhang, W. et al., 2015. Ankyrin Repeats Convey Force to Gate the NOMPC Mechanotransduction Channel. *Cell*, 162(6), pp.1391–1403.
Zhang, Z., 2014. Chondrons and the Pericellular Matrix of Chondrocytes. *Tissue engineering. Part B, Reviews*, 21(3), pp.267–277. Available at: http://www.ncbi.nlm.nih.gov/pubmed/25366980.
Zheng, J., 2013. Molecular mechanism of TRP channels. *Comprehensive Physiology*, 3(1), pp.221–242.

13 Acknowledgments

I want to thank Prof. Dr. Gary R. Lewin who has given me the opportunity to pursue my PhD in his lab. His enthusiasm, suggestions and comments have been crucial for the development of my project and for me as a scientist.

I am deeply grateful Dr. Kate Poole, who devoted so much time to mentor me. Her presence was definitely inspiring and encouraging. I am grateful not just for her expertise and dedication, but also for her advices, and for being a role model from whom I learnt determination and scientific clarity.

I am very grateful to Dr. Mirko Moroni who was essential for my development as an electrophysiologist. Thanks for you never-ending constructive comments, for your encouragement and for being an excellent role model.

Thank you to Prof. Dr. Ursula Koch for accepting to be my supervisor. I want to thank Dr. Alison Barker, Dr. Jane Reznick and Dr. Mirko Moroni for your helpful comments about this thesis. Immense thanks to Dr. Anca Margineanu for all the help related to the Second Harmonic Generation imaging. I am additionally grateful to all -current and past- members from the Lewin lab, I surely learnt something from you all. Special thanks to Dr. Conni Staerkel.

My friends and family have been absolutely essential to complete this path. My dad Jorge, my mom Martha, and my sister Paulina, infinitas gracias por todo. For my friends, thank you Marta, Yu-Ting, Cristina, Angelica, you made my path brighter. Tristan, thank you for your support, patience, humor, love, and strength (physical and emotional).

14 Publication

Servin-Vences MR, Moroni M, Lewin GR, Poole K. Direct measurement of TRPV4 and PIEZO1 activity reveals multiple mechanotransduction pathways in chondrocytes. Swartz KJ, ed. *eLife*. 2017;6:e21074. doi:10.7554/eLife.21074.